THESIS

INVESTAGATION OF ECOSYSTEM DROUGHT STRESS AND ITS IMPACTS ON CARBON EXCHANGE AT TROPICAL FORESTS

Submitted by

Jun Liu

Atmospheric Science Department

In partial fulfillment of the requirement

For the Degree of Master of Science

Colorado State University

Fort Collins, Colorado

Summer 2004

COLORADO STATE UNIVERSITY

July 20, 2004

WE HEREBY RECOMMEND THAT THE THESIS PREPARED UNDER OUR SUPERVISION BY JUN LIU ENTITLED INVESTAGATION OF ECOSYSTEM DROUGHT STRESS AND ITS IMPACTS ON CARBON EXCHANGE AT TROPICAL FORESTS BE ACCEPTED AS FULLFILING IN PART REQUIREMENTS FOR THE DEGREE OF DOCTOR OF PHILOSOPHY.

Committee on Graduate Work

_____

_____

_____

_____

_____

_____
Advisor

_____
Department Head/Director

Abstract

INVESTAGATION OF ECOSYSTEM DROUGHT STRESS AND ITS IMPACTS ON CARBON EXCHANGE IN TROPICAL FORESTS

Tropical forests are subject to severe seasonal and ENSO-related inter-annual fluctuations in precipitation, yet transpiration and CO_2 exchange in these forests are resilient, partly due to their ability to extract water from deep soil reservoirs. The physiological response of forests and secondary vegetation covers to drought stress determines the seasonal and inter-annual variations in carbon and water exchange, which feed back to regional CO_2 concentrations, hydrology, and circulation patterns. Proper characterization of the responses of the tropical forest system to climate variability is crucial for analysis and prediction of carbon and water cycle changes in these areas.

In order to investigate the interactions between ecosystem-level drought stress, carbon exchange, and precipitation, and to eliminate the unrealistic severe drought stress from the simulation, the proper parameterization of root depth, soil hydrology and ecosystem stress in the simple biosphere model (SiB2) is explored, and the recently developed SiB--- SiB3 models are studied.

Model parameterizations and interpretation are evaluated at two forests sites across the Amazon Basin where long-term flux tower time series were available: Tapajos 67km and Reserva Jaru. Extreme drought stresses during the dry season were found at both sites when using the SiB2 simulation, which was inconsistent with the observed data. Two strategies were explored in order to eliminate this server drought stress. When considering the standard model may be overly sensitive to drought stress, one idea is to use alternative parameterization, which involves deep root, a new algorithm for drought stress, and less run-off for precipitation. The other idea explored is to apply the recently

developed SiB3 model, which introduced revised soil and snow structures as well as new strategies to calculate water stress, including multiple soil layers, adjusted water extraction root profile and the application of plant available water in the calculation of water stress.

Alternative parameterizations in SiB2 did not make any significant improvement in alleviating server drought stress in the dry season, suggesting that modifying the standard model itself may not solve the problem radically.

The impacts of multiple soil layers and adjusted water extraction root profile on water storage and transportation depend not only on the number of layers, but also on the location and weather conditions of the sites. For Reserva Jaru, the SiB3-10_layer model alleviated severe drought stress in the dry season but two extra deep layers at the bottom of the soil were necessary in order to eliminate drought stress completely. For the northern site, the Tapajos 67km site, the 12_layer model alleviated drought stress to around 35% but didn't allow for it to vanish completely, partly due to the smaller amount of precipitation in this area. The impacts of a multi-layer model on the carbon and energy exchange were also explored in this study. It showed that the SiB3 multi-layer model was more consistent with the observed data when compared to the SiB2 model.

Jun Liu
Department of Atmosphere Science
Colorado State University
Fort Collins, Colorado 80523
Summer 2004

ACKNOWLEDGEMENTS

I would like to thank Dr. A Scott Denning, my advisor, for consistent and patience, understanding and support of my study and thesis throughout the course of this project.

I would also like to give many thanks to my committee members Dr. David A Randall and Dr Micheal B Cougheour for taking the time for review this thesis and giving me suggestions.

I am also grateful to all the members in Denning's Group. Lixin Lu, my former officemate and best friend, who has always been there with valuable advises and help me through ups and downs in my life. Help from Ian Baker for his tremendous help on my understanding and applying SiB2 model. Help from John Kleist and Owen Leonard for their patience on my computer problems, which are very important for me to get through this research. Connie Uliasze, Aaron wang, Neil Suits, Jillian L'Ecuyer and all other members of Dr. Denning's Group have contributed to make my stay an enriching and exciting experience.

Thanks to Kelsi Nagy, from Physiology Department for her great help on the English edition of my thesis.

Special thanks to my best friends: Hui Chang, Shanshan Li for their friendship and solid support, which made the last few could-be-stressful months a pleasant experience.

This research is funded by LBA (Large Scale Biosphere-Atmosphere Experiment in Amazonia). Any opinions, findings, and conclusions or recommendations expressed in this publication are those of the authors and do not necessarily reflect the views of the LBA.

TABLE OF CONTENT

LIST OF FIGURES

LIST OF TABLES

Chapter 1

Introduction

1.1 The Interaction between Land and Atmosphere

1.1.1 The Important Role of Interaction between Land and Atmosphere

The interactions between land surface and atmosphere are significant and complex. These interactions cover a wide range of spatial and temporal scales. Land surface is an important source and sink of radiation, water, latent and sensible heat flux, momentum as well as trace gases.

Exchanges of radiation, sensible heat, latent heat, and momentum are important and significant interactions between land and atmosphere systems. These exchanges have a direct impact on fields of wind vector and precipitation. The other aspect involves the exchange of trace gases such as CO_2 and CH_4 and various N-species, which play an important role in determining the radiative transfer characteristics of the atmosphere and hence the energy budget of the planet. The importance of carbon compounds and mineral nutrients for the functioning of the biota, particularly photosynthesis and respiration, require no elaboration. Any attempt to simulate climate change without including the effects of vegetation will prove to miss a major component of an accurate model. Some examples of feedbacks include the positive feedback loop between soil moisture and precipitation (see section 1.2), the impacts of aerosol on the photochemistry in the boundary layer (Dickerson *et al*., 1997). Also, people live on the land's surface, so extra attention is needed to accurately simulate near-surface condition.

The inclusion of the interactions between land-surface and atmosphere in the climate models is also helpful in evaluating the accuracy and developing better parameterizations for assimilation of weather and climate data (Betts *et al*., 1998).

1.1.2 Land-atmospheric Processes in Climate Modeling

Energy and mass exchange between land and atmosphere are important processes in the climate. Physical and biological processes in soil-plant ecosystems control these exchanges. In atmospheric models, latent heat, sensible heat, momentum and CO_2 fluxes from land surfaces are source and sink terms in atmospheric models. The description of the interactions between land surface and atmosphere is an important part of climate modeling.

Cox *et al.* (2000) demonstrated that carbon-cycle feedbacks could significantly accelerate climate change over the twenty-first century by including the feedbacks between the climate and the biosphere. The coupled climate/carbon-cycle model was brought to equilibrium with a 'pre-industrial' atmospheric CO_2 concentration of 290 p.p.m.v, starting from an observed land cover data set provided by Wilson *et al*. (1985). The simulation results show that the atmospheric CO_2 concentration are 250 p.p.m.v higher in the fully coupled simulation than in uncoupled carbon models, resulting in a global-mean warming of 5.5K, as compared to 4K without the carbon-cycle feedback. That means there is 1.5 K difference in temperature when land-atmospheric interaction is considered as one of the key elements in the climate model. Figure 1.1a and 1.1b shows the impact of carbon-cycle-climate feedbacks on the atmospheric CO_2 concentration and consequent global warming, taken from Cox *et al.* (2000).

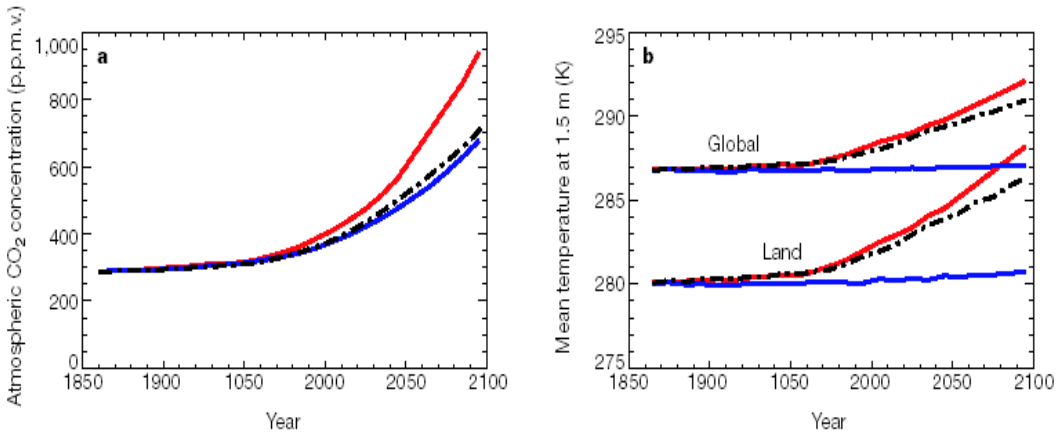

Figure 1.1: a: Global-mean CO_2 concentration, b: global-mean and land-mean temperature. Red lines indicate the fully coupled simulation with interactive CO_2 and dynamic vegetation; dot-dash lines represent a standard GCM climate change simulation with prescribed CO_2 concentration and fixed vegetation; blue lines represent the simulation without including CO_2-induced climate change.

Strategies used to represent the land surface in climate modeling can be classified into two categories (Sellers *et al.*, 1997):

(1) prescription of independent land surface parameters such as albedo, aerodynamic roughness length of plants and surface "moisture availability"(Betts *et al.*, 1998; Viterbo *et al.*, 1999).

(2) use of self-consistent biophysically process-based models such as the photosynthesis-conductance model(see section 2.1.2.2).

Tremendous developments in land surface parameterization have been made in the past few decades (Sellers *et al.*,1996), including the incorporation of a realistic canopy photosynthesis conductance submodel and the use of satellite data to describe vegetation state and phenology. However, the approach of prescription of land surface parameters is extremely limited. First, no feed back from climate to land surface can be simulated with

prescribed surface properties. Second, enormous data collection efforts have to be made in order to obtain realistic climatological fields of the surface parameters.

A more realistic approach is to base the model on biophysical principles and in doing so, capture the typical characteristic of biophysical controls within the land-atmosphere exchange processes. Biophysically based models may have the following benefits: 1) they can be used to study the various feedback processes between land surface and atmosphere by land-surface parameterization (LSP). LSP has undergone tremendous development in the past decade and now includes a higher degree of biophysical realism and is more consistent than what was being used just a few years ago (Sellers *et al.*, 1997). 2) It offers a better prospect for the use of coupled land-atmosphere models for prediction. It has been shown that biophysically-based land-surface parameterization improves the ability of numerical weather prediction models in the 1980s and 1990s to forecast weather under extreme climatic conditions such as droughts (Atlas *et al.*, 1993) and floods (Beljaars *et al*., 1996). Land-surface predictions can also be used to evaluate the accuracy and develop better parameterizations for assimilation of weather and climate data (Betts *et al*., 1998). 3) The model may provide physical-state variables rather than conceptual analogs for comparison with actual measurements and hence allows for model verification and initialization. In this respect, remote sensing data with global coverage and high temporal resolution is immensely useful.

Therefore, the effects of vegetated land on the atmosphere play an important role in the simulation of atmospheric circulation. Without including these interactions the atmospheric model would be misleading.

1.2 Soil Moisture and Drought Stress

Soil moisture is essential in evaptranspiration, which is the dominant mode of energy transfer from the surface to the atmosphere. Transpiration is the loss of water from plants in the form of vapor and it is the dominant process in plant water exchange because of the

large volume of water involved and the influence it has to control plant water status (Kramer and Boyer, 1995; see section 1.2.1). Latent heat flux involved in the transpiration process is dependent on a number of environmental and biological processes and is an essential process of mass and energy exchange between the vegetated land surface and atmosphere. The interaction between soil moisture and atmospheric circulation influence regional and global climate significantly.

The U.S. Midwest floods during the summer of 1993 were an example of climate anomalies related to soil moisture and atmospheric interaction. Figure 1.2 shows the figures from Flood Analysis by Paul Baumann (1993)

In a numerical simulation the 1993 Midwestern Flood, the sensitivity of the low-level jet, planetary boundary layer, and heavy precipitation were examined by imposing various soil moisture and surface anomalies to the model simulation (Bosilovich *et al.*, 1999). The increased surface heating, caused by a strong dry anomaly, induced a large-scale surface pressure disturbance, centered in southeastern United States that weakened the low-level jet and moisture convergence within the flood region. The correlation between saturated soil moisture since the spring of 1993 and the subsequent increase of precipitation suggests that local precipitation is enhanced by a large amount of soil moisture, a process called recycling of water (Mintz 1984; Betts *et al.*, 1994; Trenberth and Guillemot 1996). To make matters worse, floods are usually accompanied by other kinds of server weather. In addition to persistent and heavy rainfall, the Midwest region of U.S. experienced frequent storms with gusty winds and hailstones the size of quarters or larger, especially during June. Numerous funnels and tornadoes were spotted. In June, fifty-four funnels or tornados were spotted, more than twice the number recorded in the previous two months of April and May (Paul, 2001, flood analysis, 1993 Mississippi flood).

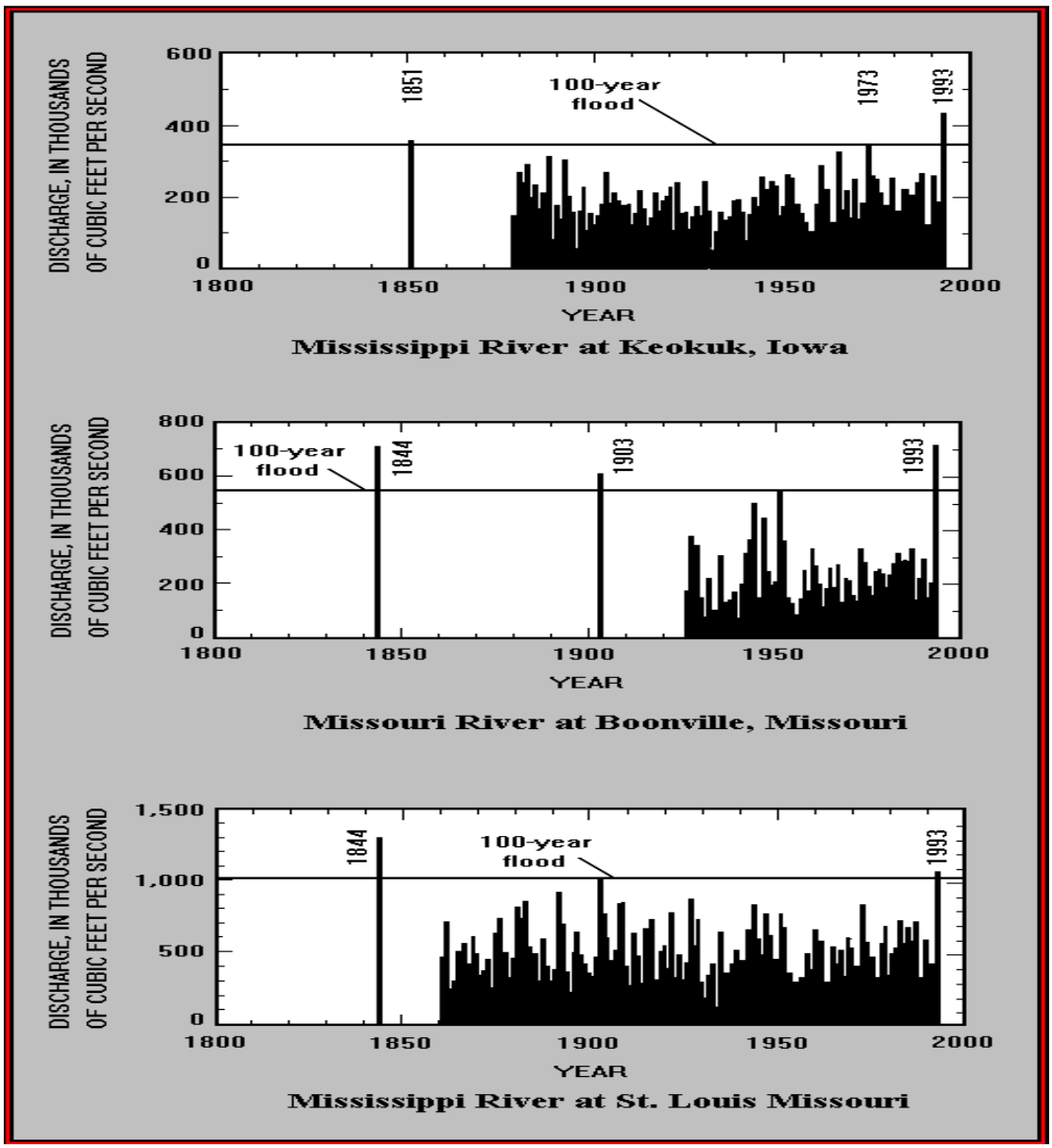

Figure 1.2: Discharge in the Mississippi River during within one century(taken from Paul Remann, flood analysis)

Climate hazards due to the positive feedback between soil moisture and precipitation (see section 1.2.1) are not the only concern. Lack of soil moisture or extremely dry atmospheric conditions will cause drought stress, which also has a significant impact on climate. Many variables play a part in order for drought conditions to be reached; these

include lack of natural rainfall, air temperature and humidity, wind conditions, sun exposure, as well as the types of soil and plant.

Drought stress takes a significant role in atmospheric circulation because of its impact on the boundary circulation. Drought stress has important effect on evaporation as well as on photosynthesis (section 1.2.1). As Boyer (1970) states, moisture stress affects the efficiency of photosynthesis through a number of mechanisms: by affecting the levels of metabolic intermediates; by inhibiting the photosynthetic electron transport system; by causing stomatal closure; and by altering rates of respiration. We will discuss the photosynthetic reaction in section 1.2.1. As a consequence, drought stress affects the energy budget as well as weather conditions, general circulation, precipitation, clouds and winds through the positive feedback loop (section 1.2.2).

Severe drought stress could cause disaster in agriculture through its influence on plants. Plants under drought conditions are vulnerable to pest damage since they are in the weakened state and their density is low. At the same time, severe drought stress will also result in disastrous climate events by disturbing the normal photosynthetic process (section 1.2.1) and positive feedback (section 1.1.2) between land and atmosphere. The worst drought in the United States has experienced in the past 50 years occurred during the last major La Niña from 1988 to 1989 (see table 1.1) when crops planted in the spring failed to receive the rain they needed to grow. Rainfall in the Midwest was as much as 85% below normal. Crops and livestock died. Millions of acres of trees were destroyed by forest fires impossible to control. A systematic decrease in monthly mean of evapotransportation(ET) has been indicated by the water vapor budget for 1988. Compared to non-drought summers, the ET rate was anomalously low. Estimated reduction in surface latent heat fluxes relative to the control years are approximately 20 W/m^2, with implied increases in sensible heating of similar magnitudes (Lyon *et al.*, 1995). Table 2.2 is taken from Lyon *et al.* 1995.

	Temperature anomalies (ºC)	Precipitation (percent of normal)
June	3.7	40
July	1.4	59
August	1.7	105

Table 1.1: 1988 temperature and precipitation anomalies

1.2.1Transpiration Processes

Transpiration is the process where water moves from the soil into the atmosphere due to the differences in water potential between soil, plants and air. The movement of water through the soil-plant-atmosphere continuum can be regarded as occurring along the decreasing water potential, which is analogous to the flow of the electron current. Equation 1.1 describes the rate of transpiration:

$$\text{Transpiration rate} = \frac{\Psi_g - \Psi_r}{r_g} = \frac{\Psi_r - \Psi_l}{r_r + r_s} = \frac{\Psi_l - \Psi_a}{r_s + r_a} \qquad (1.1)$$

where Ψ_g Ψ_r Ψ_l Ψ_a are water potentials of the soil, roots, leaves and air respectively. r_g is resistance through the soil to the root surface, r_r is resistance across the root, r_x is xylem resistance, r_s is stomatal resistance involving a phase change from water as a liquid into a vapor, and r_a is aerial boundary layer resistance.

1.2.2 Photosynthesis and the Respiration Processes

Photosynthesis is a process through which green plants extract solar energy and convert it into a form usable for other levels in food chain (Kramer and Boyer *et al.*,

1995). In this process, primary sugars, water, and oxygen are produced by chlorophyll-containing plants in the light-intermediated reaction.

$$6CO_2 + 12H_2O \rightarrow C_6H_{12}O_6 + 6H_2O + 6O_2 \quad . \tag{1.2}$$

Although the pathway is different than in photosynthesis, *respiration* is an inverse of photosynthesis. It is the function of soil moisture and soil temperature. All living things respire to produce energy. Chlorophyll is not a component of the respiration process. The irradiance level at which photosynthesis and respiration are equal is known as the *light compensation point*.

Green plants can be classified into three major groups according to their photosynthetic mechanisms: C_3, C_4 plants and CAM plants. The typical photosynthetic plant is called a C_3 plant because the first stable compound formed from CO_2 is a three carbon compound at the beginning of the Calvin Cycle. The Calivin Cycle is a metabolic pathway found in the chloroplast where carbon enters in the form of CO_2 and leaves in the form of sugar, discovered by Melvin Calvin and Andy Benson at the University of California, Berkeley. Likewise, C_4 plants are named for the four carbon compound that is first formed incorporating CO_2 . CAM is the abbreviation of Crassulacean acid metabolism. The name points at the fact that this pathway occurs mainly in Crassulacean species (and other succulent plants). The chemical reaction of the carbon dioxide accumulation is similar to that of C_4 plants but here is carbon dioxide fixation and its assimilation is not separated spatially but temporally (Peter von Sengbusch 2003; Gebauer, 1988).

Among the mechanisms through which drought stress can affect photosynthesis, the stomatal regulatory mechanism is one of the direct influences on water availability in photosynthesis through stomatal apertures. Resistance to the diffusion of carbon dioxide into leaves increases with stress, as stomates close in response to stress. Stomatal conductance takes an important role in regulating the balance between transpiration and

net uptake of CO_2. The theoretical treatment is based on the premise that stomata take such a role: on one hand, it permits CO_2 to diffuse into the leaf to support photosynthesis; on the other hand, it restricts water loss from the leaf mesophyll. Complex mechanisms adjust the opening of stomata in response to changes in environmental conditions, such as photosynthetic active radiation (PAR), humidity of the air, CO_2 partial pressure, leaf temperature, soil moisture and reflect environment, as well as the plant's own physiological conditions (Jarvis, 1976; Steward, 1988; Jones and Higgs, 1989). It has been argued that the regulatory system strikes an appropriate compromise between permitting photosynthesis and restricting water loss (Cowan, 1977). The current hypothesis concerning the stomatal regulatory mechanism states that regulated stomata should approach a theoretical optimum through natural selection. There is great experimental work that leads to supports this theory (eg. Farquhar and Sharkey, 1982).

1.2.3 Positive Feedback between Soil Moisture and Precipitation

Soil moisture has a significant influence on evaporation, surface cooling, surface energy fluxes, and mixed layer depth (Betts *et al.*, 2000), Drought stress is the stress that results from lack of soil moisture. Drought stress impacts atmospheric circulation and also on the energy budget through positive feedback between soil moisture and precipitation (Betts *et al.*, 2000)

In the energy budget between land-surface and atmosphere, conservation of the total amount of latent heat (LH), sensible heat (SH) and ground heat fluxes (G) holds (Betts *et al.*, 2000). In Betts *et al.* (2000), the difference between the diurnally averaged net radiation (R_{net}) and ground heat flux (G) is referred to as surface forcing (Q^*), also known as net available energy, which drive fluxes in sensible heat and latent heat (see equation 1.3). The evaporative fraction is defined as the ratio of latent heat flux to the total flux of latent and sensible heat flux (see equation 1.4). BR refers to the Bowen ration, which is defined in equation 1.3:

$$Q^* = R_{net} - G = SH + LH \tag{1.3}$$

$$EF = LH/(LH + SH) \tag{1.4}$$

$$BR = SH / LH \quad . \tag{1.5}$$

Given a similar soil temperature and net available energy (Q^*) while in the absence of significant horizontal advection, higher soil moisture, and the associated higher EF will lead to a higher afternoon equilibrium potential temperature q_E, and could lower base P_{LCL}. The Lifting Condensation Level (LCL) is the level where condensation (saturation) occurs if one lifts an unsaturated surface parcel dry-adiabatically. q_E is linked to soil temperature and increases with a higher soil temperature while P_{LCL} is a measurement of how far surface air is from saturation. P_{LCL} is associated with the availability of water for evaporation, the imbalance between evapotranspiration from soil moisture and the evaporation from soil, and the turbulent entrainment of dry air into the boundary layer from the free atmosphere. On a rainy day, evaporation of falling precipitation reduces P_{LCL}. Both higher q_E and lower cloud base favor enhanced deep convection and hence precipitation, A positive feedback is established (see figure 1.3). Betts *et al.* (1998) showed this positive feedback through the analysis of FIFE surface climate and site-average dataset from the year of 1987 to 1989.

Betts *el al.*, (2000) used energy budget balance to explain the positive feedback loop. When given a certain vegetative resistance R_v, sensible and latent heat flux is controlled by the radiative and evaporative cooling terms, and surface forcing term Q^* respectively. In Betts *et al.* (2000) sensible and latent flux is described as follows:

$$SH = C_P F_{0q} = rC_P g_a (q_0 - q_M) \tag{1.6}$$

$$LH = LF_{0q} = rLg_a (q_0 - q_M) \quad . \tag{1.7}$$

where *?* and C_p are the density and heat capacity of air; L is the latent heat of evaporation; $F_{0?}$ and F_{0q} are the surface fluxes of potential temperature and moisture; $?_M$ and q_M are the potential temperature and specific humidity in the mixed layer; $?_0$ is surface (aerodynamic) potential temperature, and q_0 is surface specific humidity. g_a is an aerodynamic conductance, which is the reciprocal of R_v.

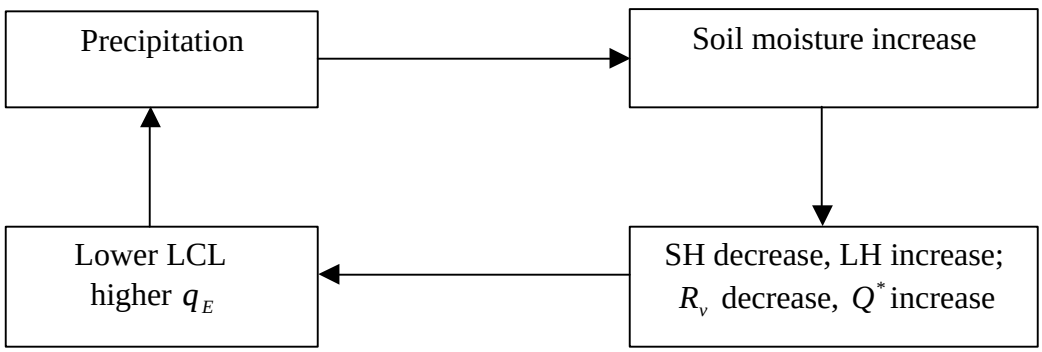

Figure 1.3: Positive feedback loop between precipitation and climate

Within the mixed layer, radiative cooling and evaporative cooling are two types of surface cooling in order to support the two balances—thermal balance as well as moisture balance. These two balances determine the long-term equilibrium of the diurnal energy cycle over land (Betts *et al*., 2000). In thermal balance,

$$F_{oq} - F_{Hq} + (\partial q_{rad} / \partial t + \partial q_{evap} / \partial t) \cdot (P_H / g) = 0 \tag{1.8}$$

the mixed layer depth is P_H (in pressure coordinates, to be defined positively), g is gravitational acceleration. $F_{H?}$ is defined in equation 1.7. $\partial q_{rad} / \partial t$ is mean mixer layer radiative cooling and $\partial q_{evap} / \partial t$ is the mean mixed layer evaporation cooling (both are to be defined negatively). Net upward SH fluxes and subsidence warming balance net radiative cooling and evaporation cooling. In moisture balance, net upward latent fluxes balance drying by subsidence (see equation 1.8):

$$F_{oq} - F_{Hq} - (C_P P_H / Lg)(\partial q_{evap} / \partial t) = 0 \tag{1.9}$$

where F_{Hq} is defined in equation 1.7.

$$F_{Hq} = -(\Omega_T / g) \cdot \Delta q \tag{1.10}$$

$$F_{Hq} = -(\Omega_T / g) \cdot \Delta q \tag{1.11}$$

where

$$\Delta q = q_T - q_M \tag{1.12}$$

$$\Delta q = q_T - q_M \tag{1.13}$$

Where q_T and q_T are air temperature and specific humidity respectively. The omega term, a cloud-base subsidence term, is the sum of

$$\Omega_T = \Omega_R + \Omega * \tag{1.14}$$

where O_R is a radiative equilibrium subsidence (to be defined positively) at the mixed layer top, and Ω^* is an additional mass flux (also to be defined positively) through cloud base associated with a shallow cumulus field, typically the upward transport of air into clouds that is moist but slightly cool (e.g., Betts *et al*., 1975).

1.3 Tropical Forest Hydrology

1.3.1Background of Hydrological Process

The hydrological processes include precipitation, interception, evaporation and runoff. Interception splits the precipitation into what is delivered to the land and water surfaces and what is caught on the forest canopy and returned to the atmosphere by evaporation. Water delivered to the land surface may run off directly, as overland flow into streams to join rivers and lakes and flow back into the sea, or it may infiltrate the soil. The surplus

that drains further down into springs maintains the steady flow of rivers. Vegetation is supplied from the soil; much of the soil water is returned by plants through transpiration into the atmosphere or evaporates directly from soil or water surfaces. Part of the water that infiltrates the soil moves laterally through the upper horizons until it reaches a stream channel and does not become part of the ground water reservoir. This portion of subsurface flow is referred to as interflow or through-flow and, together with overland flow, constitutes what is generally surface runoff, or more properly, as direct runoff or quick flow (Dickinson *el al*.,1986).

Because of its lush vegetation the tropical rain forest forms an exceptionally effective screen or climate filter between the free atmosphere above and the vegetated ground below. Salati *el at.*, 1979 and Salati and Matsui 1981 measured oxygen isotopes in rain and river water and confirmed the importance of recycled water in the hydrological balance throughout the Amazon Basin. The studies concluded that 52% of the precipitation in the Amazon region between Belem and Manaus was accounted for by inflowing moisture from the Atlantic Ocean, the remainder by recycled vapor within the local area. Interception in the forest occurs at two levels within the forest cover: in the canopy and in the ground. In the tropical interception loss values for heavy rainfalls are less than for light rainfalls. This conclusion is supported by several studies (e.g. Lockwood, 1976, Lawson, 1981). In contrast to evaporation from the *surface* soil of bare ground, dense tropical forest continues to transpire water from a deeper soil horizon. Thus the tropical forest serves as an important source of water vapor because it transpires water in larger quantities than most other vegetation. The soil-drying action of the tropical forest is considerable. Lomee (1961) found it reached 2,0002,300 mm for a 25 m rooting depth and an available moisture 4,200mm in Java and in the Congo Basin between 1,230 and 1,510 mm under forest's surface, while it was only 950-1,100mm under savanna's.

1.3.2 General Geophysiology and Climatology of the Tropical Forest

The tropical rainforest is the most productive ecosystems on the earth, exchanging as much as 5% of the mass of atmospheric CO_2 every year (Houghton *el al*., 1987). They are also undergoing very rapid change due to human land use. Altered cycles of water, energy, carbon and nutrients in Amazonian vegetation cover, are expected to have climatic and environmental consequences at local, regional and global scales.

The tropical forest is a treasure trove of different animal and plant species. It is the earth's most complex biome in terms of both structure and species. The numerous species that inhabit the rainforests are not well documented. Abundant precipitation and year around warmth occur under optimal growing conditions. There is no annual rhythm to the forest; rather each species has evolved its own flowering and fruiting season. Because tropical rainforests contains trees standing 30 to 50 meters in height creating a canopy of foliage, sunlight is a major limiting factor. The enclosed canopy shades the forest floor inhibiting the development of much undergrowth (Gash *et al*.,1996).

Trees of smaller statue than those found in the rainforest are named as *Tropical Monsoon* of *Season Forest or Shrub*. The Monsoon forest may include deciduous trees, as well as, broadleaf evergreen trees reflecting the seasonal precipitation of the *Monsoon Climate*. The tropical monsoon climate experiences abundant rainfall like the tropical rain forest climate, but is concentrated in the high-sun season when maritime equatorial and tropical air masses travel from the ocean over the land and are uplifted by either convection or condensation of the air to induce condensation. The low-sun season is characterized by a short drought season when high pressure inhibits precipitation formation. Because it is located near the equator, the tropical monsoon climate experiences warm temperatures throughout the year. The monsoon climate is generally found all over the tropical continent and increases in severity with latitude (Ritter 1997, Gash *et al.*, 1996).

1.3.3 Climate of Amazonia

The Amazon rainforest is important because of its aseasonal climate, warm temperatures and high rainfall. The Amazon covers almost half of the forested area of the Brazilian territory. UNESCO/UNEP/FAO(1978), estimates the area covered by moist tropical forest in the world is about 9.35×10^6 km², 39% of which is composed of the Brazilian evergreen rain forest (Dickinson *et al.*, 1986). Mean monthly temperatures are above 64°F; precipitation is often in excess of 100 inches a year with an brief annual season of reduced precipitation.

Dickinson *et al*. (1986) has stressed that the Amazon is an important heat source for the general circulation of the atmosphere, as a large amount of solar radiation is absorbed by the surface and transformed into latent heat. Nobre (1983) has also shown that localized and intense heat sources in the tropical atmosphere are a result of continental precipitation that gives rise to strong upward motion with associated convergence at the lower levels and divergence at upper levels, promoting large-scale subsidence outside the source region. This large-scale subsidence triggers seasonal drought conditions.

The entire Amazon Basin is located in the equatorial latitudes far from the subtropical high-pressure centers. Its tropospheric circulation is frequently disturbed by the intertropical convergence zone (ITCZ) and by squall lines of tropical instability, which cause rain (Dickinson *et al.*, 1986). A large reduction in the annual amount of precipitation appears to be related to the occurrence of strong ENSO (El Nino- Southern Oscillation). The possible relationship between ENSO and the reduction of precipitation, or droughts, has been explained by Kousky *el al.*, 1984. A stronger than normal convection is established over the abnormally warm waters of the eastern equatorial Pacific. The ascending branch of the Walker circulation, which normally resides over the western portion of the Amazon, is shifted westward over the warmer ocean and is enhanced by the strong convection. Meanwhile, the descending branch covers the entire Amazon and reaches the west coast of Africa, causing noticeable reductions in precipitation.

As mentioned above, weather in the Amazon is affected by a broad spectrum of meteorological phenomena that varies from small-scale cumulus convection to global-scale circulation patterns (Molion, 1986).The rapid removal of the tropical rain forest caused by deforestation is now a major concern of those who study the climate. In tropical areas, deforestation has been occurring throughout history. The total deforested area, as estimated by Brazil's Space Research Institute (INPE) in February 1991, was 415, 215 square kilometers. Tropical deforestation is a major component of the carbon cycle and also has profound implications for biological diversity (Skole and Tucker,1993). Skole and Tucker (1993) stated that deforestation increases atmospheric CO_2 and thus might consequently affect the climate (Houghton, 1991). Houghton *et al*. (1987) and Schimel *et al*. (1996) also declared that the recent change in land use had contributed to the release of CO_2 into the atmosphere, accounting for a significant fraction of the global anthropogenic flux. It is also likely that deforestation reduces local evaporation as indicated by numerical experiments (eg. Henderson-Sellers and Gornitz,1984). A reduction in evaporation would change the hydrology, probably reducing precipitation, since the local source of water vapor for precipitation in the Amazon is of the same magnitude as the adverted vapor (Molion, 1986). Moreover, the forest intercepts 20% of the annual precipitation, since it is composed of several small layers of strata. The intercepted rainfall cycles directly back into the atmosphere by evaporating without taking part in the soil moisture cycle. Without forest cover, the previously intercepted water will be available to increase the overland flow, drastically changing the monthly runoff pattern, resulting in larger flood peaks in the wet season and possible drought conditions in the dry season (Molion 1986). In conclusion, Large-scale deforestation of the Amazon Basin may interfere with the regional climate and possibly also with the global climate.

1.3.4 Natural vegetation and soil in Amazonia

There are more than 2500 tall tree species in the Amazonian forest, compared with a few dozen or less in most temperature-latitude forests (Dickinson *el al.*, 1986). As discussed before, the tall trees create a canopy of foliage over the surface, influencing

solar radiation, evaporation, and the global feedback of hydrological circulation subsequently.

A very important property of tropical soil is the extent to which their parent rocks are altered. Rocks are rapidly decomposed because of the hot temperature and humidity. Thus with the absence of Quaternary glaciations and the protection of the forest, the Amazonia soils have developed to a great depth (Dickson, 1986). This deep soil structure gives rise to the idea of multi-layer soil structure in Simple Biosphere Model (SiB3) (see section 2. 1. 3).

1.3.5 LBA Experiment

Large Scale Biosphere-Atmosphere in Amazonia(LBA) is a program constituted as an international research initiative led by Brail. It is to estimate the basin-scale carbon balance of Amazonia, using a combination of data collected by flux towers and regional atmospheric circulation, remote sensing, and geographic information systems. Tower flux data from sites in intact forest, regrowing forest, pasture, and savanna, are used to calibrate a model ecosystem physiology and biogeochemistry in both regional and global scale (Denning *et al*., 1997). In addition to the regional issues such as deforestation, forest regrowth and possibly CO_2 fertilization, quantification of tropical carbon fluxes is a key “missing link” in our understanding of the global carbon cycle. Rayner *et al*. (1996) used a tracer transport model to invert data, and calculated the locations of stations which would best reduce uncertainty in atmospheric CO_2 exchange with the oceans. They found that the existing observational network would best be extended by adding data over Amazon, because the uncertainties in tropical ecosystem fluxes are among the most significant uncertainty terms in the inversion budgets.

Denning (2000) declared three key elements in LBA experiment: 1) evaluation the models (SiB2 and coupled GCM-SiB2, Coupled RAMS-SiB2) across a range of spatial and temporal scales, from local fluxes and isotope isotope ratios to field campaigns in the area of the Flona Tapajos, to large regions sampled by airborne experiments; 2) a

collaborative investigation of the effects of surface water and seasonal inundated land on exchanges of energy, water, and CO_2; 3) estimation of regional and Basin-scale carbon balance on seasonal, annual, and interannual time scales by inversion of atmospheric data using tracer transport modeling. The work is undergoing with the efforts of all members in Denning's group and other colleagues.

1.3.6 Uncertainties in the research of Amazonia

Carbon cycle feedbacks are among the largest sources of uncertainty for future climate. Cox *el al*., (2001) declared that climate warming (the indirect effect of a CO_2 increase) tends to reduce terrestrial carbon storage and increase atmospheric CO_2, especially in warmer regions where an increase in temperature is not beneficial for photosynthesis. At low concentrations of CO_2, the direct effect of CO_2 dominates. Both vegetation and soil carbon increase atmospheric CO_2. However, terrestrial carbon begins to decline as CO_2 increases, since the direct effect of CO_2 on photosynthesis becomes saturated but the specific soil respiration rate continues to increase with the temperature. The transition between these two regimes occurs abruptly at around 2050 in this experiment (see figure 1.4b). The terrestrial carbon decreases by about 170 GtC from 2000 to 2100, accelerating the rate atmospheric CO_2 increases over this period. In contrast, Friedlingstein *el al*. (2001) concluded that atmospheric CO_2 would in fact be higher than the level reached if climate change does not affect the carbon cycle, by using climate carbon three dimensional models forced by a 1% per year increase in atmospheric CO_2 (see figure 1.5a and b). Therefore, given nearly identical human emissions, different models project dramatically different futures.

Cox *el al*., (2001) also addressed that vegetation carbon in South America begins to decline, as a drying and warming of Amazonia initiates loss of forests. This is driven purely by CO_2-induced climate change (see figure 1.4a). It was concluded by Cox *et al*. (2001) that the reduction in terrestrial carbon after 2050 onward is associated with widespread climate-driven loss of soil carbon (see figure 1.4b).

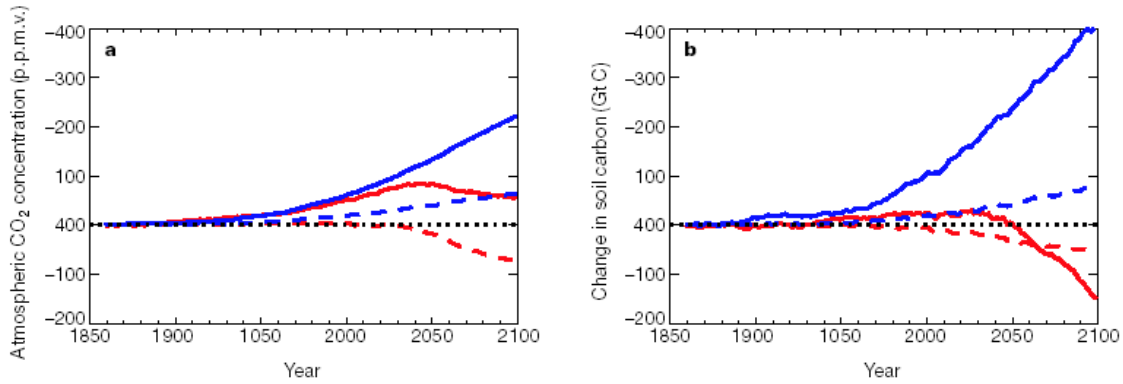

Figure 1.4: Effect of global warming on changes in land carbon storage. The red lines represent the fully coupled climate/carbon-cycle simulation, and the blue lines are from 'offline simulation' which neglects direct CO_2-induced climate change. The figure shows simulated changes in vegetation carbon (a) and soil carbon (b) for the global land area (continuous lines) and South America alone (dashed lines). This figure is taken from Cox *el al*., 2001.

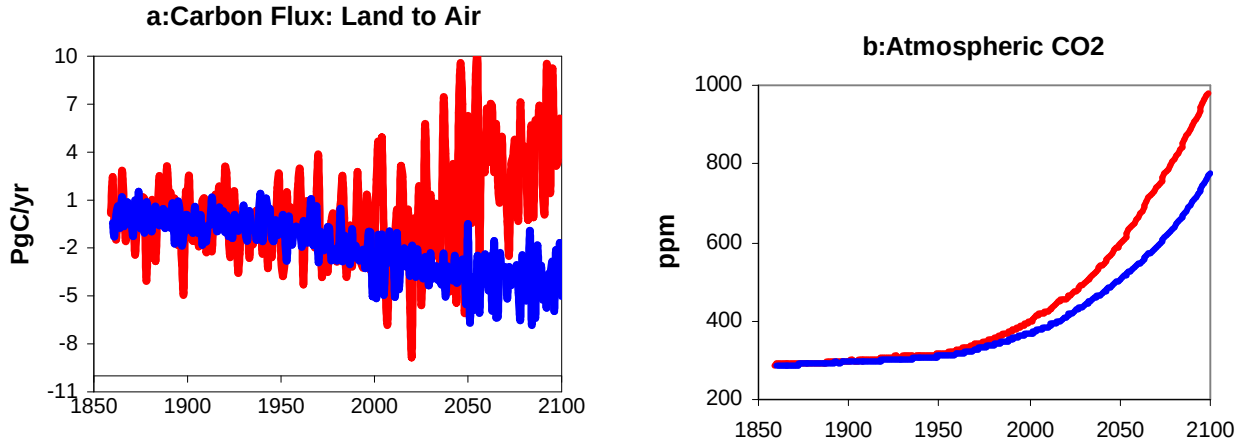

Figure 1.5: Effect of global warming on carbon changes. The red lines represent simulated results from Cox *et al.* 2000 and the blue lines are from Friedlingstein *et al*. 2001.

However, Saleska *et al.* (2003) stressed that biometric observations confirmed the net loss of carbon but imply that it is a transient effect of the recent disturbance

superimposed on long-term balance. They compared the measured net ecosystem exchange of CO_2 in two old growth forest sites near Santarem, Brazil to the model predictions. In contrast to the model results, the observation data shows the tropical forest is quite resilient with its release of CO_2 in the wet season and uptake of CO_2 in the dry season. Natural episodic disturbances complicate estimates of the regional carbon balance. However, when using the alternate SiB2 model (see section2.1.2) simulated NEE is consistent with the observed data (see section 3.2.1)

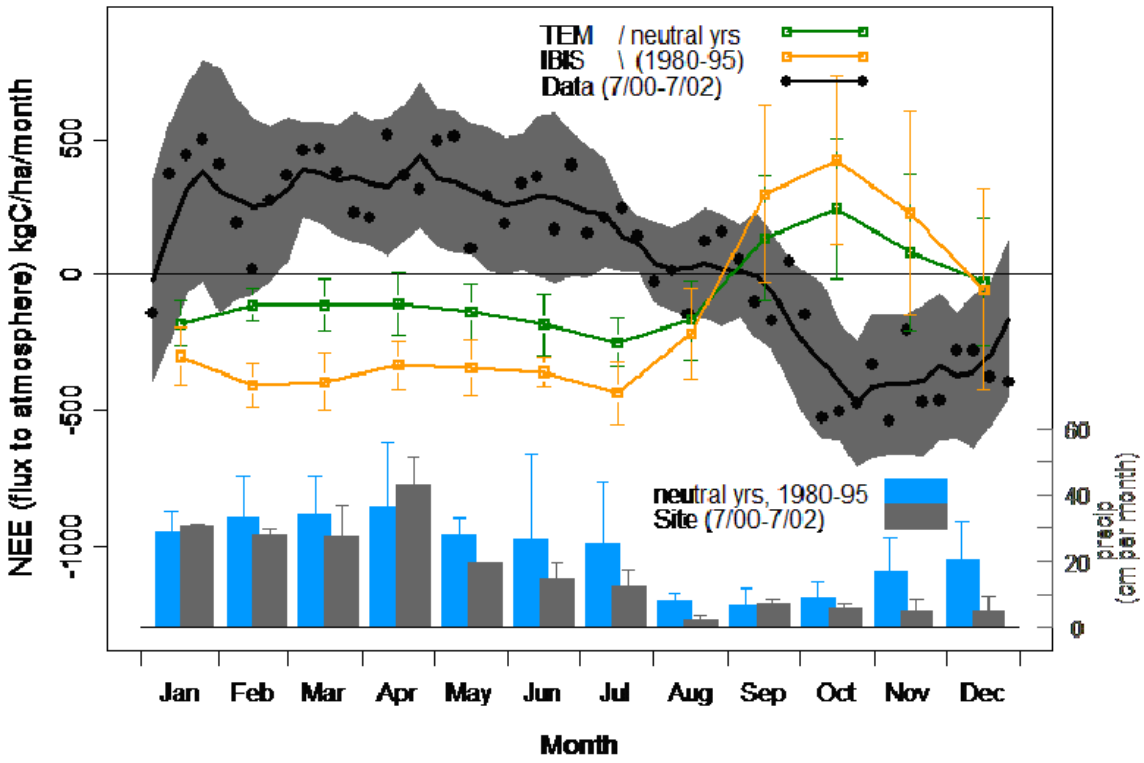

Figure 1.6: NEE flux and precipitation at the site of Tapajos 67km

Figure 1.6 is provided by Scott Saleska from Harvard University. Model output is mean of 4 grid points: -55.5<longitude<-54.5, -3.5<latitude<-2.5, the simulation time is 1980-1981, 1984-1985, 1990 and 1993-1995, which can be considered as neutral years. The data is from Tapajos 67km flux tower. The black dot represents the observed data and black line is moving average, showing the trend of NEE variation, and the green and yellow lines are the results of the two models---TEM and IBIS respectively. Obviously,

the trend of NEE from the simulation is not consistent with what has been observed and even indicates the opposite.

1.4 Objective in This Research

Tropical forests are subject to severe seasonal and ENSO-related interannual fluctuations in precipitation (Garreaud and Aceituno, 2000 and Garbriel *et al*., 2002), yet transpiration and CO_2 exchange in these forests are resilient, partly due to their ability to extract water from deep soil reservoirs. The physiological response of forest and secondary vegetation covers to drought stress determines the seasonal and interannual variations in carbon and water exchange, which feed back to regional CO_2 concentrations, hydrology, and circulation patterns. Proper characterization of the response of each of these systems to climate variability as well as the hydrology in the soil are therefore crucial for analysis and prediction of carbon and water cycle changes in these areas as well as regional and global climate changes.

In this research, the interaction between ecosystem-level drought stress, net ecosystem exchange, and precipitation are studied by using Simple Biosphere Model (SiB2 and SiB3) and the CSU GCM. Better understanding of the storage and transportation of water in the soil and its effects on the fluxes of CO_2 and energy are detected. More realizable models, which include new parameterization and new structure of soil layers, are explored.

Chapter 2

Methods

The arrangement of this chapter is as follows. In the model description section (section 2.1), general information of CSU BUGS is introduced (section 2.1.1). The Simple Biosphere model is then introduced and discussed with a focus on the simulation of photosynthesis and transpiration processes, both of which are crucial to the mass and energy exchange between land-surface and atmosphere (section 2.1.2). Then, the recently developed version of SiB, named SiB3, is introduced in section 2.1.3, which tries to eliminate the simulated severe drought stress in the Amazon Basin (see Chapter 3). Section 2.2 discusses the biology and climate features of the two sites as well as the observed methods. In the third section (Section 2.3), general information of data input and model simulation strategy are discussed.

2.1 Model Description

2.1.1 General Circulation Model (CSU GCM)

CSU GCM is an outgrowth of earlier work on the general circulation modeling performed at UCLA. AGCM introduces a more realistic parameterization compared to UCLA. This includes parameterization of solar and terrestrial radiation (Harshvardhan *et al.*, 1987), land and atmosphere interaction (Sellers *et al.*, 1986, 1987, 1992a, b, c, 1996a, b), as well as both convective and stratiform clouds (Fowler *et al.*, 1994). In addition, higher conservation is reached by using geodesic grids. The grid allows a longer time step, while incorporating an explicit PBL depth, with a modified sigma coordinate.

Recently, more and more attention has been focused on understanding land-atmosphere interactions as well as clouds and convection. The revised parameterization

of terrestrial and solar radiation by Harshvardhan *et al.* (1987) has improved the relevant model describing the interaction between land surface and atmosphere. Solar radiation parameterization includes Rayleigh scattering and absorption by water vapor and ozone, while terrestrial radiation includes radioactive flux divergence caused by water vapor, carbon dioxide, and ozone.

2.1.2 Introduction to Simple Biosphere Model

2.1.2.1 General information of Simple Biosphere Model

One limitation of the early GCM during the early 1980s was that it excluded a realistic parameterization of land-surface processes. The land surface process has an essential role in atmospheric circulation. In order to remedy this, a project was undertaken with Piers Sellers and other scientists that ultimately led to the development of SiB, the Simple Biosphere Model, which has been very influential in the land-surface modeling arena.

Several reasons can be proposed for the popular attention of land-atmosphere interaction compared to sea-atmosphere interaction: 1) the land surface fluxes are influenced by a large number of parameters. These include soil temperature, soil moisture, and many other parameters, whereas the ocean surface fluxes mainly depend on one ocean variable, namely sea surface temperature (SST). 2) In contrast to SST, land surface moisture shows steep gradients on both the regional and subgrid scales due to the presence of orography, the variety of the physiography, and the heterogeneous distribution of soil moisture and snow. 3) The land surface shows a strong diurnal cycle and day-to-day variability, while SST evolves relatively slowly into the atmosphere (Douville, 2003).

Simple Biosphere Model, developed by Sellers *et al*. (1986), is a simple yet realistic model that is used to calculate the transfer of energy, mass, and momentum between the atmosphere and the vegetated surface of the earth. It provides the General Circulation Model (GCM) with methods to determine the flux of radiation, water vapor, sensible heat, latent heat flux, and momentum across the lower boundary of the atmosphere in order to simulate the general circulation of the atmosphere.

A two-layer model is utilized in SiB to represent the morphology of different types of vegetation (Sellers *et al.*, 1986). The vegetation layers are classified into two layers: an upper layer and a lower layer, based on their species. The upper layer of vegetation includes the perennial canopy of trees or shrubs, while the annual ground cover of grass and other herbaceous vegetation are represented in the lower layer. From a local point of view, the distribution of the vegetation may be fractional, the individual vegetation elements are treated as evenly spaced and their roots are regarded as being uniformly distributed throughout the GCM's grid area. The depth and density of the root systems determines the amount of soil moisture available for evaportranspiration. The physical and physiological properties of the vegetation, such as the Leaf Area Index (LAI) are taken into accounts as well as canopy temperature and root depth when determining the flux of radiation, water vapor, sensible heat, latent heat flux and momentum between the vegetated surface and the atmosphere. In Sellers *et al.*1996a and b, this two layer vegetation canopy structure was then reduced to one layer (see section 2.1.2.2).

2.1.2.2 The Simple Biosphere Model (SiB2)

Spittlehouse and Black (1981), Sellers and Lockwell (1981) proposed that the energy and water balance of a region can be highly dependent on its physiology, which determines the transpiration rate. The energy and water balance of a region is also dependent on the region's morphology, which controls the interaction loss rate of precipitation. Goudriaan (1977), Otterman (1981) and Kimes (1984) stated that vegetation structures also have a significant influence on radiation absorption by trapping

light in multiple reflections of the plant elements Therefore, radiation absorption is attributed to the following factors: 1) the spectral reflection of multiple leaves, 2) the biophysical control of evapotranspiration by a plant's metabolism that is based on the photosynthetic reaction, 3) momentum transfer as a result of the vegetation canopy's roughness and porous surfaces, 4) soil moisture availability determined by the depth and density of the vegetation root systems, and 5) insulation, which is related to the dense vegetation canopy are all factors treated as key elements when modeling the interaction between land surface and atmosphere.

The surface fluxes of sensible and latent heat were determined using the Simple Biosphere (SiB) parameterization developed by Sellers *et al.* (1986). Then in the mid 1990's, SiB underwent substantial modifications (Seller *et al.*, 1996a, b; Randall *et al.*, 1996), and is now referred to as SiB2. In comparison to its first version the improvement can be summarized as follows:

(1) The incorporation of a realistic canopy photosynthesis-conductance model in order to describe the simultaneous transfer of CO_2 and water vapor into and out of vegetation respectively.

(2) The number of biome-specific parameters has been reduced, and most are derived directly from processed satellite data rather than prescribed from the literature.

(3) Modification of the hydrological submodel to give a better description of base flows and a more reliable calculation of interlayer exchanges within the soil profiles.

(4) Incorporation of a "patchy" snowmelt treatment, which prevents rapid thermal and surface reflectance transitions when area-averaged snow cover is low and decreasing.

(5) The original two layer vegetation canopy structure of the original SiB has been reduced to a single layer SiB2.

In the original version of SiB, seven prognostic physical-state variables were prescribed. These variables are related to the physical and physiological properties of the vegetation and included canopy and ground cover temperature; canopy and ground cover

water stores as well as soil moisture stores related to vegetation root systems, hydraulic diffusion and gravitational drainage (Sellers *et al.*, 1986). However, in SiB2, the second vegetation layer (ground cover) has been moved, but the model otherwise has a similar structure to that shown in figure 2.1. The other substantial modification to the model is the calculation of stomatal and canopy conductance which will be discussed later.

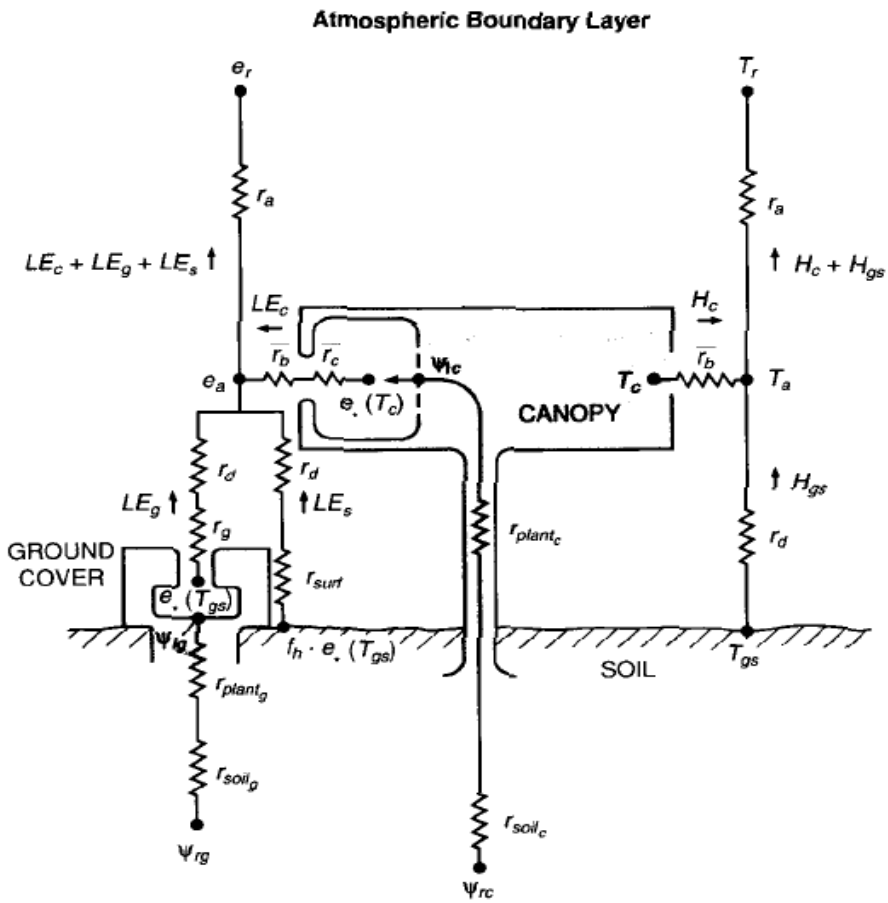

Figure 2.1: Structure of the SiB model after Sellers *et al.* (1986). Fluxes are indicated by arrows (H is sensible heat flux and LE is latent heat flux) and are calculated as gradient of the scalar quantities (T for temperature, e for vapor pressure, y for water potential) divided by empirically defined resistances r.

The important concept of "Biomes" has been pointed out in SiB2 to describe the vegetation cover type. Nine cover types are defined in SiB2 by combining or redefining twelve vegetation cover types of the earlier version of SiB (*cf.* Dorman and Sellers, 1989;

see table 2.1). Vegetation cover type is an essential concept for the model because it impacts the soil energy budget (evaporation, sensible heat flux and ground heat flux). Since the soil under a dense vegetation canopy intercepts less radiation and may be aerodynamically shelled, the energy available to the covered soil is small, and the component terms of the soil energy budget are correspondingly reduced (Denning, 1994). In the SiB3 model, which will be discussed in section 2.1.3, the classification of vegetation cover type continues to be employed.

Table 2.1 Biome types used in SiB2 and SiB3

	SiB2
Type	Name
1	Broadleaf evergreen trees
2	Broadleaf deciduous trees
3	Broadleaf and needle leaf trees
4	Needel leaf evergreen trees
5	Needel leaf-deciduous trees
6	Short vegetation/C4 grassland
7	Broadleaf shrubs with bare oil
8	Tundra
9	Cultivation/C3 grassland

Vegetative canopies also take an important role in determining the soil energy budget and boundary conditions, first by influencing the water reception of soil, and then through selective radiation absorption (see section 1.3). Vegetative canopies can intercept atmospheric precipitation and can also store the equivalent of several mm of water on the leaf surface. The evaporation of the intercepted water reduces the precipitation that the soil absorbs, which will reduce the soil moisture in the water reservoir. Then, in contrast to bare ground, which exhibits a gradual increase in reflectivity with wavelength over the interval of 0.4-4.0 micrometers, vegetative canopies can absorb photosynthetically active radiation (PAR), in the wavelength interval 0.4-0.72 micrometers and reflect moderately in the near-infrared region 0.72-4.0 micrometers. Direct-beam components as well as diffuse components are two streams of incoming short wave radiation. These are used to determine the surface albedo and the radiation absorption by the canopy and the surface, as functions of spectral properties and angular orientation of the stems and leaves.

Stomatal conductance is predicted in the CSU GCM by a new method, which includes the explicit treatment of the carbon assimilation rate by photosynthesis (Collate *et al.*, 1991, Collate *et al.*, 1992; Sellers *et al.*, 1992a, b; Sellers *et al.*, 1996a). As discussed in section 1.2, the stomatal regulatory mechanism takes an optimization role, such that it makes plants seek to maximize their ability to absorb atmospheric CO_2 and at the same time minimizes water loss from the soil. Therefore, since both are based on the stomatal regulatory mechanism, the uptake of CO_2 by plants and water loss from the soil layers are calculated together following Farquhar *el at.*, (1980) and Berry and Farquhar (1978). The C_3 photosynthesis model of Farquhar *et al.* (1980), as expanded on by Collats *et al*., (1991) and others, the C_4 model of Collatz *el al.* (1992) (see figure 2.2), and the stomatal model of Ball (1988) are the basis for the leaf photosynthesis-conductance model used in SiB2. In SiB2 model, photosynthesis and conductance are explicitly connected (see figure 2.2), following the models of Collatz *et al.* (1991, and 1992). For a complete description of the model refer to Seller *et al.* (1996).

The principle motivation for formulating SiB2 was to provide more realistic estimates of sensible heat and latent heat fluxes over continents. An extra set of variables for CO_2 concentration have been added to the stomatal conductance model: CO_2 concentration in the interior of the plant (C_i), CO_2 concentration at the leaf surface inside the laminar leaf boundary layer (C_s), and CO_2 concentration outside the leaf boundary layer in the canopy air space (C_a). The mass and energy fluxes, including fluxes of water vapor, sensible heat flux, and CO_2 are expressed in the equations as difference in potentials divided by resistance. The sensible heat flux, H is:

$$H = \frac{T_s - T_a}{r_b} = g_b (T_s - T_a) \tag{2.1}$$

where T_s and T_a represent the temperature at the leaf surface and in the atmosphere respectively. r_b is the leaf boundary layer resistance, which is equal to the reciprocal of the leaf boundary layer conductance g_b. Similarly, water vapor flux is given as:

$$E = g_s(H_i - H_s) = g_s(H_s - H_a) \tag{2.2}$$

where H_i, H_s and H_a are water vapor concentration (%), which is the proportional water vapor pressure to the saturated water vapor pressure e_i , e_s and e_a. H_i, H_s, H_a represents vapor concentration in the leaf interior, at the leaf surface and in the canopy air space respectively. The water vapor in the leaf interior is assumed to be saturated in the model, so that H_s / H_i is equal to h_s, which is the relative humidity at the leaf surface. g_s represents stomatal conductance.

Net Ecosystem Exchange is a way to express the net exchange of CO_2 between land-surface and atmosphere. NEE can be calculated as follows:

$$NPP = GPP - R_a \tag{2.3a}$$

$$NEP = NPP - R_h \tag{2.3b}$$

$$NEE = -NEP \tag{2.3c}$$

where NPP, GPP, NEP represent net primary production, gross primary production and net ecosystem production in the ecosystem respectively; R_a and R_h are autotrophic and heterotrophic respiration. NEE is calculated as the difference of GPP and respiration in SiB2 (see equation 2.5). GPP is the diffusive flow of CO_2 into the stomata, which is referred to as net assimilation A_n and is expressed as follows:

$$A_n = \frac{g_s}{1.6}\frac{C_i - C_s}{p_s} = \frac{g_b}{1.4}\frac{C_s - C_a}{p_s} \tag{2.4}$$

where p_s is the surface pressure in Pa. The constant factor of 1.4 and 1.6 account for the difference between molecular diffusive CO_2 and water vapor in the leaf boundary layer and the stomatal pores, respectively. A_n is expressed in mol $m^{-2}s^{-1}$. The pressure of CO_2

in the canopy air space is assumed to be a uniform constant of 355 *ppm* times p_s. Through the equation (2.5), which is derived from (2.4), the concentration of CO_2 in the leaf interior can be gained:

$$C_i = C_s - \frac{1.6A_n}{g_s} p_s \quad . \tag{2.5}$$

Respiration is an inverse process of photosynthesis except that it does not need Chlorophyll (section 1.2). It is determined by the total net assimilation for a specific year. The difference between respiration and net assimilation is referred to as the net ecosystem exchange, which is treated as conservation for a specific year so that net assimilation is equal to respiration. Respiration depends on soil scale and respiration factors in the SiB model. Formula (2.6) and (2.7) demonstrate the relationship:

$$R = \sum_{1yr} \sum_{i} \sum_{i} ss(i) \bullet Rf(i) = A_n \tag{2.6}$$

$$Rf = \frac{A_n}{\sum_{1year} ss} \tag{2.7}$$

where Rf is the respiration factor as unit A_n (mol $m^{-2}s^{-1}$), ss represents soil scale and is determined by soil temperature and soil moisture for each layer. i counts the number of soil layers. There is an optimum soil moisture value for respiration. When the soil moisture is below this optimum value, respiration increases with soil moisture; whereas when soil moisture is beyond this certain value, respiration drops as soil moisture increases. However, respiration always increases with soil temperature exponentially.

The critical equation that relates stomatal conductance, photosynthesis and transpiration processes is as follows:

$$g_s = m\frac{A_n}{C_s}h_s P + b \qquad . \qquad (2.8)$$

The intercept b in the equation represents the resistance when the stomata are completely closed, named the cuticle resistance, which is derived from observation with the value equal to 0.01 μmol $m^{-2}s^{-1}$ for C_3 and 0.04 μmol $m^{-2}s^{-1}$ for C_4. The slope m is a non-dimensional empirical coefficient derived from observation that is equal to 9 for vegetation, 4 for C_3 plants and 6 for C_4 conifers. An iterative procedure is used in SiB2 to solve for g_s, A_n and C_s. By using the scheme that relaxes the new value of g_s toward the predicted equation (2.8), while using the old value of g_s to get A_n and C_s, g_s is updated as a prognostic variable in SiB2. Leaf conductance for the influx of CO_2 and the simulations efflux of water thus are linked through a simple dependence on relative humidity, CO_2 concentration, air pressure and two empirically vegetation-dependent constants m and b.

The photosynthesis-conductance model used in SiB2 is a considerable improvement compared with the empirical stomatal model applied in the original SiB model. Additionally, it requires much smaller sets of parameters. And one of the most important parameters in SiB2, FPAR (fraction of PAR absorbed by green vegetation canopy), can be derived from satellite data.

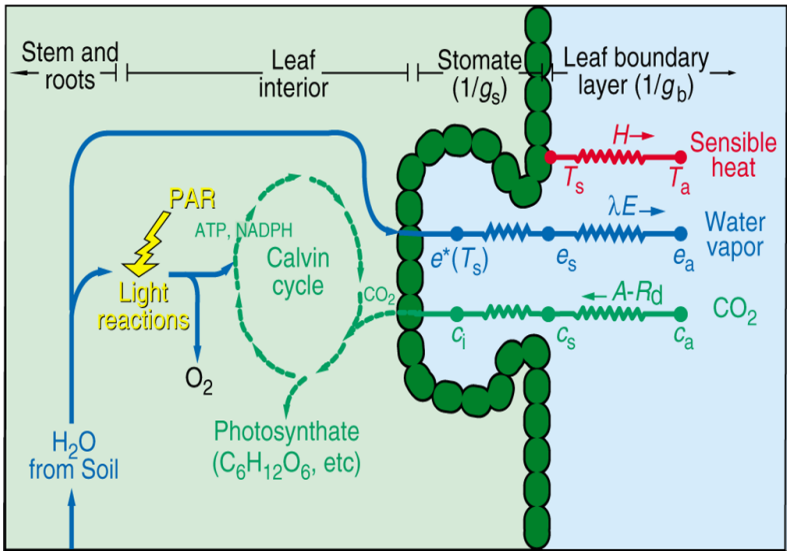

Figure 2.2: Details of stomatal structure in SiB2 described by Collatz *et al.* (1991) and illustrated by Sellers *et al.* (1992a).

Sellers *et al.* (1992a) expresses the net assimilation A_n and stomatal conductance g_s for the entire canopy as a closed-form which can be solved analytically by using Beer's Law for interception and absorption of PAR. Canopy PAR uses parameter Π, which is used to calculate the coupled photosynthesis and transpiration and can be expressed as follows (Sellers *et al.*, 1996b):

$$\Pi = \frac{\overline{FPAR}}{\bar{k}} = \frac{1-\exp(-\bar{k}LAI)}{\bar{k}} \tag{2.9}$$

in which $\bar{k}$ is the time-mean (radiation weighted) extinction coefficient for PAR. $\overline{FPAR}$ is a time-mean fraction of PAR absorbed by a green vegetation canopy. LAI is the leaf area index (leaf area per unit ground surface area). All these three quantities in this formula can be estimated from spectral vegetation indices (such as NDVI).

There exist four types of stress factors in SiB2: root zone water stress factor, humidity stress factor as well as high and low temperature stress. The experiments suggest the crucial role of drought stress is the influence on net ecosystem exchange and energy flux; therefore, I focus my attention only on the water stress factor in this study.

The root zone water stress results from the lack of moisture in the soil. Soil moisture potential is modeled as a power curve combined with a short parabolic section near saturation to represent gradual air entry by using a simple infiltration equation (Clapp *et al.*, 1978). The power curve representing the moisture characteristic is:

$$y = y_s W^{-b} \tag{2.10}$$

$$W = \frac{q}{q_s} \tag{2.11}$$

where y_s is soil tension at saturation and W is the soil wetness which is the volumetric fraction of saturation. q is the volumetric soil moisture fraction (m^3 of void space per m^3) and q_s is the saturated water content or the total porosity (m^3 of void space per m^3). The exponent b is an empirical coefficient based on soil type.

RSTFAC2 in SiB2 represents the water stress factor in the soil. The value of it decreases to zero under the condition of extremely strong stress and increases to one when enough water is available and no stress exists. It is multiplied by stomatal conductance to result in reduced photosynthesis and transpiration as drought stress increases. The relationship between root zone soil moisture and the water stress factor described in SiB2 can be explained in figure 2.3. Water stress increases abruptly as soil moisture drops down below 50%. It is calculated as follows (Sellers *et al.*, 1986, 1996a):

$$rstfac2 = \frac{1}{1 + \exp(b * (c + y))} \tag{2.12}$$

where c is equal to half the leaf critical water limit, which is from the boundary condition that represents the water potential at the 1/2 stress point. b and y are empirical constant and soil tension respectively. www2 in figure 2.3 represents the root zone water saturation(%) in SiB2.

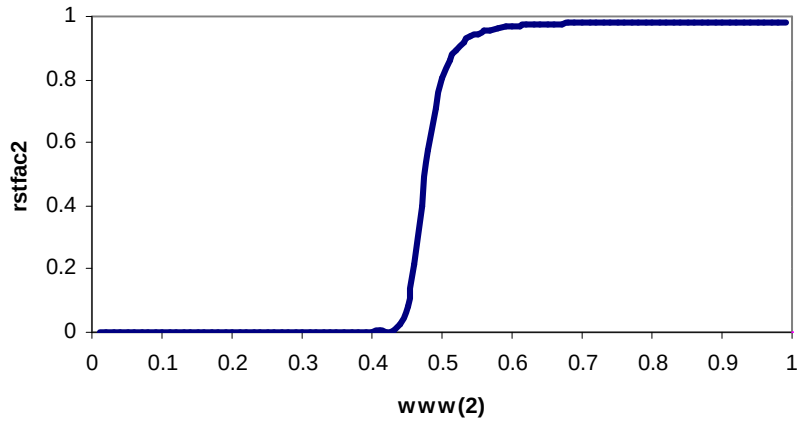

Figure2.3: SiB2 water stress parameterization

The disadvantages of using equation 2.12 in SiB2 are as follows: 1) it was developed to accommodate plant scale, but is being applied to ecosystems or even a GCM grid scale; 2) the equation is applied to a bulk root zone whereas in nature, both root density and soil moisture vary vertically. These inconsistencies may lead to the inaccurate simulation of water stress, which will be the focus of Chapter 3.

The ability to calculate coupled energy, water, and carbon fluxes throughout the continents with the use of plausible physiological models with suitable boundary conditions that can be derived from satellite data looks to have a promising future interpreting certain important earth-science problems.

2.1.3 SiB3

A revised model based on SiB2 has been developed in order to improve the accuracy of the description of energy and the water budget between land-surface and atmosphere. This new version of SiB is called SiB3.

There are five major improvements in SiB3 (see figure 2.4) compared to SiB2:

- The original three soil layer structure has been modified to 10 or 12 soil layer structure. With an increased number of soil layers and a revision of the soil's structure, the model is more favorable to water storage and is also a more realistic account of water transportation throughout the soil layers.
- Instead of a three-layer model in which roots are simply pooled into the second layer, SiB3 projects adjusted water extraction root profile throughout all the layers. The advantage of including root distribution analysis is that the model allows for a more realistic hydrological process in soil layers, especially vertical water transportation through soil layers.
- Plant available water (PAW) replaces root zone water to be used in the calculation of the water stress factor. This method is a simple but plausible way to deal with the entire plant-soil system (see section 3.3.3).
- Prognostic temperature, water vapor, CO_2, heat and water fluxes are introduced in "canopy air space".
- Snow structure and a multi-layer soil model based on CLM (Dai *et al*., 2001) is applied in the model, which is also a more realistic assessment of the soil's hydrological process.

As discussed in section 1.2, soil moisture is one of the significant parameters in land-atmosphere interaction. Soil moisture variability leads to a clear and wide variation in seasonal climate variability (Douville 2003). The lack of soil moisture causes drought stress, which will result in insufficient moisture supply to the plants stems and leaves. The important impact of drought stress on regional and global hydrological and climatic circulation has been discussed in Chapter 1.

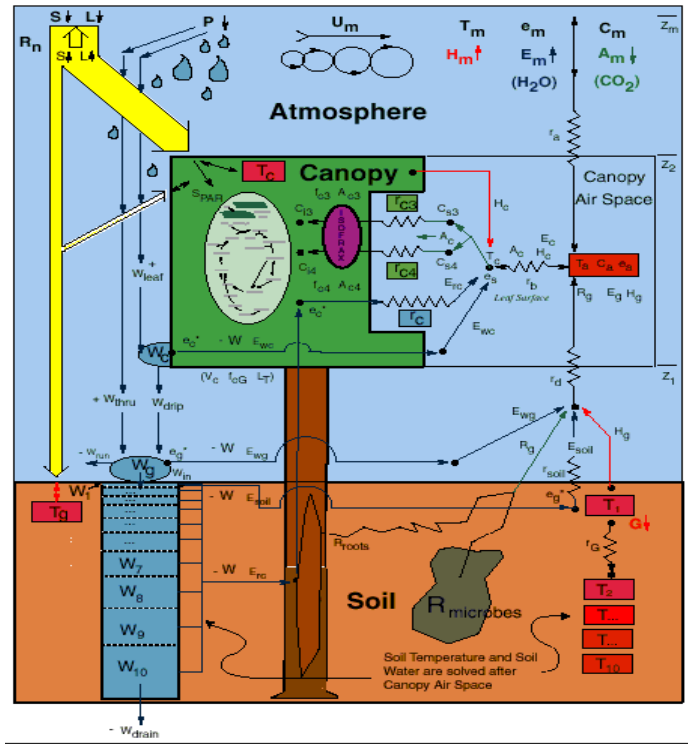

Figure 2.4: Structure of SiB3 model

Shukla and Mintz (1982) and others have demonstrated that changing even a small amount of available soil moisture may have a large feedback effect on the continental climate. In order to investigate the seasonal cycle of drought stress due to the lack of soil moisture, the Simple Biosphere Model (SiB) is used to simulate the interaction between the land-surface and the atmosphere in this study

Soil moisture is one of the significant elements in SiB and is influenced by many factors.

First, soil moisture is affected by natural precipitation in the atmosphere. Two elements of precipitation are described in the model: a convective component and a grid area component. The former presents the shower-type locally precipitation, which will run off much faster than the grid area precipitation, which is more uniform, and has larger scale. As discussed in section 2.1.2, the input of precipitation into the soil is influenced by vegetative canopies, which can be treated as indirect influential elements.

Second, the root distribution throughout the entire soil also makes impacts on variation of soil moisture. In the second version of SiB—SiB2, three-layer model is employed. The upper layer is the thin layer, where water evaporates into the boundary of the atmosphere directly once the pores of the soil are at or near saturation. The second layer is the root zone, where all roots of plants centralized in. These upper two layers of soil consisted of perennial plants with persistent roots assigned to a fixed depth taken to be the bottom of the second soil layer, and the ground cover is made of the annual vegetable that may have a time-varying root depth. Beneath the root zone, there is an underlying recharge layer, where the transfer of water is governed only by the gravitational drainage and hydraulic diffusion. In the higher version of SiB, ten-layer or twelve-layer models is employed based on the deep root fact in the tropical forest and plant roots are considered exponentially distributed throughout the whole soil layers.

Third, the variability of soil texture is one of the key elements that influence soil moisture. Soil texture is used to describe soil types by how much sand, silt and clay are present. The ability to hold water varies across the different types of soils. Sand is the largest particle in the soil and cannot hold water well; while clay is the smallest of particles. Clay is smooth when dry and sticky when wet. It retains water and doesn't allow much water go through it well. Silt is a soil particle whose size is between sand and clay, and its ability to hold water is between that of sand and clay.

2.2 Site description

2.2.1 Site locations

Tropical forests play a major role in determining the current atmospheric concentration of CO_2 as both sources of CO_2 following deforestation and sinks of CO_2 probably as a result of the simulation of forest photosynthesis (see section 1.3). The

studies of the interactions between CO_2 exchange, soil hydrology and precipitation in tropical forest areas hence have an influence on global climates models (Malhi, 2000).

As mentioned in section 1.3, the Amazonian vegetation cover change results in altered cycles of water, energy, carbon and nutrients, which have significant impact on local, regional, and global scales to both climate and environment. Therefore, research in Amazon Basin plays an important role in the study of the climate.

The study area of this project includes two tropical forest sites in the Amazon Basin, one is Tapajos with a latitude of 2.875ºS and a longitude of 54.959ºW, the other is Reserva Jaru（ 13.6S and 57.8W）, 11º south of Tapajos . Site locations are shown in figure 2.5.

Figure 2.5: the locations of Tapajos and Reserva Jaru

The Tapajos site is featured by a primary forest (at km 67 Santare-Cuiaba highway), and is one of the research areas in LBA (Large Scale Biosphere Experiment in Amazonia; section 1.3.5). The site receives 1920 mm year^{-1} on average of rainfall and has a 7-month

wet season (months with >100 mm of precipitation), representing the 25th to 30th percentile of each metric unit among Amazon forests (see Saleska *et al*., 2003). The mean annual temperature of this site is 27ºC.

The climate is favorable to the growth of evergreen plants with deep roots and the biotype of this region is broad leaf evergreen trees. Net ecosystem exchange (NEE) is measured by using eddy covariance methods simultaneously with fluxes of momentum, CO_2, H_2O, sensible heat, net radiation, PAR, atmospheric and soil profiles of temperature, CO_2 and H_2O, as well as wind profiles. All of which are also measured continuously using automated instruments on a 65km meter radio tower. Figure 2.6 shows the exact location of the km 67 tower.

Reserva Jaru shares similar biological characteristics and as well as a similar climate to Tapajos, but is featured by more notable dry season. It is a forest reserve owned by the Brazilian Environmental Protection Agency (IBAMA) and is located about 80 km north of Ji-Parana at 120 m above sea level. The mean height of the forest canopy is 33 m.

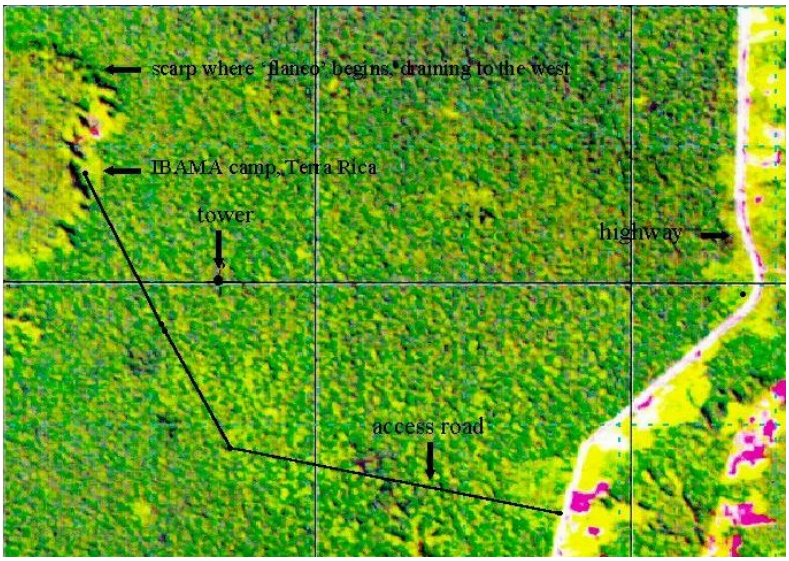

Figure 2.6: Location of the km 67 tower in Tapajos

According to the precipitation amount less or greater than 100 mm throughout the year, the climate in Tapajos and Reserva Jaru can be divided simply into wet and dry

seasons. But there are no obvious boundaries between the wet and dry seasons. In Tapajos, the period between July and November can be considered as the dry season (see figure 2.7a.), while in Reserva Jaru, the dry season is from April to August (see figure 2.7b, dataset are from Niall Hannan). The total precipitation for Tapajos was 1882mm in 2002, and the average rainfall of Reserva Jaru was 2228mm in 1993. Two different years are included in this study - 2002 for Tapajos 67km and 1993 for Reserva Jaru - both of which are considered as normal years for the sites.

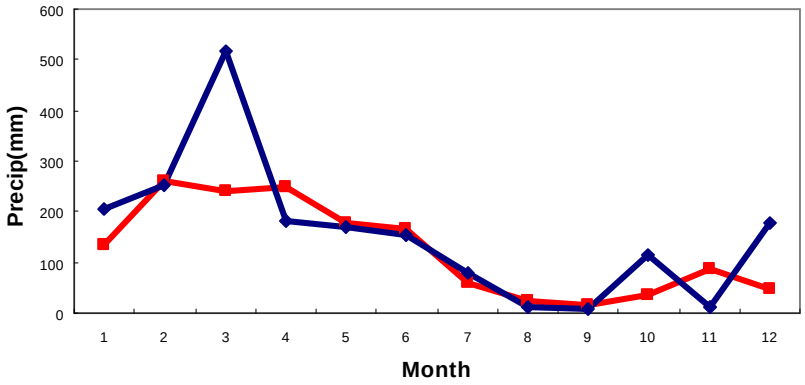

Figure 2.7a: 2002 Tapajos 67km precipitation. Red line is the observed data and blue line is NCEP reanalysis data. We use NCEP reanalysis data as meteorological driver data in the simulation

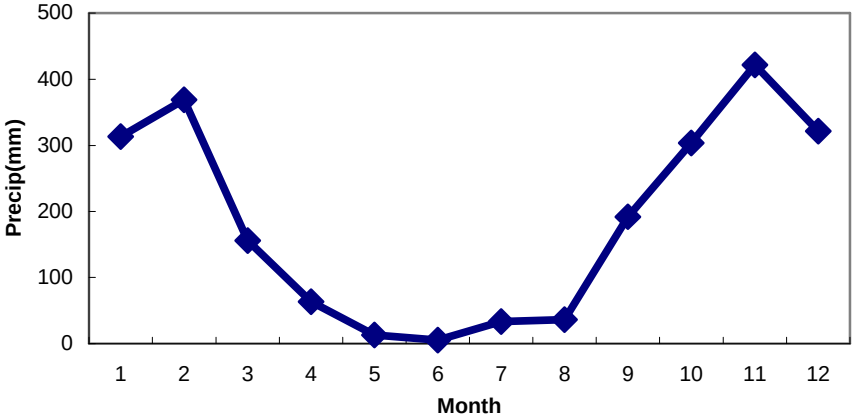

Figure 2.7b: 1993 Reserva Jaru observed precipitation

2.2.2 Methods of Measurement

For the Tapajos 67km site, three instruments have been employed in flux measurements since April of 2001: eddy-covariance instruments at 60m (above all trees), 45m (maximum height of emergent trees), and a profile system for measuring the through-forest CO_2 concentration profile. The arrows in figure 2.8 indicate the location of 60m and 45m eddy-covariance instruments.

Figure 2.8: LBA tower. The arrows show the locations of the instruments

The instrument systems are a new design for eddy-covariance measurements which consist of modular, largely self-contained units (approximately 1m×0.6m×0.2m). These house all key measurement and datalogging instrumentation. The instrument system has the advantages of a closed and an open path design. For example, the closed-path design contributes to the precise instrument calibration, while minimal air disturbance of the air sample before measurement is attributed to the open-path design. The units in the instruments are mounted on the tree directly, minimizing sample tube length (~2m in the case) between air sampling ports and the closed-path measurement device. This system is particularly suitable for the deployment in the very tall vegetation of a primary forest where very long sample-tubes from the top of the tower to a ground-based measurement device would be impractical.

For the Reserva Jaru site, the 52 m forest tower was installed and instrumented in October 1991 with an automatic weather station mounted at the top of the tower.

2. 3 Model Data Input Description

2. 3. 1 Variable and Parameters in SiB3

2. 3. 1. 1 Boundary Condition

Boundary conditions for the SiB2 model (Sellers *et al.*,1996a) characterize land surface conditions at a location using a combination of land cover types (Hansen *et al.*, 2000), a monthly maximum Normalized Difference Vegetation Index (NDVI) derived from Advanced Very High Resolution Radiometer (AVHRR) data (Teillet *et al.*, 2000), and soil properties (Soil Survey Staff 1994). Sellers *et al.* (1996a) describe the principle variables and parameters used in SiB as boundary conditions via loop-up tables. The variables and parameters include: (1) atmospheric boundary conditions, (2) time-invariant parameters, (3) time-varying parameters, (4) soil physical properties and (5) prognostic variables.

The boundary condition includes atmospheric boundary-layer temperature, vapor pressure, wind speed, partial pressure of CO_2 and O_2, and reference height, as well as incident solar radiation, incident thermal infrared radiation (diffusive only), convection, a large-scale precipitation rate, and atmospheric surface pressure.

Time invariant vegetation parameters are a set of constant value in the model. These parameters include morphological properties, optical properties, and the physiological properties of vegetation. In contrast, time-varying parameters change with time, and most of them are related to the properties of the canopy. These parameters involve FPAR

(fraction of incident radiation absorbed by green canopy), total LAI (leaf-area index), canopy greenness fraction and roughness length, canopy zero plane displacement, bulk boundary-layer resistance coefficient, ground to canopy air-space resistance coefficient, mean canopy extinction coefficient and canopy thermal infrared transmittance.

Soil physical properties include soil water potential at saturation, soil hydraulic conductivity at saturation, soil wetness and water content at saturation. Canopy temperature, soil surface temperature, deep soil temperature, canopy interception liquid water and snow-ice store, soil interception of liquid water and snow-ice store, surface soil wetness, root zone soil wetness, deep soil wetness, and canopy conductance to water vapor are elements of prognostics variables in the model.

In order to explore the importance of spatial resolution in the SiB simulation, tower flux data is used in the simulation of the Reserva Jaru site as meteorological driven data. In the studies of Tapajos 67km site, NCEP data with a 1x1 degree of resolution is applied.

2.3.1.2 Initial Conditions

Canopy temperature and soil temperature for different layers are taken from observation. The saturated soil moisture is used in the initial step to detect any abnormal processes that may occur in the simulation. The similar initial data for Tapajos 67km and Reserva Jaru are employed in the study. As an example, table 2.2 demonstrates the initial condition applied in SiB2 in 1993 at the Reserva Jaru site, there are three soil water layers and ten soil temperature layers.

In SiB3, the number of soil layers has been increased to 10 or 12 with 10-12 soil water and temperature layers. There are 5 surface snow/ice layers. Under the initial condition, the snow/ice in the surface layers are all set to be zero and saturation is also forced into the soil layers for the first step.

We are studying the development of drought stress in the model. Detailed progression of simulated soil and vegetation conditions depend on initial conditions which are not well known for the specific sites. Therefore, we initialize the model with completely saturated soil and run a 10-year initialization experiment in which a single year at driver weather was cycled repeatedly 10 times, and then results for the 11th year are analyzed.

Table 2.2: Example initial condition for SiB2

Parameters		Value
Canopy Temperature(ºK)		296.748
Ground Temperature(ºK)		297.251
Stomatal resistance $molm^{-2}s^{-1}$		901.727
TKE(w/m^-2)		1.0
Deep Soil Temperature(ºK)	Level 1	296.765
	Level 2	296.995
	Level 3	297.022
	Level 4	296.885
	Level 5	297.030
	Level 6	297.427
	Level 7	297. 828
Surface Water(%)	vegetation	0.000516
	ground	0.0500
Surface Snow/Ice(%)	vegetation	0.0
	ground	0.0
Liquid Water Content (%)	Layer1	1.0
	Layer2	1.0
	Layer 3	1.0

Chapter 3

Results and Discussions

As we have discussed in Chap 2, soil moisture plays an essential role in land-atmosphere energy exchange. Lack of soil moisture in the Amazon would cause a very strong drought stress, which would result in variations in evapotranspiration within the ecosystem that may effect regional precipitation and climate subsequently. The relationship between drought stress and the climate can be summarized as a positive feedback loop, as shown in figure 1.1. Variations in photosynthesis and respiration in tropical forests are strongly influenced by soil moisture, precipitation, runoff, infiltration, gravitational drainage, evaporation and transpiration (see section 1.3.1) and hence make impacts on the net ecosystem exchange of carbon dioxide. Ecosystem response to seasonal and interannual drought can help us test the ability of models that represent physiological stress in tropical forests.

In studies of two tropical forest sites – Tapojos 67km site and Reserva Jaru – the SiB2 simulation projects severe drought conditions in the Amazon Basin during the dry season which, when coupled with GCM (see fig 3.7) lead to carbon loss in the dry season(see figure 3.7). This is an unrealistic account of what is actually the case. The stress may be a result of over sensitivity to water saturation in the standard model (SiB2) since positive feedback with the atmosphere which could amplify the stress response. This may be due to the inaccurate model description of moisture storage and transportation of moisture through the soil layers. In the following research, I try to find the cause of the drought stress and the optimal solution for eliminating it by studying the soil moisture variability, net ecosystem exchange as well as energy fluxes in the local areas.

Several sensitivity experiments are performed in order to investigate the problem of the simulated sever drought stress. First, alternative parameterizations in SiB2 are explored, including a deeper root, new parameterization of stress factor and decreased precipitation

runoff. Second, a new multi-layer structure of soil along with adjusted water extraction root profile, PAW (plant available water), as well as prognostic temperature, water vapor, CO_2, heat and water fluxes in canopy air space, which is referred to as SiB3 (discussed in Section 2.1.3) are developed and calculated in the revised model.

3.1 Results from Original Version of SiB2

3.1.1 Net Ecosystem Exchange

Figure 3.1a shows the comparison of seasonal net ecosystem exchange (NEE) between Tapajos 67km and Reserva Jaru, in 1993. In contrast to the result from Saleska *et al.*, (2003) (see section 1.3.6; figure 1.5), simulated NEE in SiB2 indicates the release of CO_2 in the wet season and uptake of CO_2 in the dry season, consistent with the observed data.

Figure 3.1b and figure 3.1c demonstrate the comparison of the annual cycles of net photosynthesis and respiration between Tapajos 67km and Reserva Jaru in the year of 1993. Reserva Jaru is 11° south of the Tapjajos 67km site. In Tapajos 67km, photosynthesis stays almost constant throughout 1993 and respiration drops slightly from October to December. In contrast, not only respiration but also photosynthesis decreases drastically in the dry season, suggesting that drought stress plays an essential role in both processes. Instead of having an obvious seasonal cycle in Tapajos 67km site, NEE is more complicated in Reseva Jaru because of the release and uptake of CO_2 alternatively during the dry season. The simulation for Tapajos 67km is the work of Ian Baker.

As discussed in Chapter 1, photosynthesis is affected by radiation as well as soil moisture (see equation 1.1). In the dry season, the increase of radiation due to fewer clouds will make photosynthesis more active; however, at the same time, the lack of soil moisture will prevent photosynthesis. When the drought stress is strong enough to offset the impact of greater radiation and plays a dominant role in photosynthesis, the activity of

photosynthesis decreases. Photosynthesis drops to its minimum value in September, one month after respiration reaches its lowest level, suggesting that drought stress may have a lag effect on photosynthesis. Moreover, neither of them begin to decline after April, the beginning of the dry season (see figure 2.7b), indicating that the water reservoir takes an important role in keeping the normal soil hydrology. As soon as there is plenty of precipitation in September, photosynthesis and respiration begin to go up again. Photosynthesis goes back to the same level with that at the beginning of the year after November whereas respiration is 10% lower than the initial value. It may suggest that soil moisture contributes more to photosynthesis than it does to respiration.

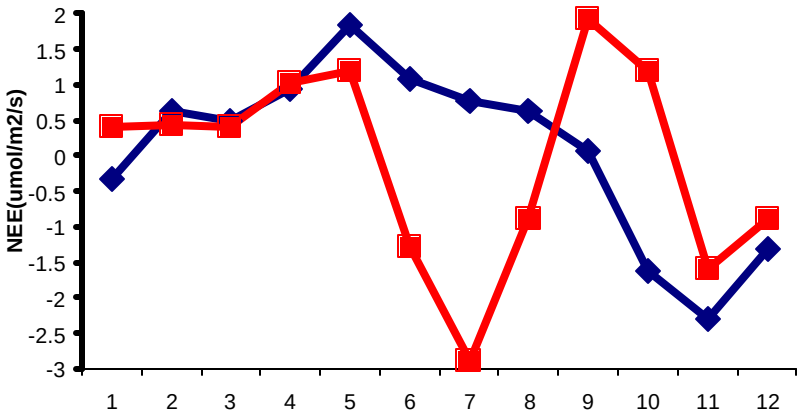

Figure 3.1a: SiB2: 1993 Comparison of net ecosystem exchange between Tapajos 67km site and Reserv Jaru. The red line and blue line represent simulated results in Resev Jaru and Tapajos 67km site respectively.

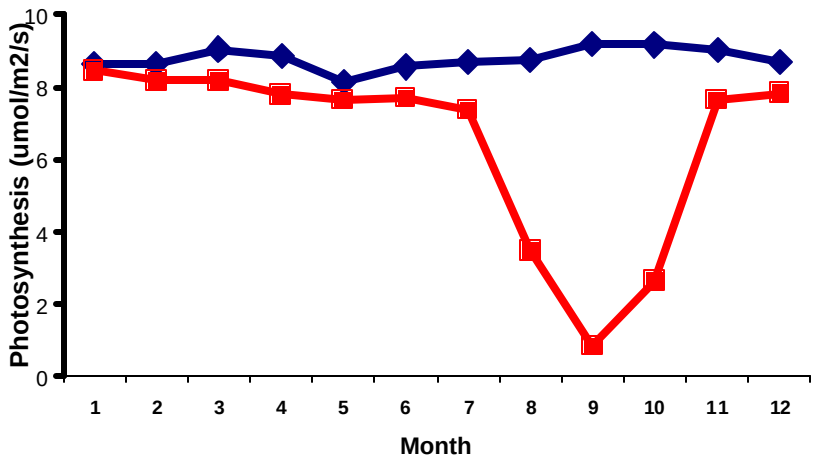

Figure 3.1b: SiB2: 1993 comparison of net photosynthesis between Tapajos 67km site and Reserv Jaru

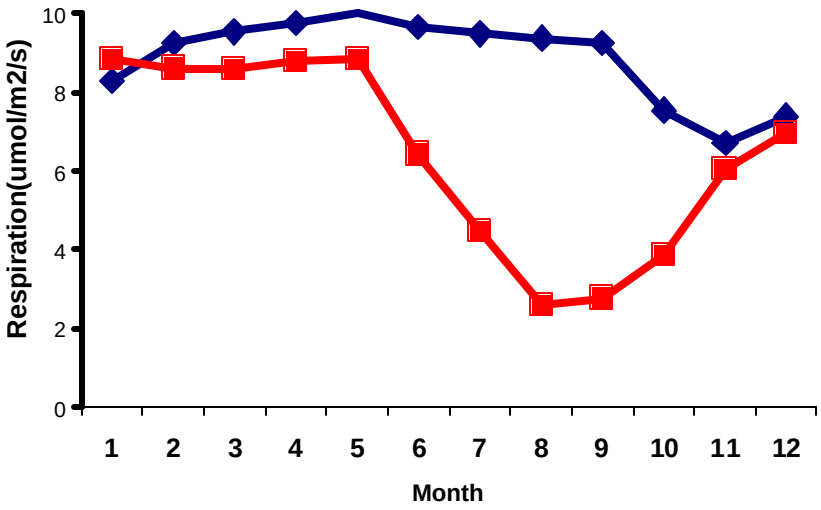

Figure 3.1c: SiB2: 1993 comparison of respiration between Tapajos 67km site and Reserv Jaru

3.1.2 Water Stress and Energy Budget

Latent heat flux, sensible heat flux and ground flux are three components of the energy budget, with the summation of them equal to net radiation in SiB2 (see equation 1.1). As discussed in section 2.1.2, they are related to evaporation and transpiration processes and

are key elements in the positive feedback between surface climate and precipitation (see section1.2). The study of the energy budget greatly contributes to understanding the abnormal drought stress simulated in the dry season.

Figure 3.2a compares the simulated and observed seasonal cycles of latent and sensible heat flux at Tapajos 67km site in the year of 2002. Observed latent heat flux increases slightly in the early dry season, then drops in November and December, with BR(see equation 1.3) less than one all the year (see figure 3.2a). The summation of latent and sensible heat flux is referred to as surface forcing (see equation 1.1). Simulated latent heat flux shows a response to the increasing surface force until September, and then BR goes up. Simulated latent heat flux decreases in the first two months of the year, showing the same trend in simulated sensible heat flux. After that, the variation of latent heat flux demonstrates an inverse trend compared to the sensible heat flux, decreasing with the increase of sensible heat flux, and vice versa (see figure 3.2a). The observed sensible heat shows good constancy throughout the whole year with slight increases after July and then decreases after September (see figure 3.2a). In the SiB2 simulation, sensible heat flux continues to increase from May to November when the weather becomes quite dry and decreases in December when precipitation increases (see figure 2.7a). It is obvious that latent heat flux has been underestimated in the SiB2 simulation while at the same time sensible heat flux has been overestimated.

Surface forcing is consistent with the observed value from March to September (see figure 3.2b). It is higher during the dry season when there are fewer clouds, and lower in the wet season. The simulation overestimates the surface forcing from January to February and from October to December. The simulated surface forcing exceed 145 w/m^2, whereas the observed value is around 130 w/m^2. This difference maybe due to the extremely low projected albedo in the SiB2 simulation.

The daily diurnal cycle of energy fluxes are shown in figure 3.2c. During the daytime, simulated latent heat flux is less than the observed value except for a few hours, whereas, observed sensible heat flux is greater than the simulated results. The maximum latent and

sensible heat flux appear at around 9o'clock in the morning, three hours before observation, corresponding to projected absorbed short wave radiation by the ground (see figure 3.2d). The reason why there are apparent differences between simulated and observed value may not only be related to the limitation of the model itself but also to error in observations as well.

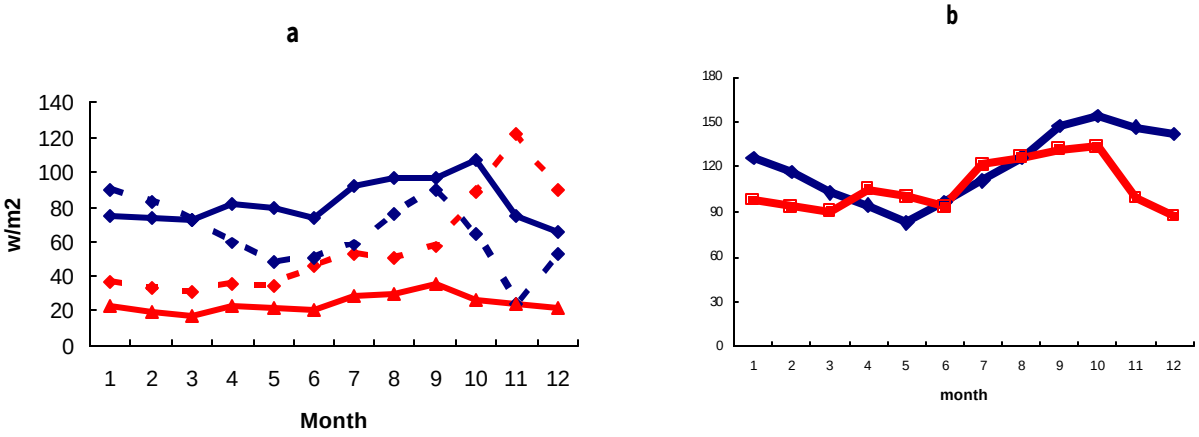

Figure 3.2: a: SiB2: 2002 Tapajos 67km energy flux. b: Surface forcing. Red lines are sensible heat flux and blues lines are latent heat flux. Solid and dashed lines represent observed and simulated data respectively.

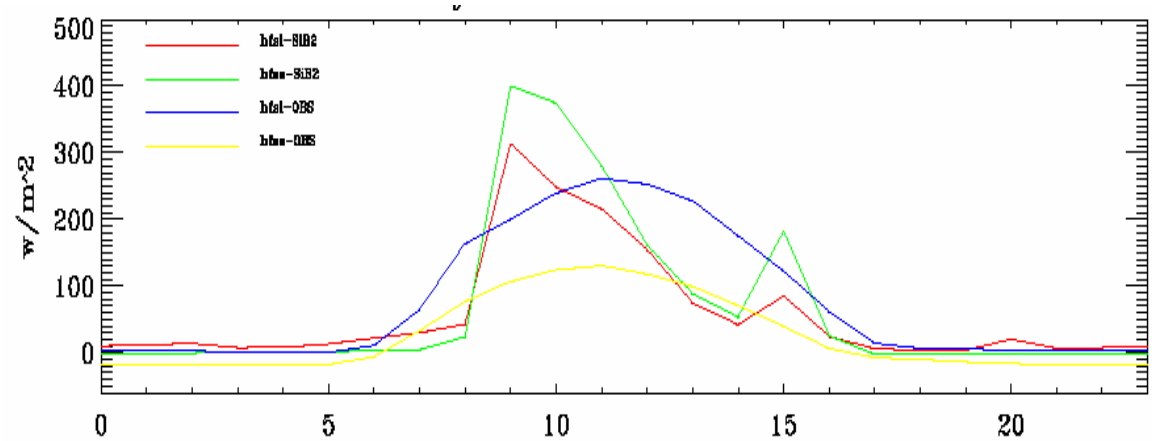

Figure 3.2 c: 2002 Tapajos 67km annual mean diurnal cycle of latent and sensible heat fluxes. Red and green lines are simulated latent and sensible heat fluxes respectively. Blue and yellow lines are latent and sensible heat fluxes from observed data. X-axis represents the number of hours.

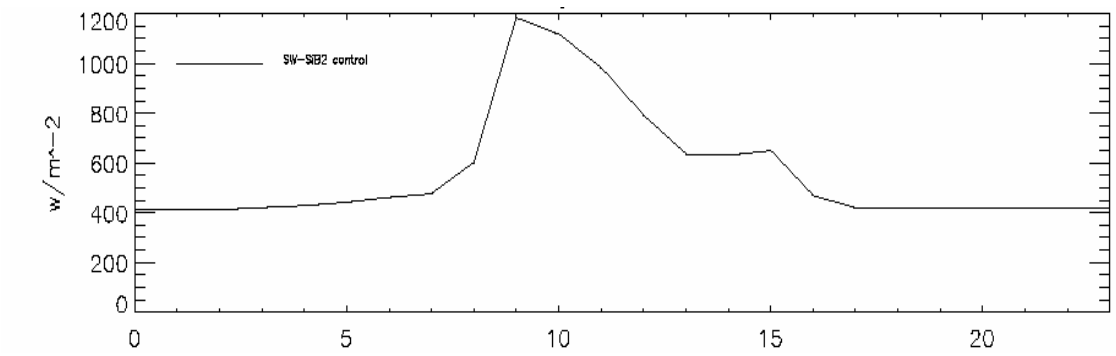

Figure 3.2 d: 2002 Tapajos 67km annual mean diurnal cycle of absorbed short wave radiation

Figure 3.3 shows the SiB2 simulated root zone water saturation and drought stress based on the curve in figure 2.3 (see equation 2.11). For Tapajos 67km site in the year of 2002, there is no water stress from March until August, when there is plenty of precipitation or plenty of moisture in the soil water reservoir (see figure 2.7a). Although precipitation starts to be less than 100mm after July and root zone water saturation begins to decrease correspondingly, severe water stress does not appear until October, indicating the important contribution of the soil water reservoir (see figure 3.3). The abrupt increase of drought stress from September to October shows the high sensitivity of drought stress to water saturation when soil moisture saturation is below 50% (see figure 2.3). It can be concluded that the severe drought stress from October to December (see figure 3.3) caused the reduction of latent sensible heat flux and the increase in sensible heat flux (see figure 3.2a).

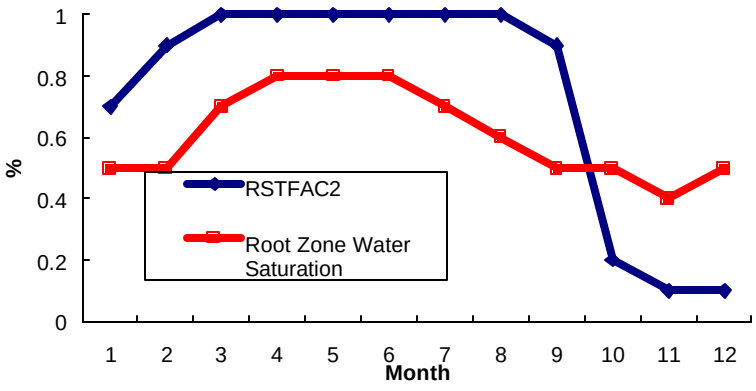

Figure 3.3: SiB2: 2002 Tapajos 67km water stress factor and root zone saturation

As the meteorological driver data are not available at Reserva Jaru in the year of 2002, I choose the year of 1993 as the research year. As shown in figure 3.4a, latent heat flux decreases from August through October and arrives at its minimum value in September, right after the last month of the dry season (see figure 2.7b) when drought stress is its most severe (see figure 3.5) and then goes back to the normal value when soil moisture is available and drought stress is alleviated in November (see figure 3.5). Correspondingly, sensible heat flux goes up when latent heat flux goes down, and vice versa. Surface forcing increases in the dry season due to lack of cloud cover.

The average daily diurnal cycle over 114 days (from April 4th to July 27th) of latent and sensible heat flux is demonstrated in figure 3.4b. Similar to the simulation in Tapajos 67km in the year of 2002, the latent heat flux is underestimated while sensible heat flux is overestimated in SiB2 compared to the observed data. Observed data is only available for 114 days in the dry season (from April 4th to July 27th) so that we cannot do the comparison between simulation results and observation throughout the entire year. Figure 3.4c and 3.4d show the comparison of daily mean energy fluxes between simulated results and observed data. The red line and blue lines represent observed and simulated data respectively. It can be seen that simulated latent heat flux is consistent with the observed data quit well, while simulated sensible heat flux is around 30% higher than observed data.

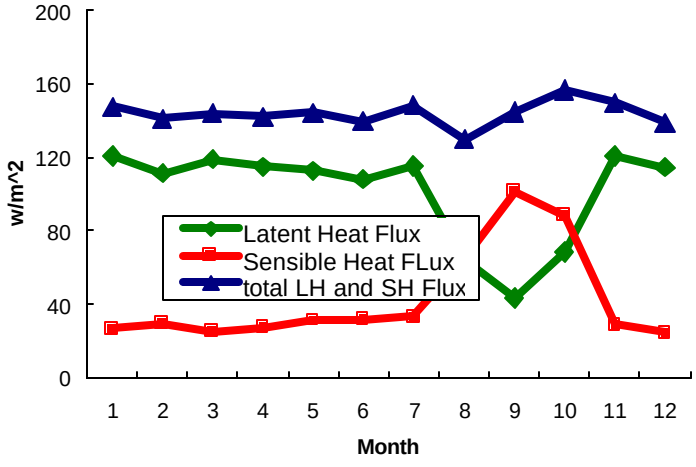

Figure 3.4 a: SiB2: 1993 Reserva Jaru energy flux

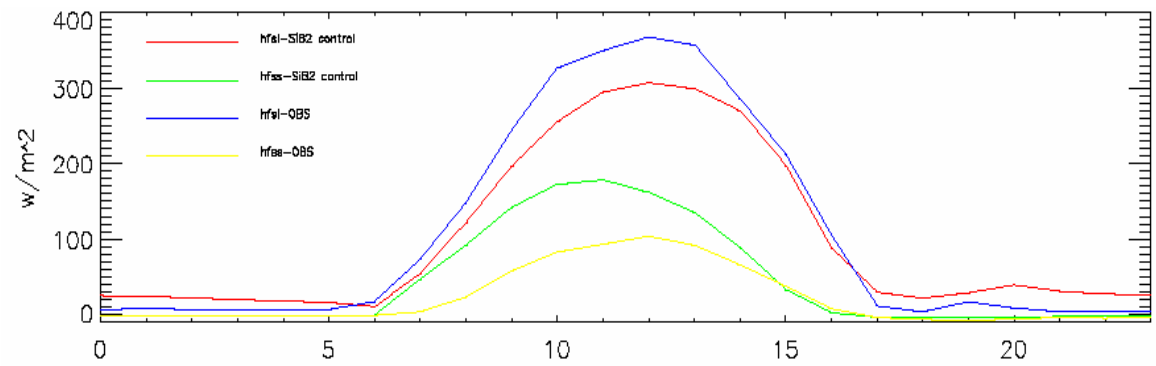

Figure 3.4 b: 1993 Reserva Jaru diurnal cycle of latent and sensible heat fluxes. Red and green lines are simulated latent and sensible heat fluxes respectively. Blue and yellow lines are latent and sensible heat fluxes averaged over 114 days (April 4th to June 27th) from observed data. X-axis represents the number of hours.

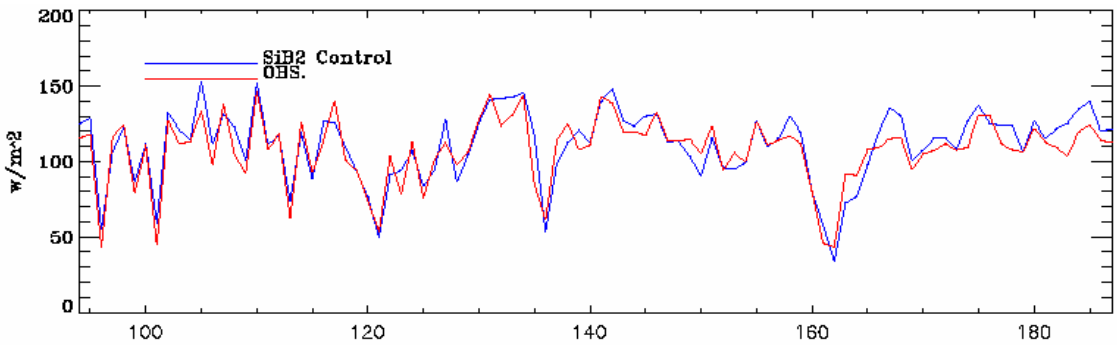

Figure 3.4 c: 2002 Tapajos 67 km daily mean of latent heat flux.

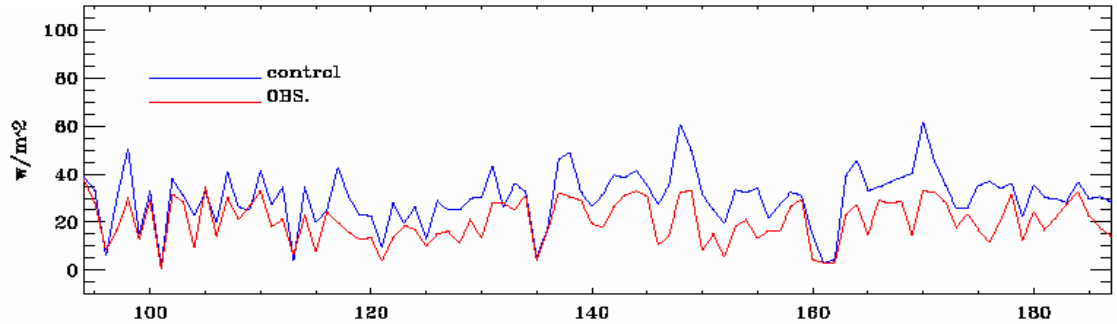

Figure 3.4 d: 2002 Tapajos 67 km daily mean of sensible heat flux.

Reserva Jaru is featured by more pronounced dry weather in the year 1993 (see figure 2.7b). Water stress increases abruptly in August and stays high until October. Instead of increasing at the beginning of the dry season, water stress does not become severe until

August even though the root zone water saturation begins to decline after April. This may be due to the relatively lower sensitivity of water stress to water saturation when soil moisture saturation is above 50%. This severe drought stress results in the collapse of photosynthesis (see figure 3.1b), reduction of latent heat flux and increase of sensible heat flux in the dry season (see figure 3.4a).

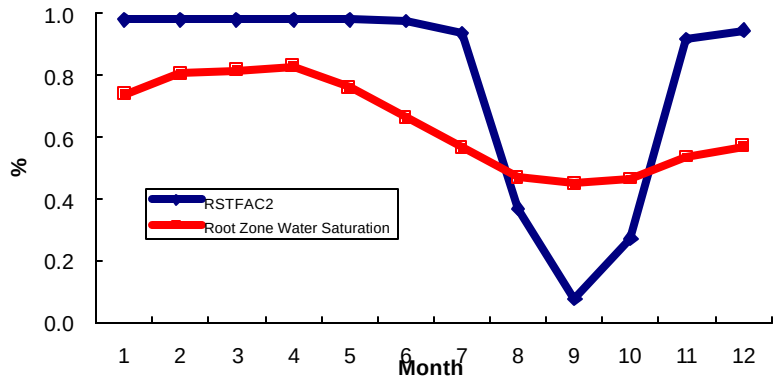

Figure 3.5: SiB2: Reserva Jaru water stress factor and root zone saturation

3.1.3 Coupled SiB2-GCM

As we have talked about in Chapter 2, SiB2 is coupled with GCM, playing an essential role to describe the mass and energy exchange between land-surface and atmosphere. In the simulation, an initial condition is modified from a previous run by setting all tropical forest soils to 100% saturation. Furthermore, climatologically SSTs are used, indicating the normal year simulation.

Three years of coupled SiB2-GCM models demonstrate the positive feedback loop interaction between precipitation and ecosystem stress (see figure 3.6). When there is less precipitation in the atmosphere, soil moisture decreases, and lack of soil moisture will lead to drought stress. Severe drought stress suppresses transpiration. As a result, there is less latent heat flux while more sensible heat is released due to lack of transpiration, which consequently results in the dry and hot boundary layer. The dry and hot boundary layer is not favorable to atmospheric precipitation. The positive feedback loop is then established.

Figure 3.7a and 3.7b show the results of a 3-year coupled simulation of SiB2 –GCM. Positive feedback can be seen clearly from the results. With less precipitation, soil moisture stress in the root zone goes up from zero to extremely high, less than 2%. Latent heat flux decreases and sensible heat flux increases correspondingly to the total latent and sensible heat stabilize around 140w/m2. The latent heat flux during the third year is almost half of that at the beginning of the year, while the sensible heat flux increases almost ten times, which is a result of the abnormal drought stress. The thickness of PBL increases 46*mb* to 58*mb* with the maximum depth of 64*mb*. The increase of PBL potential temperature is around 5.5 ^{o}K. The extremely high value of both PBL depth and the potential temperature is consistent with the amount of precipitation, root zone soil moisture stress factor, as well as sensible and latent heat flux.

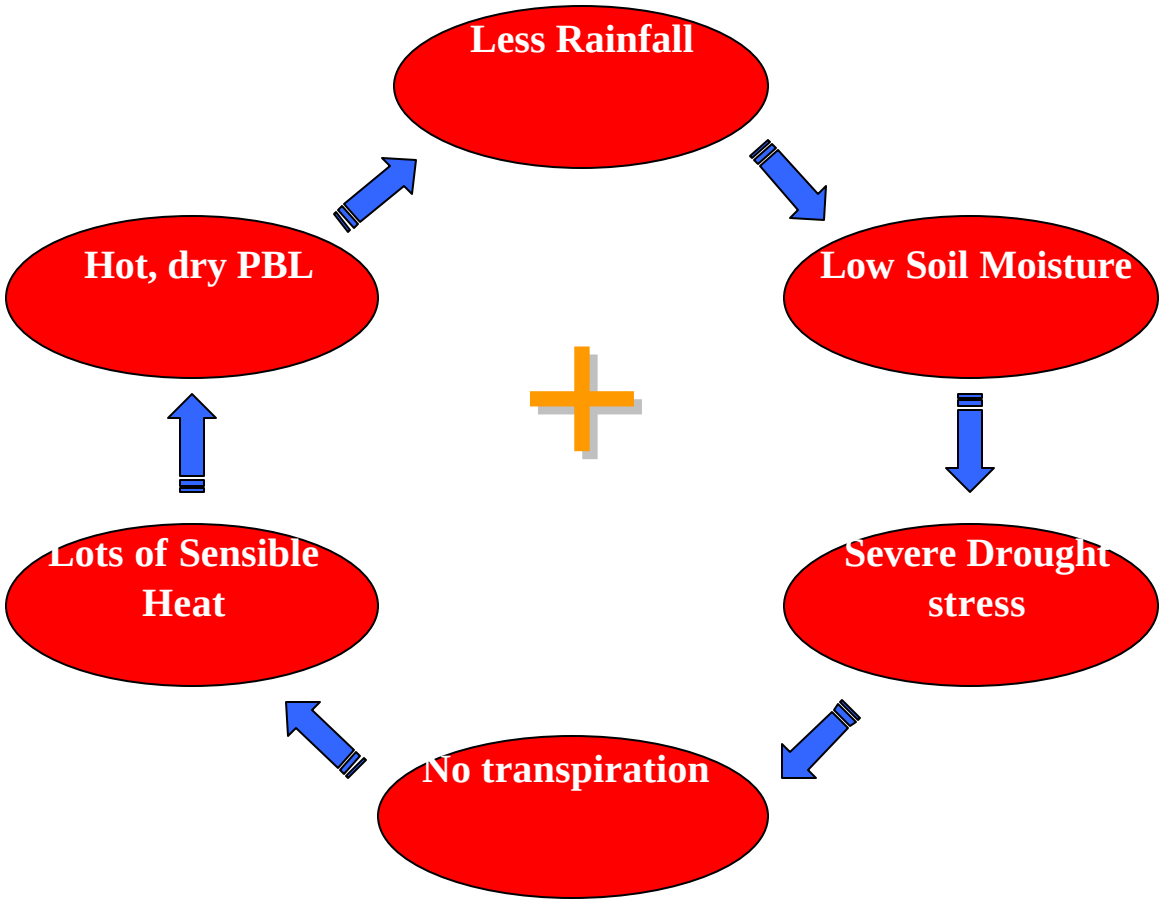

Figure 3.6: Positive feedback loop of precipitation and ecosystem stress

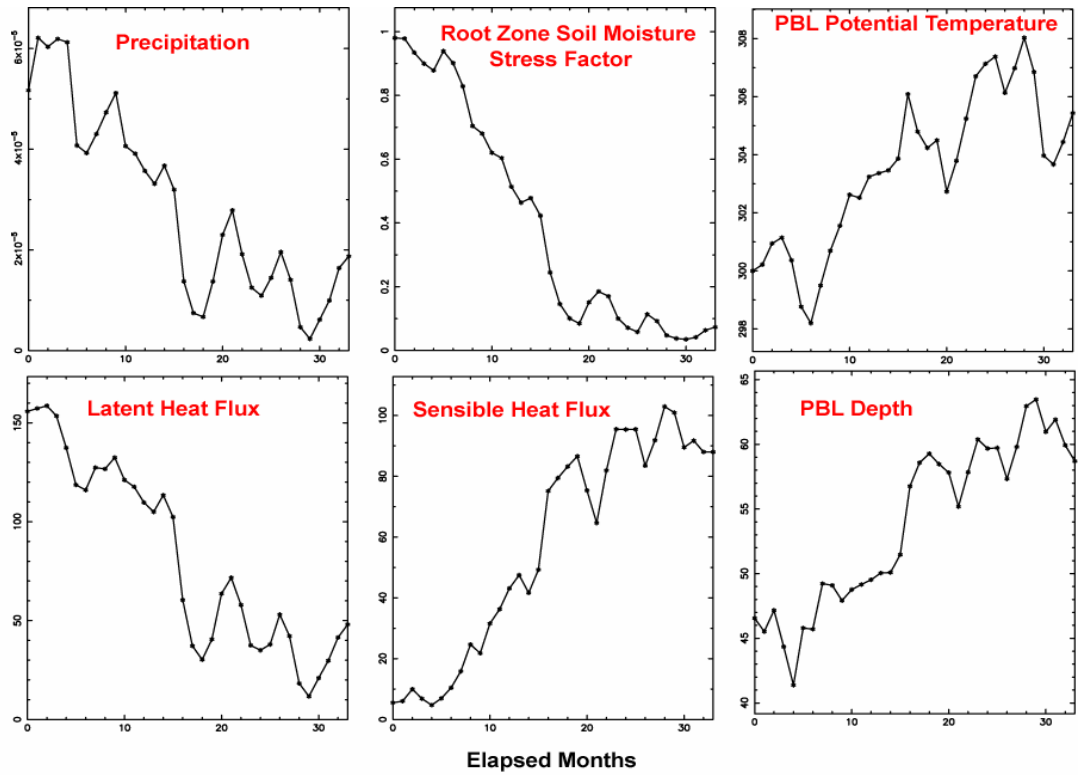

Figure 3.7a: 3-year coupled simulation: SiB2-GCM. The units are as follows: meters for precipitation, % for root zone moisture stress factor, ^{o}K for PBL potential temperature, w/m^{2} for latent and sensible heat flux and *mb* for PBL depth.

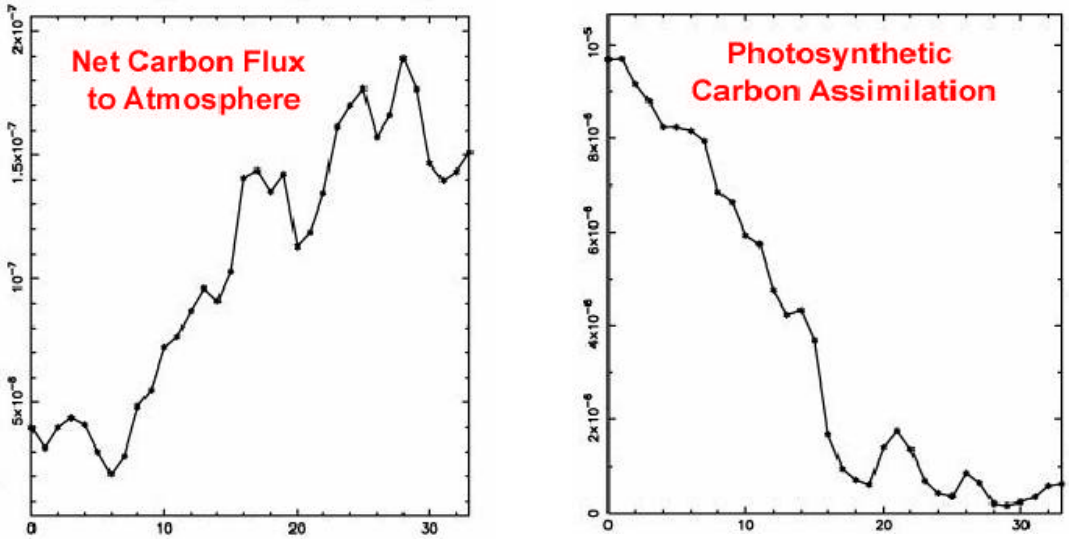

Figure 3.7b: 3-year coupled aimulation: SiB2-GCM. The units of photosynthetic carbon assimilation and net carbon flux to the atmosphere are mol/m/sec.

Photosynthesis starts to drop at the beginning of the simulation and then collapses during the third year. The forests cannot stay alive if photosynthesis collapses. Clearly, this simulation is not compatible with the observed climate of the Amazon.

Therefore, it may be concluded that the positive feedback loop of precipitation and drought stress is exaggerated in the coupled model.

3. 2 Alternative Parameterization of Drought Stress

In order to solve the unrealistic drought stress problem in the Amazon Basin, alternative parameterization experiments, including the effect of deep root, a new algorithm to calculate root zone drought stress, and less run-off precipitation, are explored in the following study. Reserva Jaru is chosen as the simulation site since it has a more notable dry season throughout the year and can be representative of other sites.

3.2.1 Effects of Deep Root

The biome type defined in SiB2 for the tropical forest is broadleaf evergreen trees (see section 2.1.2). Broadleaf evergreens are plants that will keep their foliage throughout the year including the dry season, instead of shedding it in the fall. Unlike deciduous plants, evergreen trees tend to have "fibrous" roots with numerous small roots that reach deep into the ground (Galetta Nurseries 2000). A root structure such as this enables the trees to absorb water from the deeper soil layers and a large amount of water is crucial to keep the trees alive. I hypothesize that deeper root zone storage could mitigate seasonal drought stress (Nepstad *et al.*, 1994; Saleska *et al.*, 2003) in this experiment.

Deep roots can reach more than ten meters into the soil layers, and thus are propitious to the extraction of stored water. Therefore, the root zone thickness is increased to 10m from the original thickness of 1.5m and the underlying recharge zone thickness to 5m from

2m in the SiB2 deep root simulation experiment. Boundary conditions, except for the root thickness and meteorological driver data are the same as those in the control experiment and the model scheme stays unchanged once I initialize the model with completely saturated soil and then run a 10-year initialization experiment in which a single year of driver weather was cycled repeatedly ten times. The results of the 11th year are then analyzed (see section2.3.2). Unfortunately, the simulation gives us even worse results than the original model (see figure 3.8 to 3.14).

The soil moisture saturation in the root zone stays at around 45% from the beginning of the year without any significant difference between the wet and dry season. Correspondingly, instead of increasing in the dry season and decreasing in the wet season, severe drought stress is persistent throughout the whole year without any significant seasonal cycle even after a 10-year spin-up from the initial saturated condition (see figure 3.8-3.9).

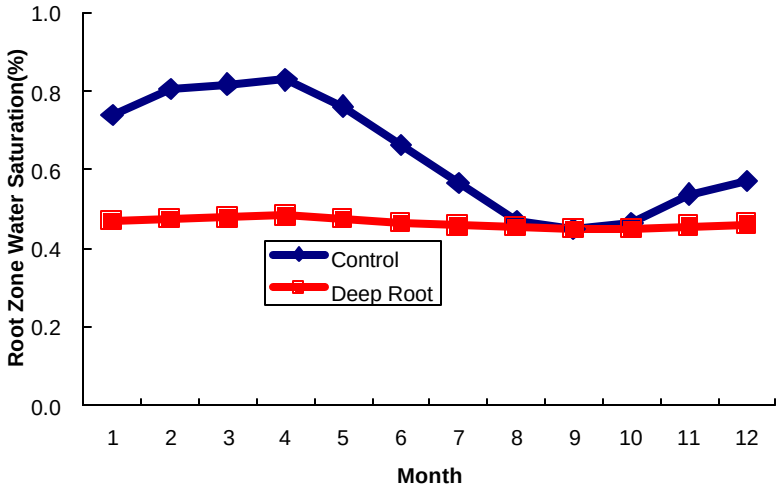

Figure 3.8: SiB2: 1993 Reserva Jaru root zone water saturation in deep root experiment

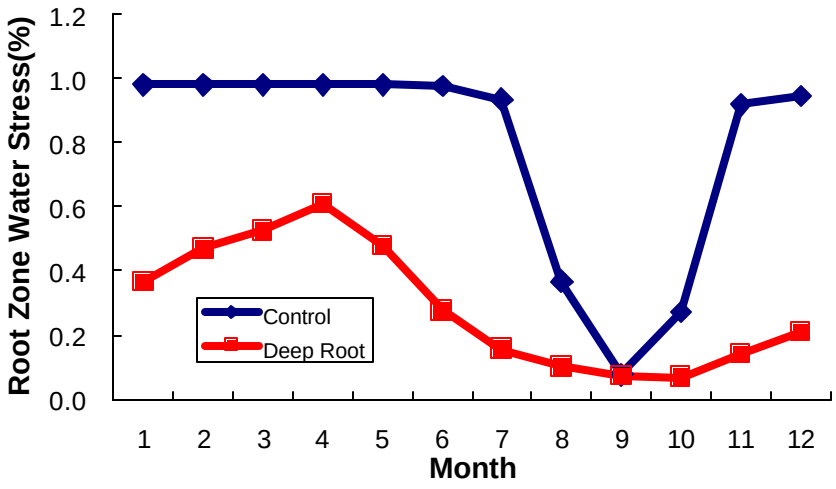

Figure 3.9: SiB2: 1993 Reserva Jaru root zone water stress in deep root experiment

The reason why root zone water saturation remains so low is because the same amount of annually available water is "spread out" through a greater volume of root zone pore space in the deep root experiment. The porosity is the saturation moisture content of the soil matrix such that the entire soil porosity is saturated with water, (%v), and dependant only on the soil texture and is unaffected by salinity or gravel. For deep roots, the porosity of the soil in the root zone is about 45%, which means the total saturation percentage can not be above 45% (see figure 3.32). Therefore, root zone saturation does not exceed 45%.

A surprising consequence of deep root is that the seasonal cycle of simulated NEE reverses its signs in this experiment---negative in the wet season while positive in the dry season---indicating an uptake and release of CO_2 correspondingly (see figure 3.10). The average value of photosynthesis in 1993 is about 52% lower than it was in the control experiment (see figure 3.11) and the activity of respiration also shows a much lower activity throughout the year (see figure 3.12). These results are the consequence of less root zone water saturation and subsequent severe drought stress, which also results in higher activity of sensible heat flux and lower activity of the latent heat flux in contrast to the original SiB2 model (see figure 3.13-1.14).

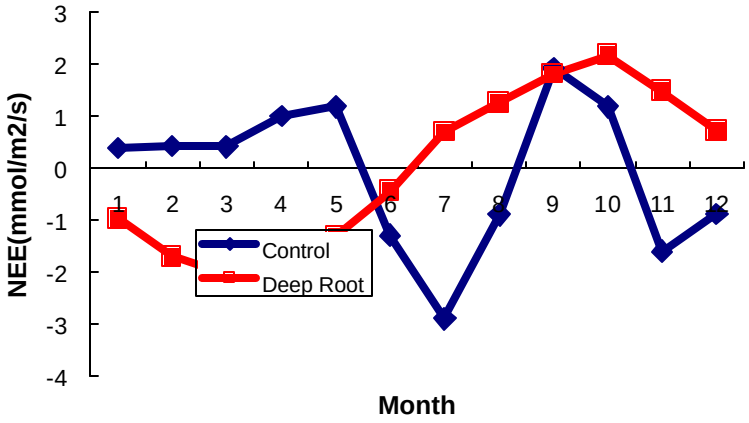

Figure 3.10: SiB3: 1993 Reserva Jaru net ecosystem exchange in deep root experiment

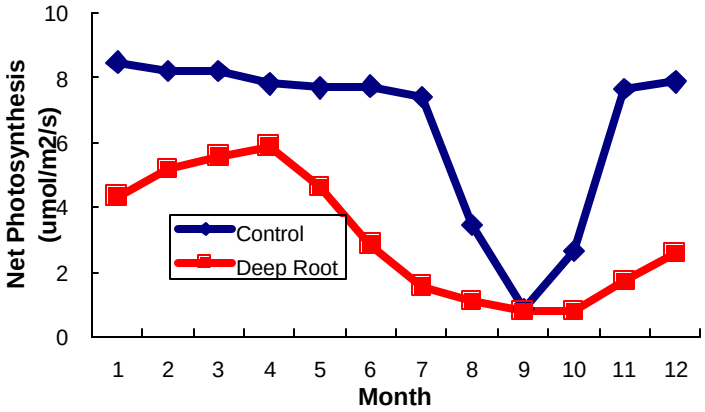

Figure 3.11: SiB3: 1993 Reserva Jaru net photosynthesis in deep root experiment

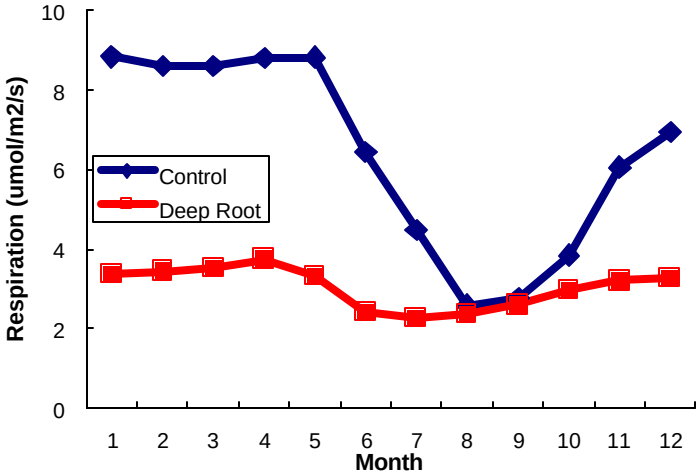

Figure 3.12: SiB3: 1993 Reserva Jaru respiration in deep root experiment

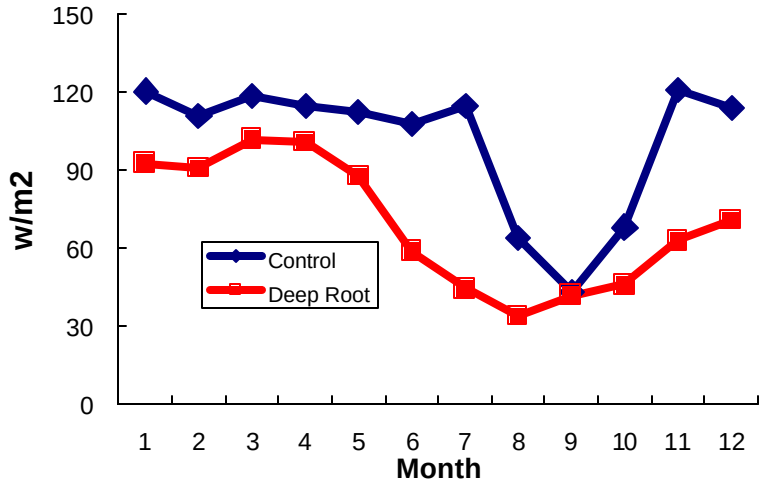

Figure 3.13: SiB3: 1993 Reserva Jaru latent heat flux in deep root experiment

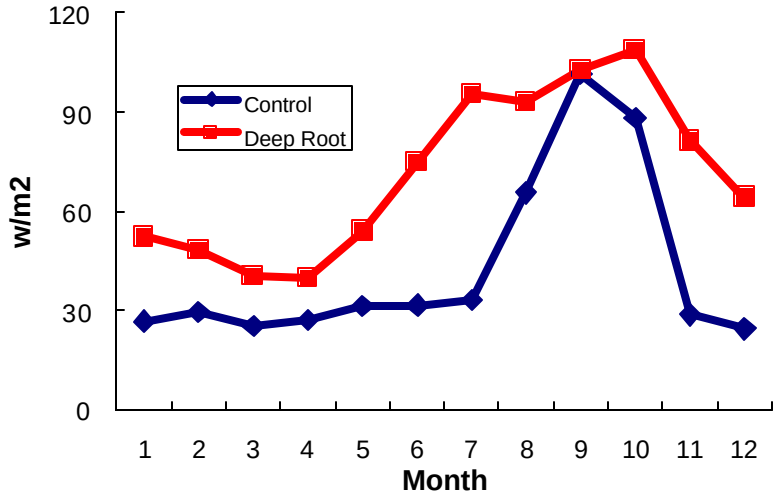

Figure 3.14: SiB3: 1993 Reserva Jaru sensible heat flux in deep root experiment

3.2.2 Revised Parameterization of Physiological Stress

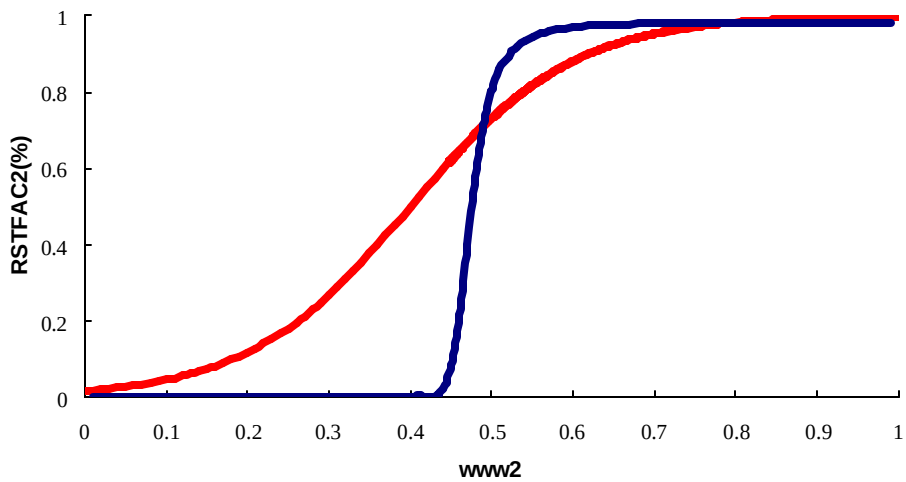

Figure 3.15: Parameterization of physiological stress. The red line is the proposed new stress formulation and the blue line represents the original relationship between root water saturation and stress.

In the original parameterization of water stress (the blue line in figure 3.15), the sudden increase of drought stress from wet season to dry season seems to overlook the importance of horizontal variations in root zone moisture over a larger scale. The motivation for the revised parameterization is the idea that horizontal variations in root zone moisture produce a smoother response on average (over an ecosystem or grid cell) than for a single tree. In order to reduce the supposed over sensitivity of drought stress to root zone water saturation, new parameterization is explored taking account of horizontal variation in root zone moisture over a larger scale (see figure 3.15). The formula used to describe this curve is given as follows:

$$rstfac2 = \frac{1}{1 + \exp(-b * (www2 - c))} \tag{3.1}$$

where $www2$ is a volumetric fraction of root zone saturation in the root zone and c is the half stress parameter the same as that in formula (2.12). b is a constant parameter that is

adjusted to make the curve more smooth and plausible. This formula slows down the sharp increase in water stress during the inter periods between the wet and dry season.

However, figure 3.16 to figure 3.22 suggest that there is no significant improvement when using this new strategy. Root zone water saturation is even less in the dry season, with the volumetric fraction of saturation dropping to around 30% in October (see figure 3.16), which indicates that reduced stress allows more moisture to be removed from the soil. Severe water stress still exists during the dry season in this case, although the curve is slightly smoother than that in the control experiment and a smoother variation of root zone water stress produces smoother behavior of fluxes throughout the year (see figure 3.17). Both root zone water saturation and drought stress reach their extreme values in October, suggesting that the rising of drought stress is synchronized with the decrease of root zone water saturation. Meanwhile, their extreme values do not appear until one month later than those in the control experiment, suggesting a contribution of the revised curve; however, this contribution is not significant.

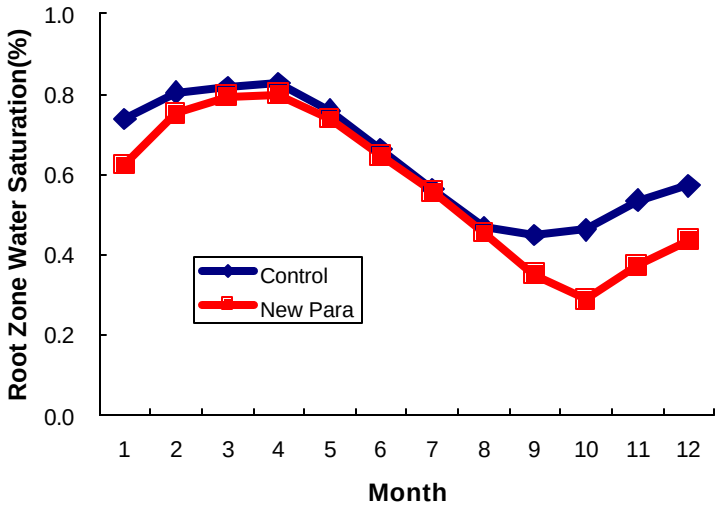

Figure 3.16: SiB2: 1993 Reserva Jaru root zone water saturation in new parameterization experiment

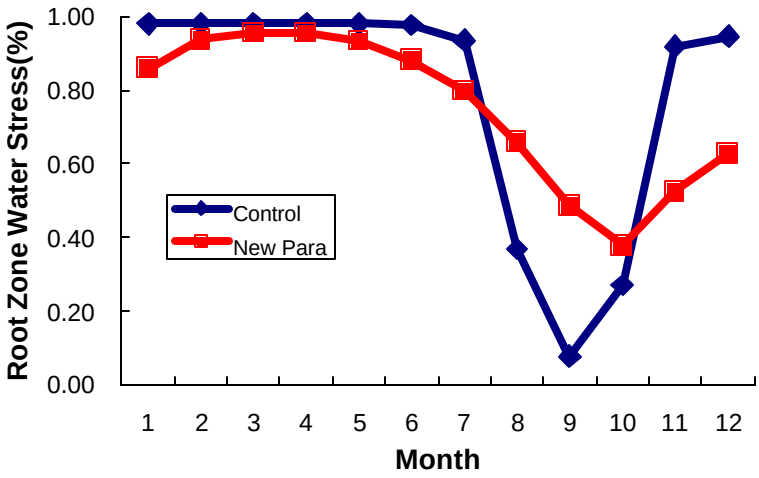

Figure 3.17: SiB2: 1993 Reserva Jaru root zone water stress in new parameterization experiment

NEE variation in this experiment shows the same pattern as in the control experiment but with a more obvious seasonal cycle. Larger absolute value of NEE indicates more CO_2 released in the wet season and taken in the dry season (see figure 3.18). Photosynthesis in the new parameterization experiment does not experience as severe a collapse in the dry season as that in the control experiment. It begins to decline in the beginning month of the dry season and reaches its lowest value in October, one month after the control experiment and the same month that root zone water saturation reaches its minimum level (see figure 3.19), consistent with the variation of drought stress. Respiration demonstrates almost the same value as that in control experiment (see figure 3.20).

Latent and sensible heat flux show a similar variation as that in the control experiment with the exception of greater latent heat flux and smaller sensible heat flux in the dry season than in the control experiment, which is consistent with increase in root zone water saturation (see figure 21-22).

It can be concluded that reducing the sensitivity of drought stress to root zone water content would not solve the extreme drought stress problem during the dry season.

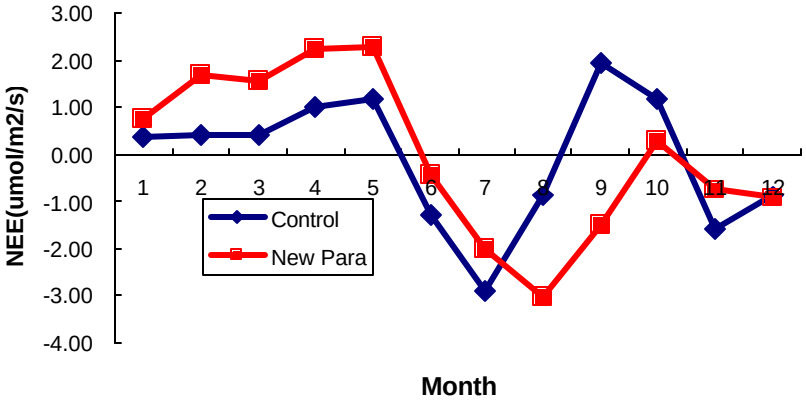

Figure 3.18: SiB2: 1993 Reserva Jaru net ecosystem exchange in new parameterization experiment

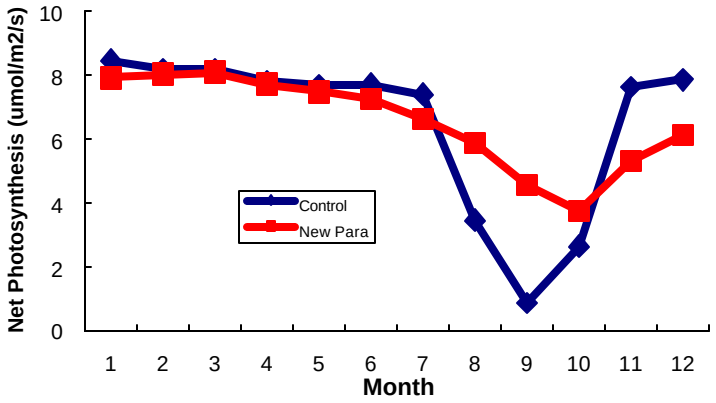

Figure 3.19: SiB2: 1993 Reserva Jaru net photosynthesis in new parameterization experiment

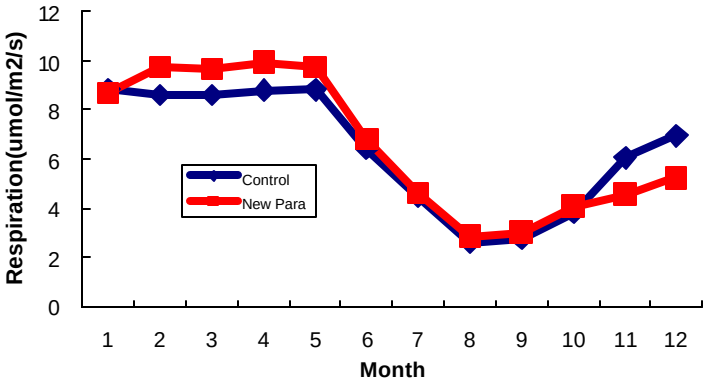

Figure 3.20: SiB2: 1993 Reserva Jaru respiration in new parameterization experiment

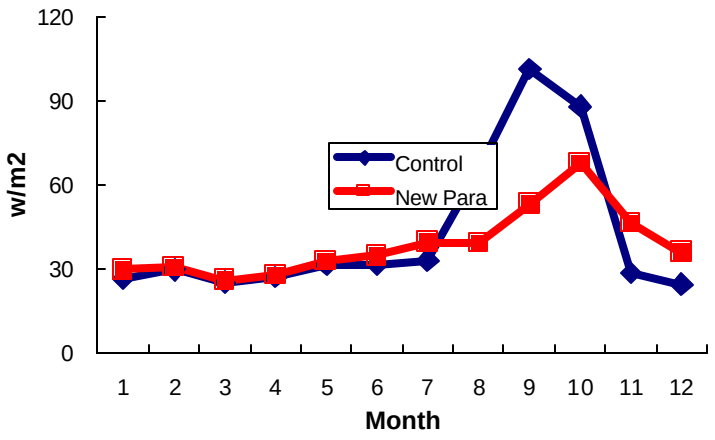

Figure 3.21: SiB2: 1993 Reserva Jaru latent heat flux in new parameterization experiment

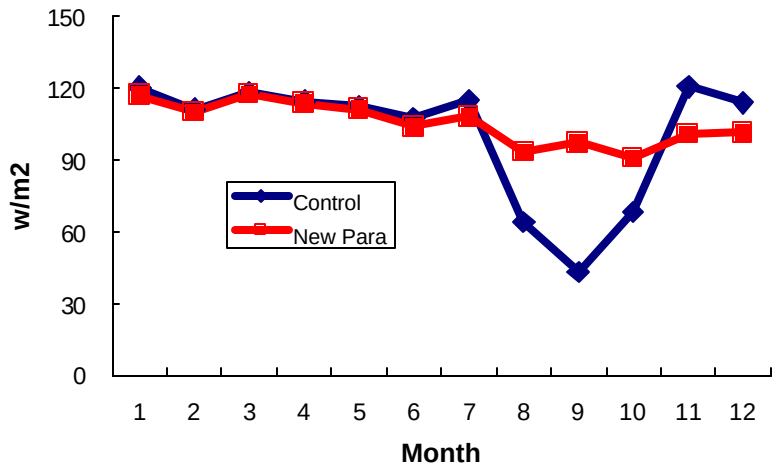

Figure 3.22: SiB2: 1993 Reserva Jaru sensible heat flux in the new parameterization experiment

3.3.3 Effects of Less Run-off Precipitation

After precipitation falls reaches the ground, part of it will immediately run off the surface of the soil while the remaining water may infiltrate into the soil, and subsequently will contribute to the soil water reservoir (see section 1.3.1). Obviously, the amount of runoff precipitation would reduce precipitation input into the soil and thus affects the water

storage in shallower soil layers. The runoff amount depends on the type of precipitation and also on the vegetative canopies as discussed in section 2.1.2. Soil texture at the surface is also important for water input into the soil. In this experiment, sandy texture was chosen to reduce soil tension at saturation, and simultaneously increase the hydraulic conductivity. A sensitivity experiment was performed in which runoff was reduced to allow greater infiltration.

Soil tension, also known as soil water potential is a way to describe the ease by which water can be extracted from the soil. Water held in pores by capillary storage is held in the soil at a certain tension. The less soil tension at saturation, the more water can be extracted by the soil. Soil porosity or pore space measures the free space between soil particles or structural units of soil. Coarse textured sandy soils have larger pores but much less pore space than finer textured clay soils. A porosity of 40% is used in this experiment. Hydraulic conductivity is the function of soil water potential and conductivity measures the ease with which water moves through the soil. Hydraulic conductivity increases drastically with the increase of water content (see figure 3.23; Brikowski, 2002). The decrease in conductivity as the soil dries is due primarily to the movement of air into the soil to replace water. As air moves in, the pathways for water flow between soil particles becomes smaller and more restricted, and flow becomes more difficult. Higher hydraulic conductivity is favorable for the flow of soil water which increases storage, but at same time, also favors gravitational drainage, which decreases water storage. The simulation results will be significantly influenced depending on which one turns out to be the dominant factor.

Unfortunately, the results do not show any improvement (see figure 3.24 to figure 3.30). Root zone water is even 30% less compared to the results from the control simulation, which means water is removed from the soil by gravitational drainage. There is no increase in drought stress, even with less root zone water saturation (see figure 3.24) because there is less soil tension in sand than in clay. Other variables, drought stress, NEE, photosynthesis, respiration, fluxes of latent and sensible heat in the reduced runoff simulation are very close to the results of the control simulation.

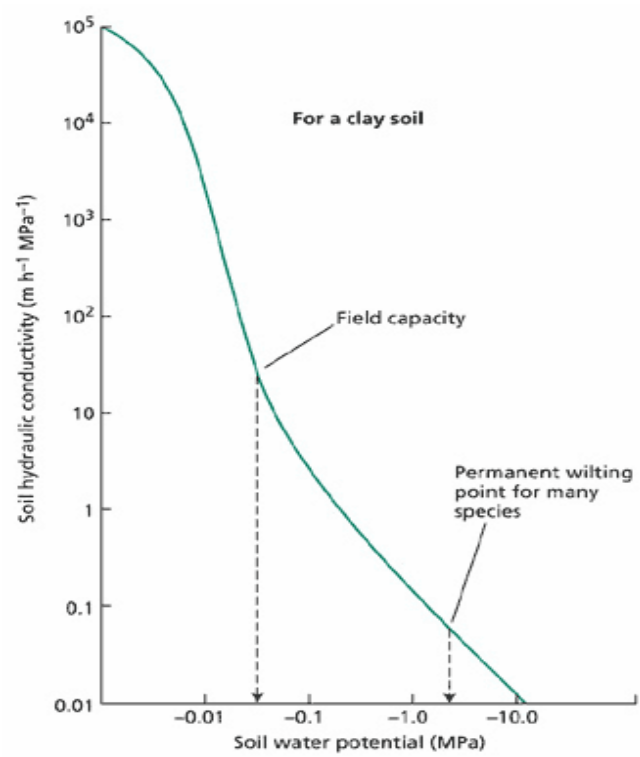

Figure 3.23: Soil hydraulic conductivity as a function of the water potential of the soil. The overall shape of this curve is representative of many soils, but the shape for a particular soil may be influenced by the size distribution of its particles and by its organic matter content. The field capacity is the amount of water the soil is able to retain against gravitational forces. The permanent wilting point is the soil water potential value at which plants cannot regain turgor pressure even at night, in the absence of transpiration. The figure is taken from plant physiology on line.

This experiment suggests that less runoff of precipitation at the surface cannot guarantee the input of enough water into the soil layers or the soil's ability to hold water. Water can loose through gravitational drainage.

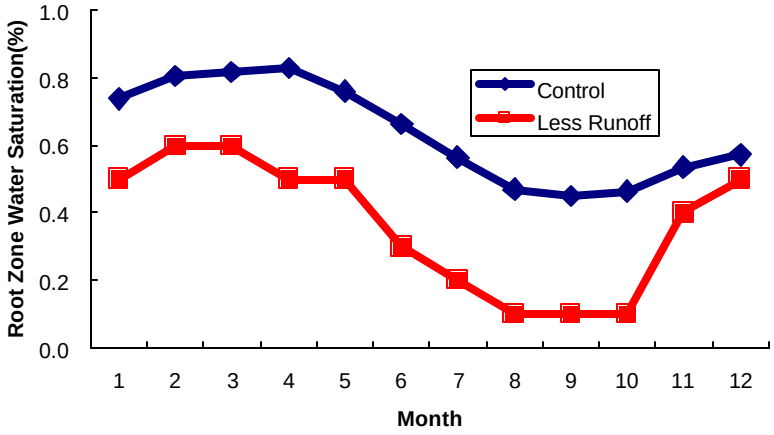

Figure 3.24: SiB2: 1993 Reserva Jaru root zone water saturation in less runoff experiment

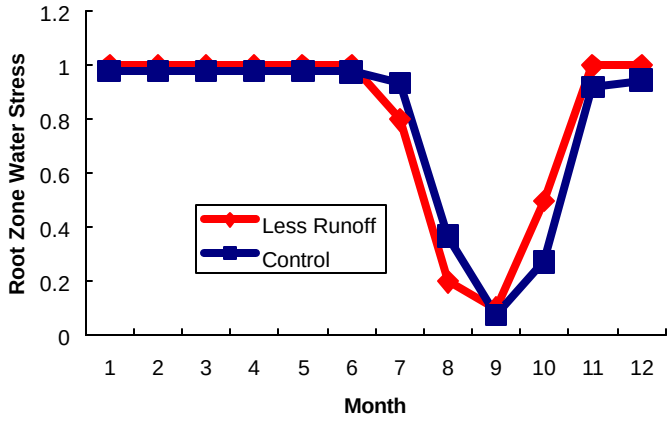

Figure 3.25: SiB2: 1993 Reserva Jaru root zone water stress in less runoff experiment

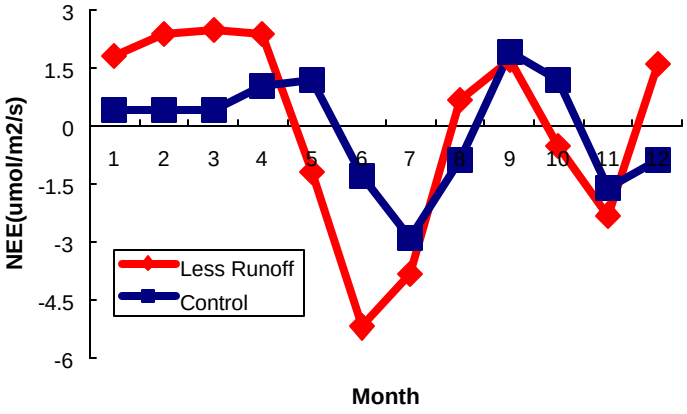

Figure 3.26: SiB2: 1993 Reserva Jaru net ecosystem exchange in less runoff experiment

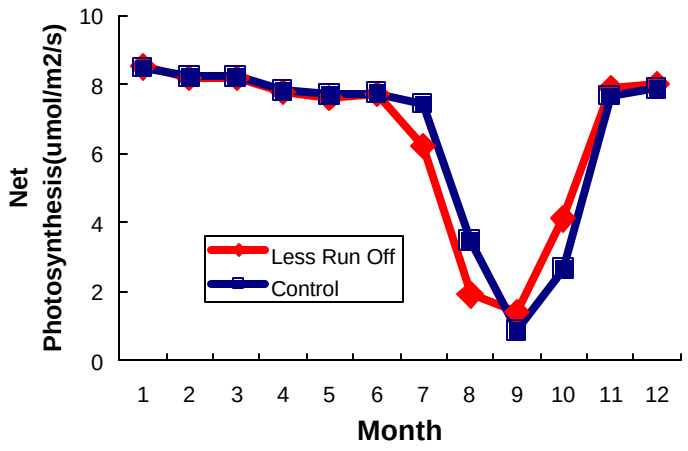

Figure 3.27: SiB2: 1993 Reserva Jaru net photosynthesis in less runoff experiment

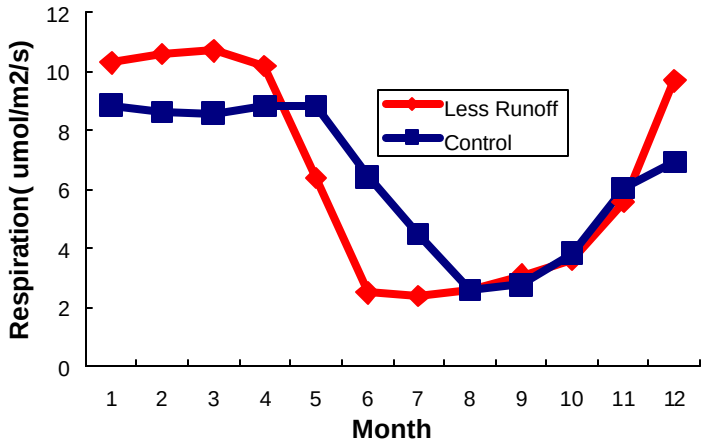

Figure 3.28: SiB2: 1993 Reserva Jaru respiration in less runoff experiment

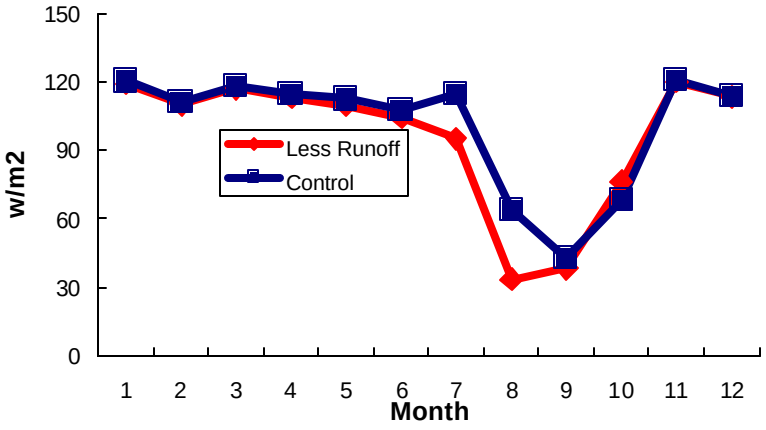

Figure 3.29: SiB2: 1993 Reserva Jaru latent heat flux in less runoff experiment

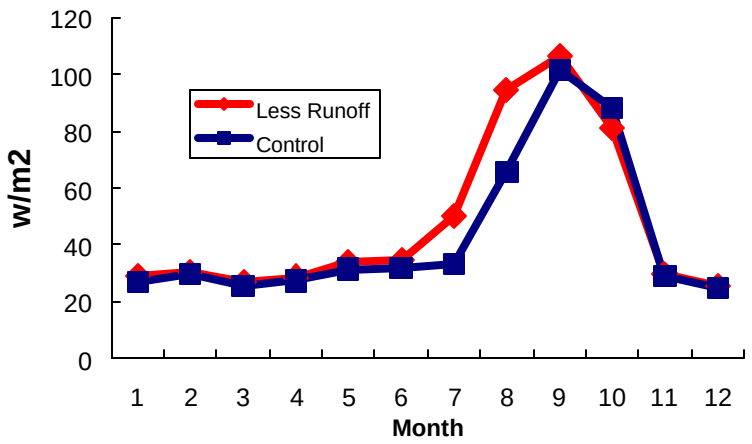

Figure 3.30: SiB2: 1993 Reserva Jaru sensible heat flux in less runoff experiment

3.3 SiB3 simulation

After exploring the alternative parameterization in SiB2, another proposal is to improve the model performance by increasing the number of soil layers, revising the root distribution through the soil layers, and using PAW (plant available water) to calculate the water stress factor.

3.3.1 Structure of Soil Layers

In the SiB2 deep root simulation, there are three soil water layers: the top 2cm of the soil, root zone soil moisture, and deep soil moisture, along with seven soil temperature layers. In SiB3, soil layers are modified to ten soil water layers and ten soil temperature layers (see figure 3.31).

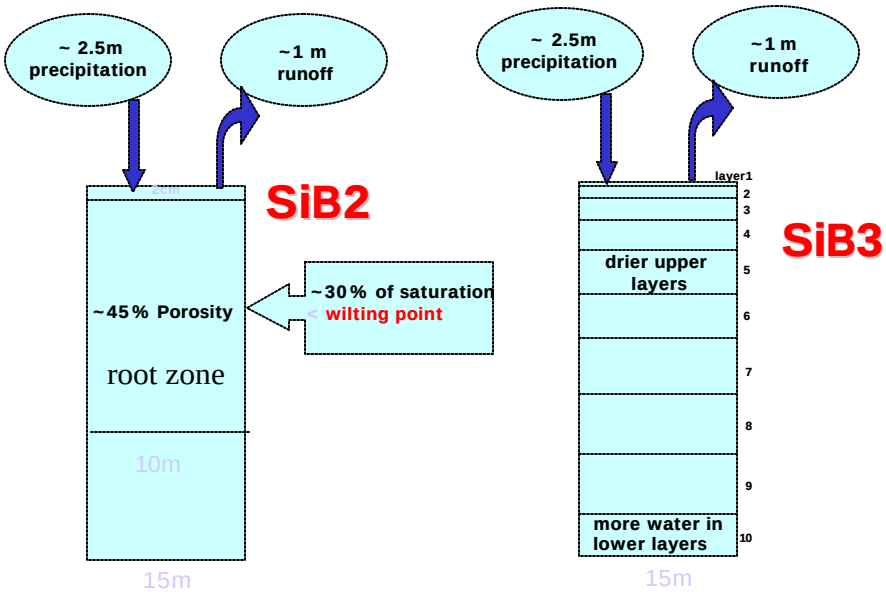

Figure 3.31: Comparison of soil layer structure between SiB2 and SiB3

There are three advantages of a multi-layer soil structure. First, increasing the number of soil layers from three to ten or from three soil moisture layers and seven soil temperature layers make it possible to simulate the vertical movement of water through the soil more realistically after precipitation occurs. Tree roots have an adjusted water extraction profile in SiB3 because they run throughout the soil. This vertical distribution of water in the soil is more accurate with a larger number of soil layers.

Second, soil moisture layers do not necessarily occupy the same depth as soil temperature layers in the SiB2 model. In contrast, the SiB3 model has soil moisture layers and soil temperature layers co-located, which is more plausible when calculating transpiration and evaporation.

Third, soil moisture is parameterized in regard to liquid and ice explicitly, with five layers of snow at the surface of the soil and ten layers of soil liquid water underneath following CLM (Dai *et al.*, 2003). Because it never snows in the Amazon, the snow depth is set to be zero in this study.

The calculation of soil layer depth follows the use of scale depth, which is equal to 0.025 in CLM (Common Land Model for land-atmosphere interaction). The formula is as follows:

Let *z, dz, lz* represent the thickness from the top to the middle point of each soil layer, the thickness for one soil layer and the depth of the cumulative soil layers respectively (see figure 3.32).

$$z(i) = 0.025\exp(0.5(i-0.5)-1) \tag{3.2}$$

where i is the number of layer. For the first layer:

$$dz = (z(1)+z(2))/2 \quad . \tag{3.3}$$

For the last layer:

$$dz = z(10)-z(9) \tag{3.4}$$

$$lz = z(10)+dz(10)/2 \quad . \tag{3.5}$$

For the between layers:

$$dz = (z(i+1)-z(i-1))/2 \tag{3.6}$$

$$lz = (z(i)+z(i+1))/2 \quad . \tag{3.7}$$

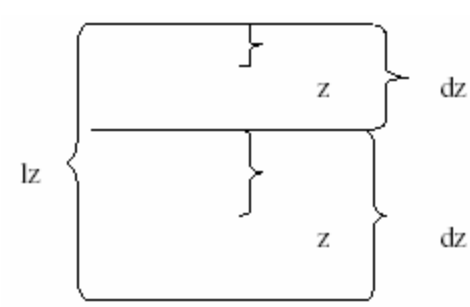

Figure 3.32: Soil layer depth and thickness in SiB3

3.3.2 Exponential Root Profile

Instead of pooling all the roots into one root zone of the three-soil layer model, roots are distributed exponentially throughout all soil layers (see figure 3.31; figure 3.33). This

distribution allows water input into the deeper layers of the soil and the water reservoir more efficient.

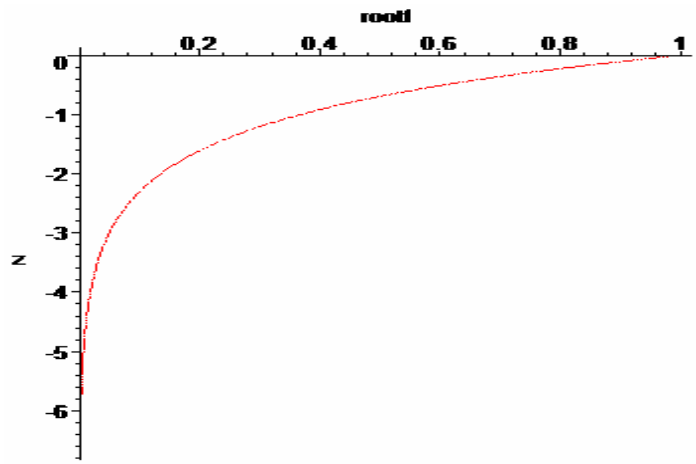

Figure 3.33: Root faction distribution with soil depth. The unit of depth is measured in meters

The multi-layer soil structure and adjusted water extraction root profile also make it possible to simulate transpiration more realistically. Two aspects of transpiration control must be parameterized in SiB3: 1) the allocation of water (fractional withdrawal) from each soil layer to supply the plant for transpiration; and 2) physiological stress resulting from dry soil.

For allocation of transpiration throughout the soil, soil layers are separated into two parts: the top layer and the remaining layers beneath the first layer. Ground interception, evaporation and transpiration take place simultaneously at the first layer if the ground temperature is greater than zero degrees Celcius, which is always the case in the Amazon. Transpiration allocation within soil layers can be described as follows:

$$rootr(i) = \frac{1-q_{wilt}}{1-q_{fc}} \cdot \frac{rootf(i)}{\Sigma rootr(i)} \qquad (3.8)$$

where *rootr* is a fraction of the total transpiration which is withdrawn from a certain layer

i, rootf is the root fraction in each layer (see figure 3.31). q_{wilt} and q_{fc} are the wilting point and field capacity respectively (section 3.33). The physiological stress is calculated using plant available water (PAW).

3.3.3 Plant Available Water

Bulk root zone water was used to determine water stress in SiB2. The disadvantage of this method is that water stress is overly sensitive to the amount of saturation in the root zone, as discussed in section 3.1.2. For example, at 45% of saturation, there can be very little stress; however, dropping the moisture in the root zone just a little bit would result in severe drought stress, as shown in figure 2.3. Moreover, this formulation based on root zone water does not allow for deep soil water to alleviate soil water stress.

In order to overcome these disadvantages, plant available water (PAW) is introduced in the new version of SiB. PAW represents the amount of water in the soil that is available to the plant. When PAW reaches its maximum value, the soil is said to be at its field capacity, which is the maximum amount of water that a particular type of soil can hold against gravitational force. At the zero value of PAW, the soil is at its wilting point. With many soil layers, PAW serves as an index to the water status of the entire plant-soil system, rather than trying to weight the model using a rooting profile or something more complex.

Soil water potential measures the energy state of the soil water or the soil's ability to produce heat. Soil water potential is important to any processes where soil water infiltrates and is redistributed throughout the soil, or is removed from the soil by evaporation or transpiration. Water potential is always negative by definition.

The wilting point is the point at which plants loose their turgor beyond a certain water potential threshold. A plant's transpiration rate decreases due to the decrease or the negatively increase of soil water potential. The wilting point varies across soil textures,

as well as plant species. The specific wilting point of soil texture and soil species affects how much water plants can withdraw from the soil and what the minimum level of humidity is the soil can reach in the layers that are not affected by evaporation. Under conditions of strongly negative water potential in the soil, in shallow soil layers, water depletion will continue beyond the wilting point since evaporation is still active. Deeper soil layers, however, are not affected by direct evaporation. They will remain at the wilting point water potential and reach its minimum possible water content.

Maximum PAW can be gained by subtracting the minimum volumetric water content (wilting point) (%) from the percentage of soil field capacity, which varies according to different soil textures. The PAW fraction is a proportion of PAW in one soil layer to the maximum PAW in this particular soil layer. The calculation of PAW in SiB3 is as follows:

$$dq(i) = q_{liq}(i) - q_{wilt}(i) \tag{3.9}$$

$$paw = \sum_{i=1}^{nsoil} dq(i) \tag{3.10}$$

$$paw\_\max = q_{fc} - q_{wilt} \tag{3.11}$$

$$pawfrac = paw / paw\_\max \tag{3.12}$$

where q_{liq} , q_{wilt} , q_{fc} are volumetric liquid water, wilting point and field capacity respectively. $paw\_\max$ is maximum plant available water and *pawfrac* is PAW fraction. When the volumetric content of water is above field capacity and below or equal to saturation, *pawfrac* is set at one,

Drought stress is defined by parameterization expressed in (3.17). Here, another parameter is introduced in the stress coefficient formula, in order to make the curve more plausible.

$$rstfac2 = \frac{(1+s)*pawfac}{(s+pawfac)} \tag{3.13}$$

where s is the stress coefficient. The curve in figure 3.34 indicates the relationship between plant available water and water stress factor. It can be concluded that when there is no PAW, water stress is severe, though when PAW reaches or exceeds its maximum value the water stress disappears. The role of s is to determine the shape of the curve and thus to modulate the variation of water stress with respect to PAW. In our SiB3 simulation $s = 0.2$ has been chosen.

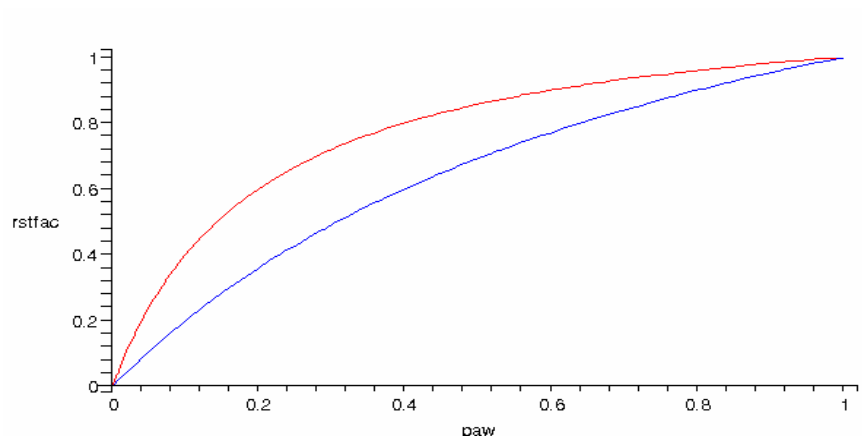

Figure 3.34: the relationship between PAW and water stress. s is chosen as 0.2 and 0.8 respectively, the red curve describes the curve when $s = 0.2$ and the blue curve shows their relationship when $s = 0.8$

3.3.4 Prognostic Tracers

Equation 3.14 through 3.18 show the calculation of temperature, water vapor, CO_2, heat and water fluxes in SiB3.

$$rC_p \Delta z \frac{\partial T_a}{\partial t} = H_c + H_g + H_s + H_m \tag{3.14}$$

$$\frac{rC_p \Delta z}{g} \frac{\partial e_a}{\partial t} = LE_c + LE_g + LE_s + LE_m \tag{3.15}$$

$$r\Delta z\frac{\partial C_a}{\partial t} = R_g - A_n - \frac{C_a - C_m}{r_a} \tag{3.16}$$

$$H_c \equiv H_c^{n+1} = \frac{rC_p}{r_b}(T_c^{n+1} - T_a^{n+1}) \tag{3.17}$$

$$LE_c \equiv LE_{Ctranspiration} + LE_{C\,interception} = \frac{rC_p}{g}(e_s(T_c^{n+1}) - e_a^{n+1})(\frac{w_c}{r_b} + \frac{1-w_c}{r_c}) \tag{3.18}$$

where, H_g, H_c, H_s are sensible heat flux from canopy, ground, snow respectively. LE_g, LE_c, LE_s , are latent heat flux from canopy, ground and snow respectively. H_m, LE_m are turbulence term. Super scribe *n* represents the time steps in SiB3. Latent heat flux can also be written as:

$$LE = b\frac{rC_p}{g}\frac{e_s(T_c) - e_a}{r_a} \tag{3.19}$$

where b is water stress factor, and the term $(e_s(T_c) - e_a)/r_a$ is referred to as evaporation demand. In the dry season drought stress will decrease the LH, but on the other hand, lower humidity will lessen the evaporation demand and makes evaporation easier. The simulated latent heat flux will be significantly influenced depending on which one turns out to be the dominant factor.

3.4 SiB3 Simulation Results at Two Tropical Forest Sites

Both 10_layer and 12_layer models, which include 10 or 12 soil layers beneath the surface respectively, have been explored in the study. When keeping everything else unchanged, a 12_layer model has extra two layers at the bottom of the soil, and both of them are very thick compared to the 10-layer model. This multi-layer structure could simulate vertical moment of water through the soil more realistically and would be favorable to water storage in the deeper layers resulting in a larger sum total of soil

moisture (see figure 3.35 also see figure 3.31 for the multi-soil layer structure).

The simulations always have a spin-up for a ten year period beginning with the saturated initial condition. The result of the 11th year is analyzed. For Reserva Jaru, the results show that drought stress develops slightly in the 10_layer model but disappears completely in 12_layer model. However, for the northern site, Tapajos 67km, there is around 18% less precipitation than Reserva Jaru throughout the year (see figure 2.7) severe drought stress develops even with 12 soil layers in SiB3.

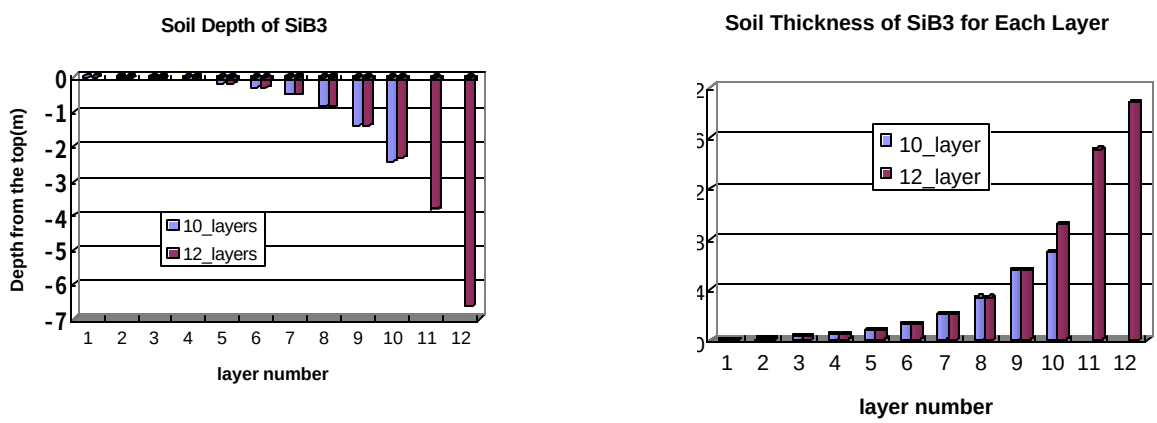

Figure 3.35: Comparison of soil depth and thickness between SiB3 10_layer and 12_layer model

3.4.1 SiB3 Simulation Results for Reserva Jaru

Figure 3.36 to figure 3.41 show the simulation results for Reserva Jaru in 1993 compared with those from the SiB2 experiment. Slight water stress develops in September and October in the SiB3 10_layer model, but is entirely gone when the two extra deep layers are applied (see figure 3.36a). Simulated plant available water is shown in figure 3.36b. The disappearance of water stress is associated with the PAW fraction (see equation 3.9-3.12) equal to one. The disappearance of water stress, in the dry season is the most significant improvement in this revised model.

Similar to the SiB2 simulation, the seasonal cycle of NEE is not as significant. Instead

of being positive through the entire wet season, it shows opposite effects, indicating the uptake of CO_2 when there is a large amount of precipitation. In spite of this, the magnitude of the NEE value shrinks down to one decimal, with the maximum absolute value of 1.2 and the minimum absolute value of 0.1, which means that there is only a tiny difference between photosynthesis and respiration for the entire year, suggesting that the processes are almost immune to the dry conditions (see figure 3.37). 10_layer and 12_layer models have similar performances in predicting net ecosystem exchange.

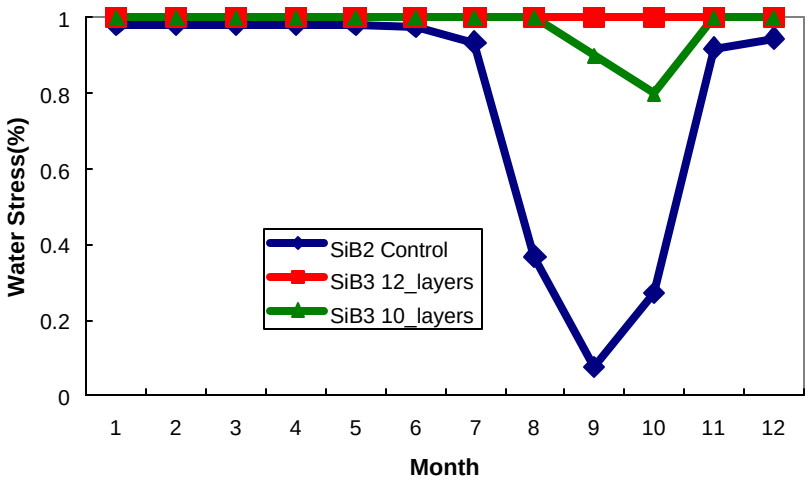

Figure 3.36 a : SiB3: 1993 Reserva Jaru water stress

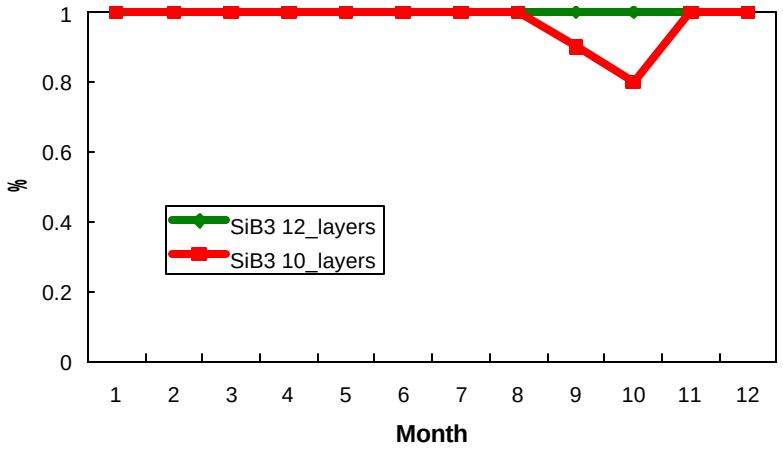

Figure 3.36 b: SiB3: 1993 Reserva Jaru plant available water (PAW) fraction

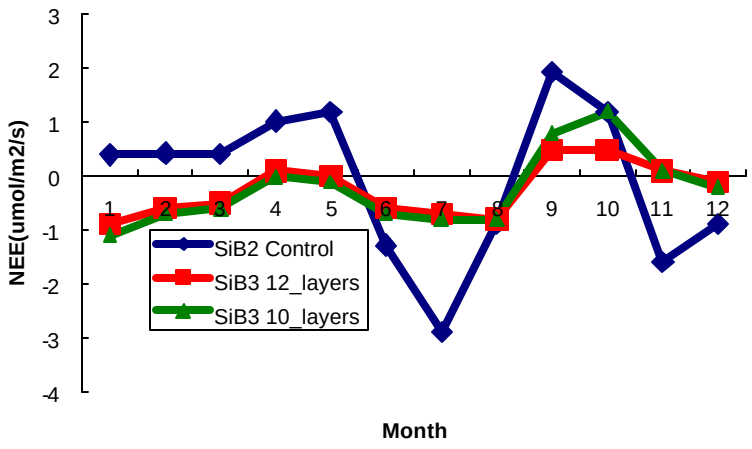

Figure 3.37: SiB3: 1993 Reserva Jaru net ecosystem exchange

Photosynthesis stays constant from the beginning of the year to the end of the year in the SiB3 12_layer model without any sign of collapse in the dry season, which is different than the SiB2 model (see figure 3.38). In the SiB3-12_layer model respiration is almost constant except for a very small increase in September, when precipitation goes up again (see figure 3.39; figure 2.7b). The consistency of photosynthesis throughout the year is due to the lack of drought stress even in dry season and enough water and radiation all year long. No water stress shows up during the year (see figure 3.36). A 10_layer model gives us results similar to the 12_layer model, with the exception of a slight decrease in photosynthesis in September and October that corresponds to slight increase in water stress during that period.

Unlike the simulation results in SiB2, the variation of latent and sensible heat flux is not as apparent throughout the year. Latent heat flux increases from 98 w/m^2 to 125 w/m^2 from June (dry season) to October (wet season) with BR less than one within the whole year. Sensible heat flux is almost persistent throughout the year (see figure 3.41). It can be seen that removal of drought stress shifts partition of latent heat flux and sensible heat flux but does not change their sum(see figure 3.42).

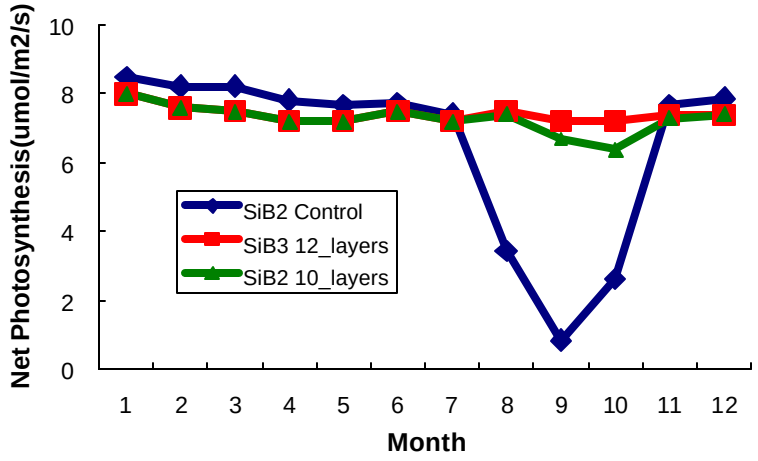

Figure 3.38: SiB3: 1993 Reserva Jaru net photosynthesis

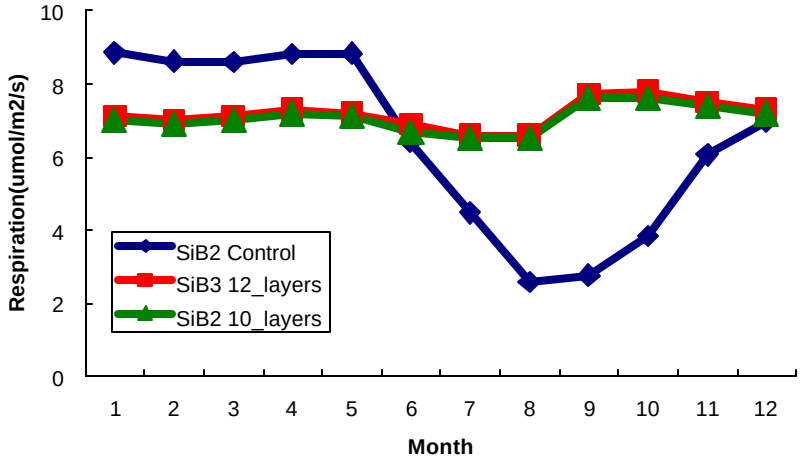

Figure 3.39: SiB3: 1993 Reserva Jaru respiration

Figure 3.43a and 3.43b show the average diurnal cycle comparison of simulated energy flux with observed data over 114 days (from April 4th to July 27th). Black lines represent simulated energy fluxes by using SiB2, blue and green lines are simulated results using the SiB3 10_layer model and 12_layer model respectively. Red lines demonstrate the observed data. Figure 3.43a shows that SiB3 multiple layer model produce more accurate latent fluxes than SiB2. However, both of these models overestimate sensible heat fluxes at around 30 %(see figure 3.43b). Figure 3.43c shows the daily mean comparison of energy

flux from April 4th and July 27th, which is part of the dry season. Green lines are simulated results and red lines are observed data. It can be seen that synoptic scale variability of latent heat flux is well captured by SiB3 12_layer model, however, daily mean of sensible heat flux is around 30% overestimated.

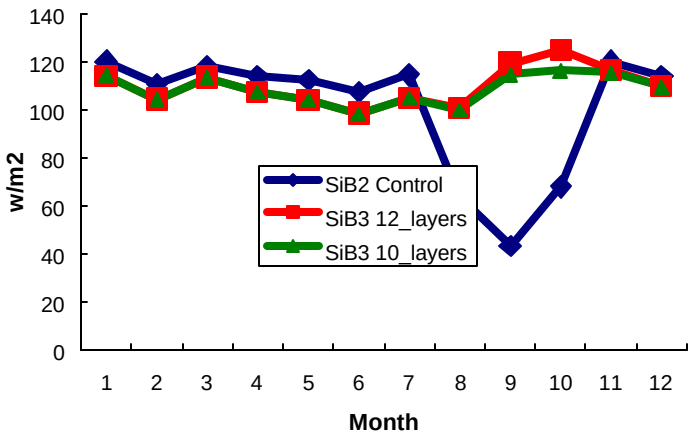

Figure 3.40: SiB3: 1993 Reserva Jaru latent heat flux

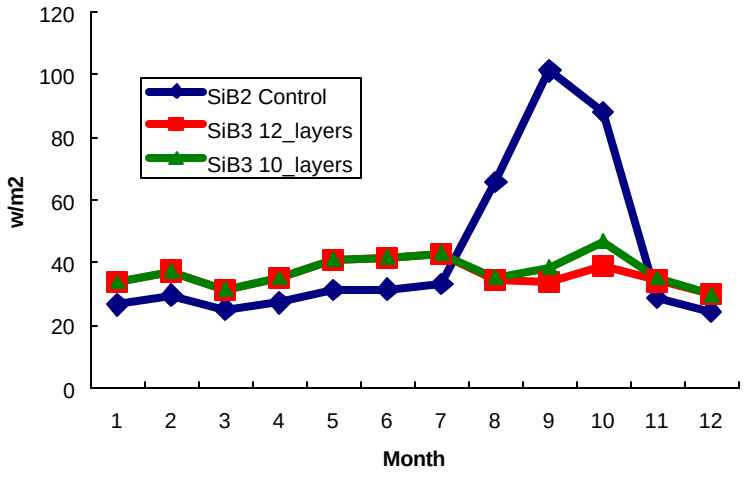

Figure 3.41: SiB3: 1993 Reserva Jaru sensible heat flux

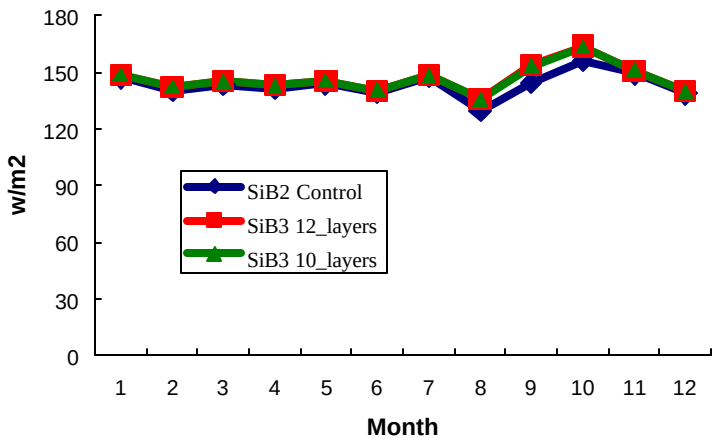

Figure 3.42: SiB3: 1993 Reserva Jaru total latent and sensible heat flux

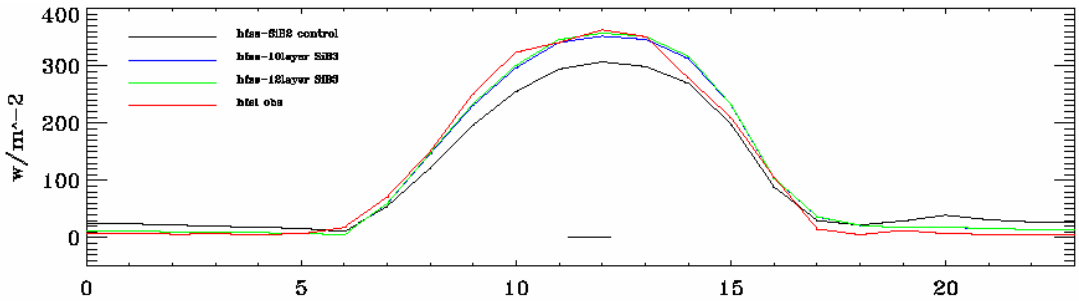

Figure 3.43 a: 1993 Reserva Jaru diurnal cycle of latent heat flux averaged over 114 days (from April 4th to July 27th)

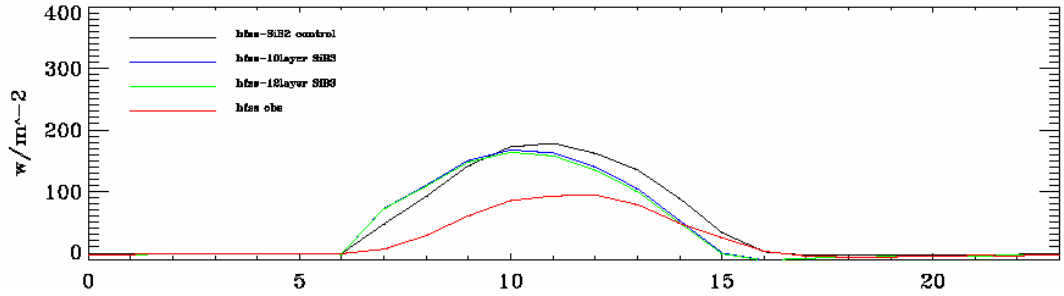

Figure 3.43 b: 1993 Reserva Jaru diurnal cycle of sensible heat flux averaged over 114 days (from April 4th to July 27th)

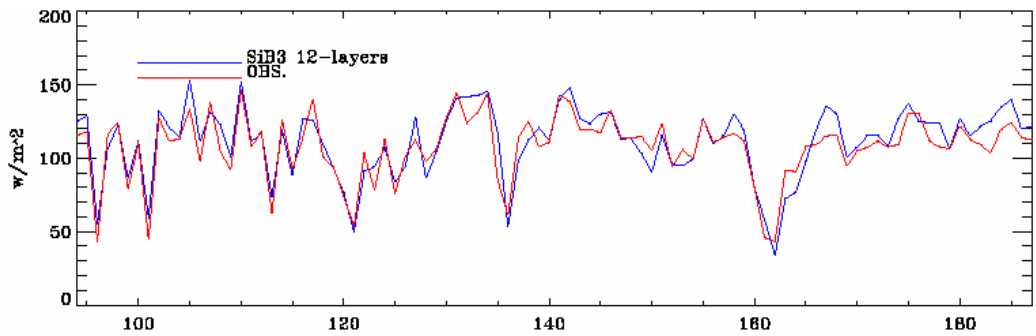

Figure3.43c: 1993 Reserva Jaru daily mean of latent heat flux.

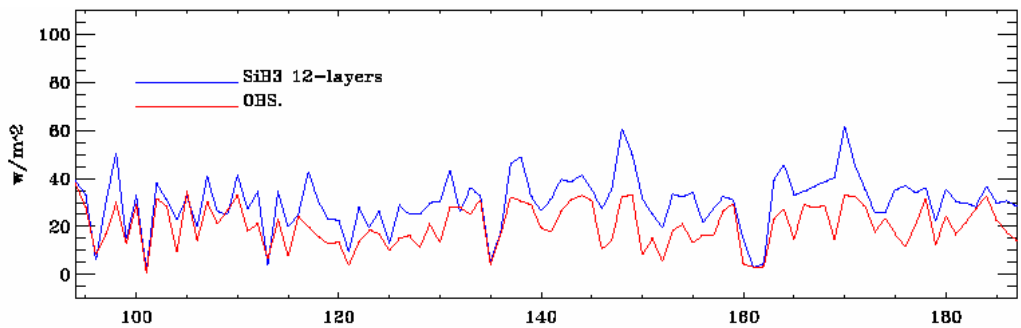

Figure3.43d: 1993 Reserva Jaru daily mean of sensible heat flux.

3.5.2 SiB3 Simulation Results for Tapajos 67km

In order to show that the SiB3 multi-layer model is plausible in all cases, a simulation of the Tapajos 67km site is also included in this study. Figure 3.44 shows the monthly mean of the water stress factor and plant available water fraction in the year 2002. The water stress is alleviated around 35% in the dry season although it does not disappear completely, suggesting the importance of a deep water reservoir.

Net ecosystem exchange in the SiB3 12_layer model demonstrates the opposite direction to what was observed (see figure 3.45). The opposite pattern of observed CO_2 to the seasonal cycle of both tree growth and model prediction may be a transient effect of recent disturbances superimposed on long-term balance (section 1.3. 6; Saleska *et al*, 2002).

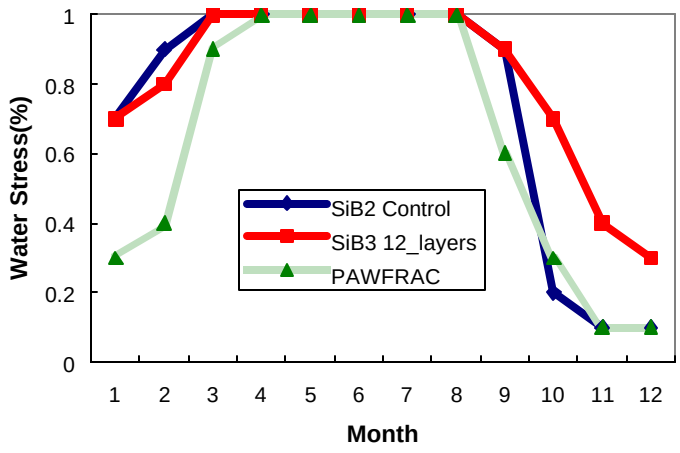

Figure 3.44: SiB3: 2002 Tapajos 67km water stress and PAW

Figure 3.46 shows the comparison of annual mean diurnal cycles of NEE among SiB3 multi-layer model and observations. The black line is NEE from SiB2, the blue line represents simulated NEE from SiB3-12_layer model and the red line is observed data. It is obvious that the maximum and minimum of NEE are well simulated by the multi-layer model but the gradual decrease in GPP in the afternoon has not been captured by the model.

Photosynthesis is determined by soil moisture and radiation. In the dry season, water stress will suppress photosynthesis while stronger radiation due to fewer clouds will favor photosynthesis. A sharp reduction of photosynthesis during the dry season from the SiB3-12_layer model simulation suggests that water stress takes a dominant role in the photosynthetic process compared to radiation (see figure 3.47). Although the collapse of photosynthesis still happens in the multi-layer model, the average net photosynthesis for the entire year is around 50% greater than from the SiB2 control experiment. This may be due to the high level of water in the soil.

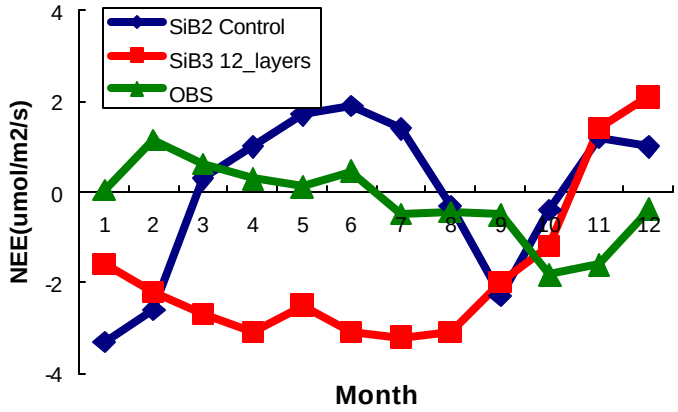

Figure 3.45: SiB3: 2002 Tapajos 67km net ecosystem exchange

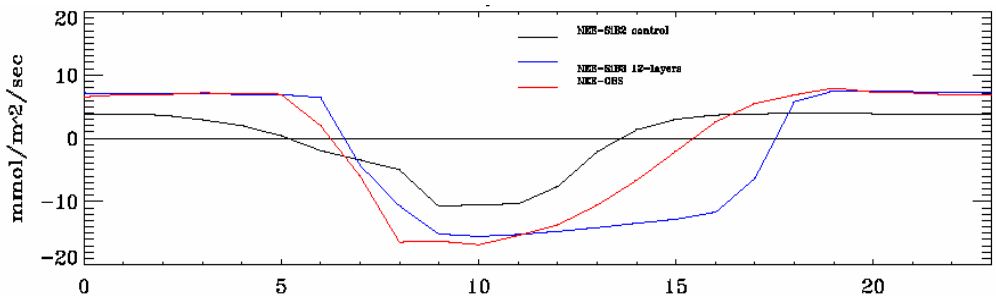

Figure 3.46: 2002 Tapajos 67km annual mean diurnal cycle of net ecosystem exchange

Respiration stays almost constant in the dry season in SiB3-12_layer model instead of decreasing in the dry season as the SiB2 simulation projected (see figure 3.48). However, respiration increases around 5% in the dry season. It is due to the much larger amount of CO_2 (see figure 3.51a and 3.51b.) at the surface in spite of lower volumetric water content (see figure 3.49) and soil temperature at the top layer (see figure 3.50). The high levels of respiration show the continuous activity of plants even in dry conditions, which may indicate plenty of water is available in the soil layers. We can attribute this to the alleviation of drought stress (see figure 3.44). From the SiB3 12_layer model the average respiration during the year is about 40% greater than the average respiration projected in the SiB2 control simulation (see figure 3.48).

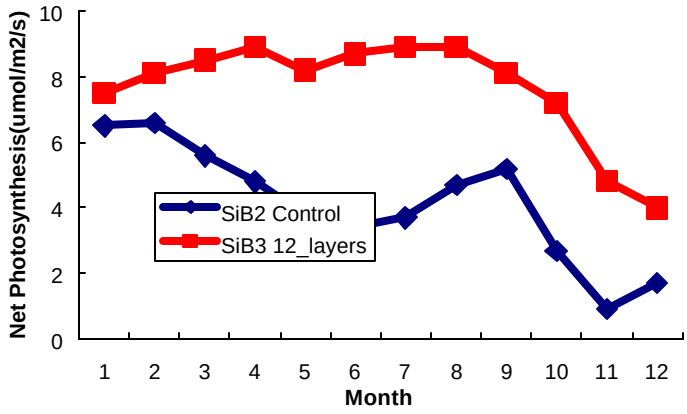

Figure 3.47: SiB3: 2002 Tapajos 67km net photosynthesis

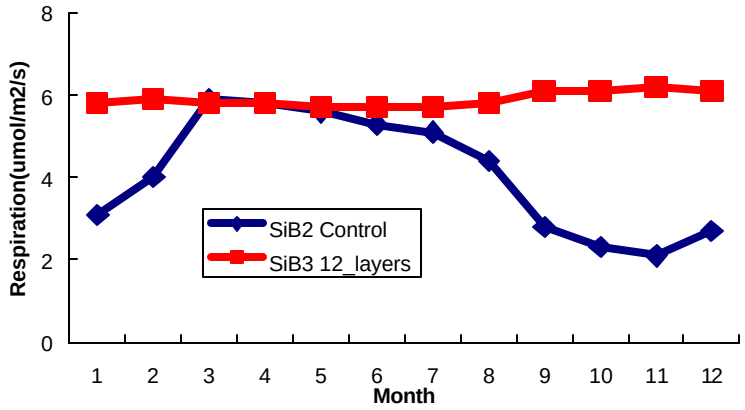

Figure 3.48: SiB3: 2002 Tapajos 67km respiration

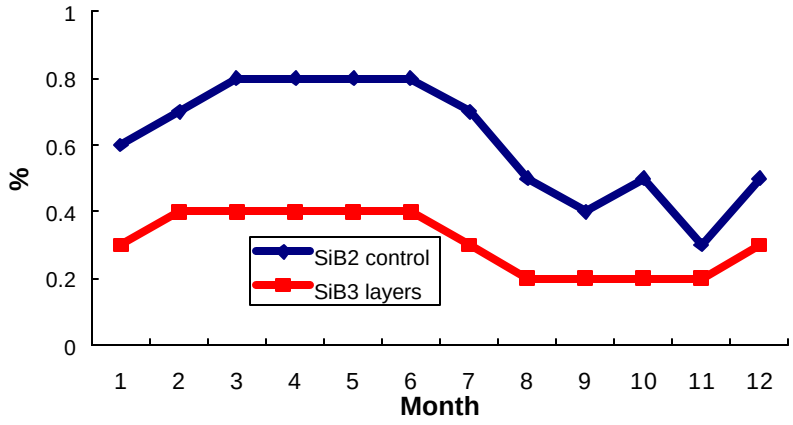

Figure 3.49: SiB3: 2002 Tapajos 67km volumetric water content at the top layer

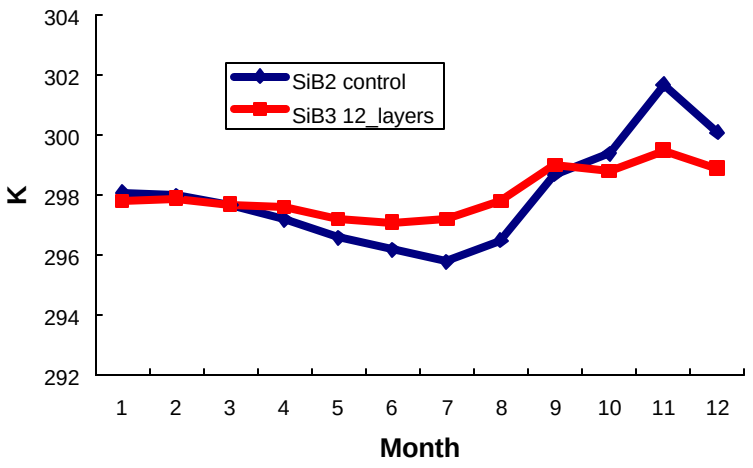

Figure 3.50: SiB3: Tapajos 67km soil temperature at the top layer

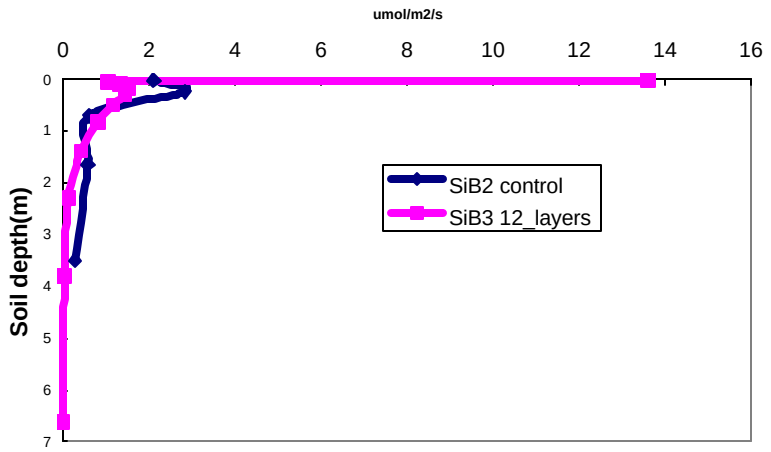

Figure 3.51 a: SiB3: Tapajos 67km the respiration factor profile throughout the soil

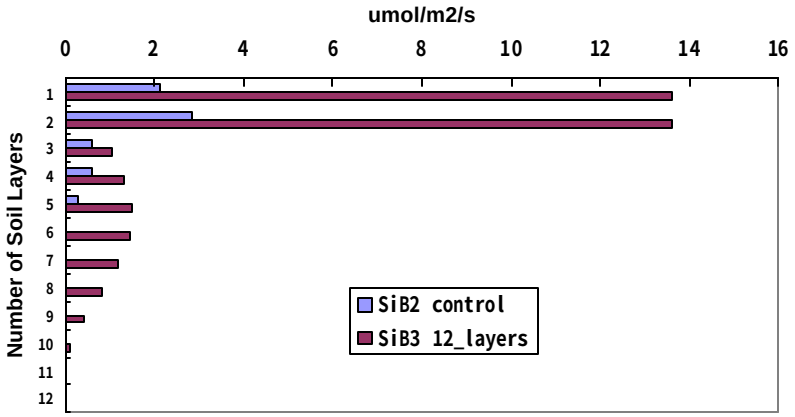

Figure 3.51 b: SiB3: Tapajos 67km the respiration factor profile throughout the soil

Latent and sensible heat fluxes suggest a huge difference between the SiB3 12_layer model simulation and the SiB2 control experiment. Overall, when compared to the observed data, latent heat flux is overestimated by about 17% by the multi-layer model while being underestimated at about 22% by the SiB2 three-layer model(see figure 3.52). From January to July and from November to December, the simulated latent heat flux is quite consistent with the observed data, but it is much higher in the dry season. This is due to the mitigated drought stress (see figure 3.44) and the relative low amount of humidity, which results in a lower evaporation demand (see equation 3.19).

The sensible heat flux is overestimated at around 75% in the multi-layer model, due to water stress. However, in contrast to the severe overestimation of sensible heat flux during the dry season in SiB2 control experiment, SiB3-12_layer model has performs better throughout the year except for the last two months (see figure 3.53). Therefore, the SiB3 multiple layer model performs better when considering latent and sensible heat separately (see figure 3.52-3.53), although it is the results from the SiB2 control simulation that are closer to the observed data (see figure 3.54), when concerning the summation of latent and sensible heat flux. The SiB3 12_layer model overestimates the total latent and sensible heat flux.

Figure 3.55 a and b show the annual mean diurnal cycle comparison of energy fluxes among the SiB2 control experiment, SiB3 multi-layer model, and observed data. Black lines are energy fluxes from the SiB2 control experiment; blue lines are energy fluxes from the SiB3-12_layer model. It is apparent that the SiB3-12_layer model has a more realistic performance although it overestimates both latent heat flux and sensible heat flux.

The reason why simulated latent and sensible heat flux are higher than observed data in the multi-layer model may by proposed as follows: 1) projected albedo in the model is too low; 2) short wave and long wave radiation in the meteorological driver data is too high all the year; 3) the systematic underestimation of latent and sensible heat flux by eddy covariance method. The higher activity of latent heat flux is may also indicate

amplified amount of soil moisture available in the water reservoir because the existence of the stress reduces the extraction of water from the soil.

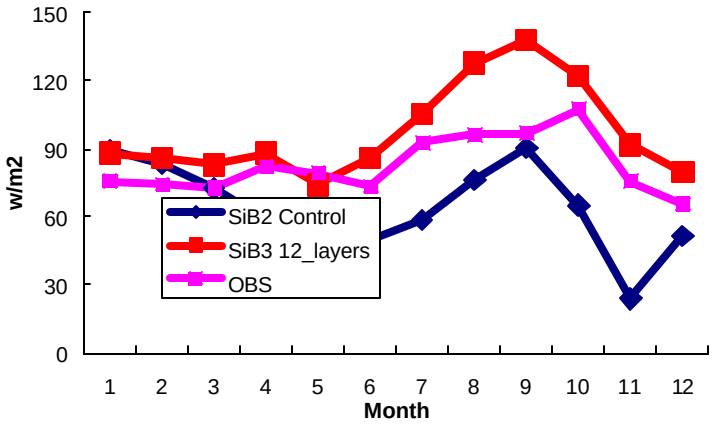

Figure 3.52: SiB3: 2002 Tapajos 67km latent heat flux

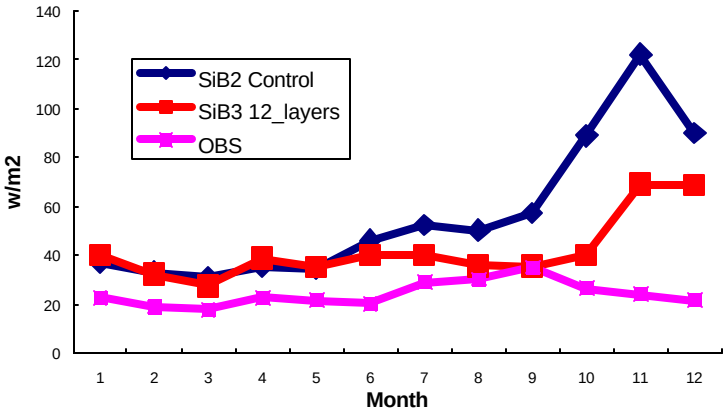

Figure 3.53: SiB3: 2002 Tapajos 67km sensible heat flux

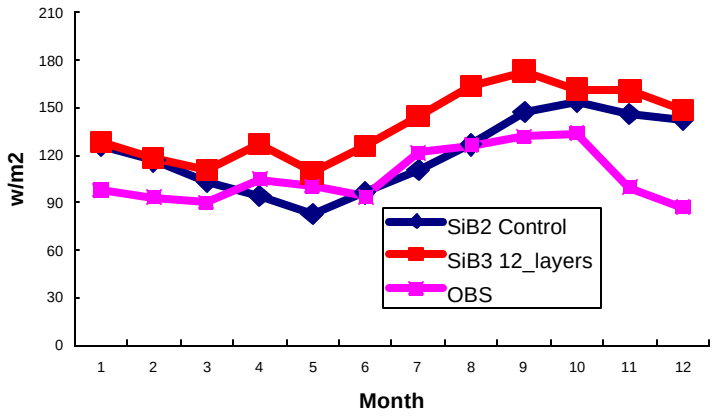

Figure 3.54: SiB3: 2002 Tapajos 67km total latent and sensible heat flux

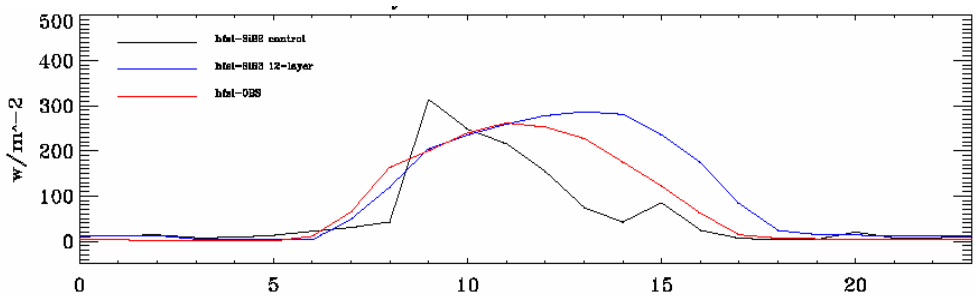

Figure 3.55 a: 2002 Tapajos 67km annual mean diurnal cycle of latent heat flux

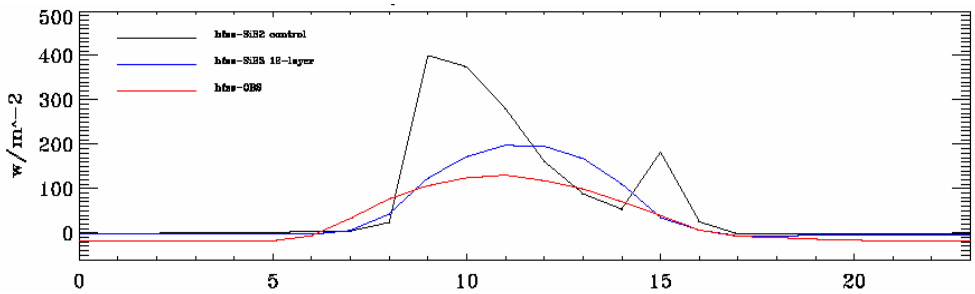

Figure 3.55 b: 2002 Tapajos 67km annual mean diurnal cycle of sensible heat flux

A question arises when comparing the simulated results between the Tapajos 67km site and Reserva Jaru The SiB3-12_layer model performs well for Reserva Jaru, however, for Tapajos 67km site water stress has been mitigated at around 35% in the dry season but still exits. The reason this has happened may be proposed as follows: the yearly average precipitation in Tapajos is around 18% less than Reserva Jaru, and rainfall is unevenly distributed throughout the year, with concentrated in the wet season from January to July

and a great reduction in precipitation during the dry season. The extremely dry conditions from August to November make it harder to eliminate water stress completely even with the two extra water reservoirs (see figure 3.56).

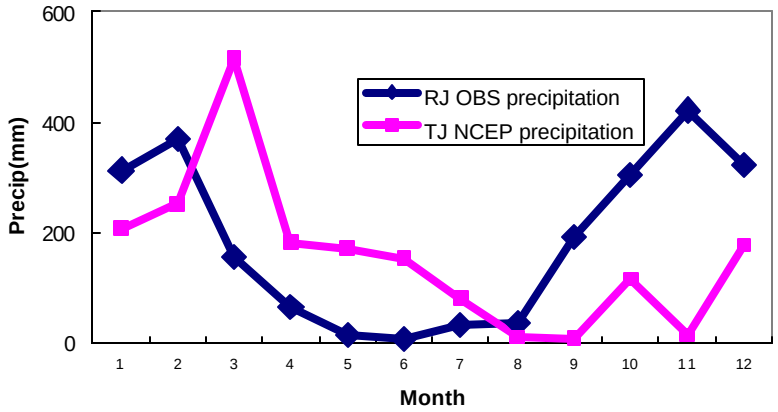

Figure 3.56: Meteorological driver data of precipitation at the two tropical forest Sites.

Chapter 4

Conclusion and Future Work

4.1 Conclusions

There are two objectives in this study:

1) To understand the seasonal variations in carbon and water exchange that feed back to regional CO_2 concentrations, the hydrology, and atmospheric circulation patterns in tropical forests.
2) To investigate the interactions between ecosystem-level drought stress, carbon exchange, and precipitation, and to explore a plausible method to eliminate any unrealistic severe drought stress from the Simple Biosphere Model simulation.

The major findings and conclusions from this study can be summarized as follows:

- The interaction between land-surface and atmosphere play an essential role in the general circulation model. An incorrect interpretation of the interaction gives rise to inaccurate simulation results when coupled with the general circulation model. The proper parameterization of root depth, soil hydrology and ecosystem drought stress are crucial in order to interpret this interaction accurately.
- Increasing the root depth results in a smaller amount of root zone water saturation and a more severe drought stress. It is because the same amount of annually available water is being “spread out” through a greater volume of root zone pore space in the deep root experiment. Latent heat flux drops significantly with a higher sensible heat flux throughout the entire year, which is consistent with the smaller root zone water content. Moreover, deep roots influence CO_2 flux by reducing net photosynthesis and

respiration simultaneously.

- Alleviating the sensitivity of ecosystem drought stress to root zone water content can relieve the drought stress only slightly. Variation patterns of energy flux change a little bit according to more constant fluxes of latent and sensible heat during the year. However the experiment does not make any significant change in CO_2 flux, with the exception of a slight increase of net photosynthesis in the dry season. These results indicate that root water zone water may not be an optimal variable to use for calculating drought water, and should be replaced by an alternative parameter.
- Increasing the amount of precipitation input into the soil by reducing the runoff of water on the surface does not contribute much to the improvement of the simulation. The results are almost the same as those in the original version. It suggests that surface runoff of precipitation is not the only way that let soil water lose. By increasing hydraulic conductivity in this experiment, gravitational drainage takes a dominant role and extracts water from the soil.
- The failure of the three experiments: deep root, the new formula to calculate drought stress, and less run-off precipitation, show that alternative parameterization based on the original three soil layer structure cannot improve the results radically. Therefore, pooling the entire root system into one soil layer without considering root distribution throughout the soil layers is not compatible with real soil hydrology.
- The multi-layer soil structure has a crucial influence on the soil water reservoir. On one hand, it allows for vertical water movement through the soil layers and efficient soil moisture, which is a more realistic account of how trees utilize water in the dry season. On the other hand, it may exaggerate soil moisture and cause the overestimation of latent sensible heat flux.
- Adjusted water extraction root profile throughout the soil layers also contributes to the alleviation of drought stress in the dry season. Exponential root distribution allows for water input into the deeper soil layers and makes the water reservoir more

efficient instead of pooling the entire root system into one soil layer.

- Using plant available water (PAW) instead of root zone water content to calculate water stress overcomes the disadvantage of over sensitivity of water stress to root zone soil moisture saturation. And this new algorithm describes the relationship between water stress and soil moisture more realistically through the use of wilting points and field capacity, which are important for determining the ability of plants to extract water from the soil. It is a simple but realistic way to describe the entire plant-soil system.
- SiB3 multi-layer model shows different performance when predicting energy flux at different sites. For Reserva Jaru, synoptic scale variability of latent heat flux is well captured and at the same time, the partition of latent and sensible heat flux is shifted due to the removal of drought stress but their sum does not change. However, not only sensible heat flux but also latent heat flux is severely overestimated in Tapajos 67km site.
- For the multi-layer model to relieve drought stress it is also somewhat dependent on the location of sites and their weather conditions. Drought stress is eliminated successfully in Reserva Jaru, However, for the Tapajos 67km site, where the yearly mean precipitation is around 18% less than Reserva Jaru, drought stress is not alleviated entirely even with the two extra deep layers added to the model.

4.2 Recommendations for Future Work

- This study focuses on tropical forest areas, which are featured by evergreen broadleaf plants and deep roots. It is very important to test whether the strategies of introducing multi-layer soil structure and adjusted water extraction root profile, which are both plausible with regard to deep root, are accurate in all locations. It is important for SiB3 multi-layer model be applied in other sites involving different biome types such as grassland, deciduous trees and so on.

- It is necessary to explore a more realistic algorithm to calculate water stress with the use of plant available water in order to alleviate drought stress completely from the model no matter what kind of weather condition the site is in, and to gain more ideal simulation results for net ecosystem CO2 exchange and energy flux. The overestimation of sensible heat flux in both sites and the slight exaggeration of respiration in Tapajo propose another challenge in the research.
- In order to predict CO2 and energy flux more realistically using the multi-layer model, it is also important to choose a more suitable number of layers and avoid the amplification in the ability of deep roots to pump water.
- Metrological driver data influence the simulated results significantly. NCEP data with the resolution of 1°x1°is employed in the simulation for Tapajos 67km site, whereas tower data is used in Reserva Jaru. The better model performance in Reserva Jaru suggests that tower data should be applied in order to get more accurate simulated results.

REFERENCES

Atlas, R., Wolfson, N., Terry, J. 1993: The Effect of SST and Soil Moisture Anomalies on GLA Model Simulations of the 1988 U.S. Summer Drought. *Journal of Climate*, **6**, 2034-2048

Ball, J. T., 1988: An analysis of stomatal conductance. Ph.D. Thesis, Stanford, CLif,. 446-476.

Beljaars, A.C.M., P. Viterbo, M. Miller, and A.K. Betts, 1996: The anomalous rainfall over the USA during July 1993: Sensitivity to land surface parameterization and soil moisture anomalies. *Mon. Wea. Rev.,* **124**, 362-383.

Beljaars, A.C.M., and P. Viterbo, 1999: Soil moisture-precipitation interaction: Experience with two land surface schemes in the ECMWF model. Global energy and water cycles. K. Browning and R. Gurney, Eds., Cambridge University Press, Cambridge, 223-233.

Berry J. A. and G. D. Farquhar, 1978: the CO_2 concentrating function of C_4 photosynthesis: a biochemical model. Proc 4th Int. Congr. Photosynthesis. Hall D., Coombs J. Coodwin T. (eds). *Biochem Sco.*, London, 119-131.

Betts, A.K., 1992: FIFE atmospheric boundary layer methods. *J. Geophys. Res.*, **97D**, 18,523-18,531.

Betts, A.K., J.H. Ball, A.C.M. Beljaars, M.J. Miller and P. Viterbo, 1996: The land surface-atmosphere interaction: A review based on observational and global modeling perspectives. *J. Geophys. Res.,* **101D**, 7209-7225.

Betts, A. K., Ball, J. H., 1998: FIFE Surface Climate and Site-Average Dataset 1987–89. *Jour. of the Atmos. Sci.,* **55**: 1091-1108

Betts, A. K. 2000: Idealized Model for Equilibrium Boundary Layer over Land. *Journal of Hydrometeorology,* **1**: 507-523.

Betts, A., J. Ball, A. Beljaars, M. Miller, and P. Viterbo, 1994: Coupling between land and surface, boundary layer parameterizations and rainfall on local and regional scales: Lessons from the wet summer of 1993. *Fifth Symp. on Global Change Studies, Nashville, TN, Amer. Metero. Soc.*, 174-178.

Bosilovich, Michael G., Sun, Wen-yih, 1999: Numerical Simulation of the 1993 Midwestern Flood: Land–Atmosphere Interactions. *Journal of Climate*, **12,** 1490-1505

Boyer, J.S 1970. Differing sensitivity of photosynthesis to low leaf water potential in corn and soybean. Plant Physics. **46**:236-239

Carson, T.R., R. Stothers, and S.K. Vemury 1981. Type II Cepheids - A comparison of theory with observations. *Astrophys. J.* **244**, 230-241.

Cazes-Boezio, Gabriel, Robertson, Andrew W., Mechoso, Carlos R. 2003: Seasonal Dependence of ENSO Teleconnections over South America and Relationships with Precipitation in Uruguay. *Jour Climate*, **16**: 1159-1176.

Collatz, G. J., J. T. Ball, C. Grivert, and J. A. Berry, 1991: Physiological and environmental regulation of stomatal conductance, photosynthesis, and transpiration: a model that includes a laminar boundary layer. *Agric. And Forest Meteorol.*, **54,** 107-136.

Collatz, G. J., M. Ribas-Carbo, and J. A. Berry, 1992: Coupled photosynthesis-stomatal conductance model for leave of C_4 plants. *Aust. J. Plant Physiol.*, **19,** 519-538

Cox, Peter. M., R. A.Betts, C.D.Jones, S.P. Spall and I.J. Tollerdell, 2002: Acceleration of global warming due to carbon cycle feedbacks in a coupled climate model. *Letter to Nature*, **408**, 184-187.

Dai, yongjiu, xubing zeng and R. E. Dickson,2001, Common Land Model(Technical documentation and users' guide).

Denning.,A. S, 1994: Investigation of the transport, sources, and sinks of Atmospheric CO2 using a general circulation model. Ph.D Dissertation, Colorado State Univeristy.

Denning, A. S. , 1997 : Spatial integration and regional carbon balance in Amazonia, proposal to LBA-Ecology.

Dickinson, R. E. 1986: The geophysiology of Amazon: Vegetation and climate interactions

Dorman, J. L. and P. J. Sellers, 1989: A global climatology of albedo, roughness length and stomatal resistance for atmospheric general circulation models as presented by the Simple Biosphere Model (SiB). *Jour. Appl. Meteorol.,* **28,** 833-855.

Farquhar, G. D., S. von Caemmerer and J. A. Berry, 1980: A biochemical model of photosynthetic CO_2 assimilation in C_3 plants. *Planta,* **149,** 78-90.

Farquhar, G. D. and T. D. Sharkey, 1982: Stomatal conductance and photosynthesis. *Ann. Rev. Plant Physiol.,* **33,** 317-345.

Fowler, L. A., D. A. Randall, and S. A. Rutledge, 1996: Liquid and ice cloud microphysics in the CSU General Circulation Model. Part I: Model description and simulated microphysical processes. *Jour. of Climate,* **9,** 489-529.

Fowler, L. A., D. A. Randall, 1996: Liquid and ice cloud microphysics in the CSU General Circulation Model. Part II: Impact on Cloudiness, the Earth's Radiation Budget, and the General Circulation of the Atmosphere. *Jour. of Climate.***9,** 530-560.

Fowler, L. A., D. A. Randall, 1996: Liquid and Ice Cloud Microphysics in the CSU General Circulation Model. Part III: Sensitivity to Modeling Assumptions, *Jour. of Climate*, **9**: 561-586.

Friedlingstein, P., L. Bopp, P. Ciais, J.-L. Dufresne, L. Fairhead, H. LeTreut, P. Monfray, and J. Orr, 2001: Positive Feedback between Future Climate Change and the Carbon Cycle. *Geophys. Res. Lett.,* **28**, 1543-1546

Garreaud, René D., Aceituno, Patricio, 2001: Interannual Rainfall Variability over the South American Altiplano, *Jour. Climate,* **14**: 2779-2789.

Gash, J.H.C., C.A. Nobre, J.M. Roberts, and R.L. Victoria: An overview of ABRACOS. pp 1.

Gebauer, G. 1988. Carbon, Nitrogen and water us of C3, C_4 and CAM of plants. Comparative Aspercts. *Acta Hort. (ISHS)* 229:73-84

Giorgi, F,. L. Mearns, C. Shields and L. Mayer, 1996: A regional model study of the importance of local versus remote controls of 1988 drought and 1993 flood over the

central United States. *Jour Climate,* **9,** 1150-1162.

Goudriaan, J. R., 1977: *Crop micrometerology: A simulation study.* Wagening Center for Agricultural Publishing and Documentation, 249pp.

Hansen, J., Mki. Sato, R. Ruedy, A. Lacis, and V. Oinas 2000. Global warming in the twenty-first century: An alternative scenario. *Proc. Natl. Acad. Sci.* **97**, 9875-9880.

Harshvardhan, R. Davies, D.A. Randall, and T. G. Corsetti, 1987: A fast radiation parameterization for general circulation models. *Jour. Atmos. Sci.*, **46,** 1922-1942.

Houghton, R. A. 1991: *Clim. Change*, **19**, 99.

Jarvis, P. G., 1989: Atmospheric Carbon dioxide and forests. *Philos. Trans. R. Soc. London, Ser. B,* **324,** 369-392.

Jarvis, P. G., 1976: The interpretation of the variations in leaf water potential and stomatal conductance found in canopies in the field. *Philos. Trans. Roy. Soc. London, Ser. B.*, **273**, 593-610.

Kimes, D. S., 1984: Modeling the directional reflectance from complete homogeneous vegetation canopies with various leaf orientation distribution. *J Opt. Soc. Amer.,* **A1,** 725-137.

Kousky, V. E. Kagano, M. T., and Cavalcanti, I. F. A., 1984: A review of the southern oscillation: Oceanic-atmopheric circulation changes and related rainfall anomalies, *Tellus*, **36A**, 490-504.

Kramer, P. J. and Boyer J. S, 1995: Water relations of plants and soils. Academic Press. pp201-204.

Lockwood, A.P.M, 1976 : Physiological adaptation to life in estuaries. pp. 98-99 in Newell, R.C., ed. Adaptation to environment: essays on the physiology of marine animals. Butterworths, London.

Lomee, O. 1961. "Effete de caractères du sol localisation la vegetation en zones équatoriale humide." In Proceedings of Symposium on Humid Tropical Zone, Abidjan, 1959, pp. 25-39. Unesco.

Lawson, T. L., R. Lal, and K. Oduro-Afiriyie. 1981. Rainfall distribution and microclimate changes over a cleared watershed. *Tropical agricultural hydrology*, pp. 141-152.

Lyon Brad., Randall M. Dole, 1995: A Diagnostic Comparison of the 1980 and 1988 U.S. Summer Heat Wave-Droughts. *Jour. Climate*, **8**, 1658-1674.

Mintz, Y. 1994: Global Climate, Cambridge, 233pp

Nepstad DC, Carvalho CJRd, Davidson EA et al. (1994): The role of deep roots in the hydrological and carbon cycles of Amazonian forests and pastures. *Nature*, **372**, 666-669.

Nobrem, C. A., 1983: Tropical heat sources and their associated large-scale atmospheric circulation, Ph.D. Thesis, Massachusetts Institute of Technology, Cambridge, MA.

Otterman, J., 1981: Plane with protrusions as ans atmospheric boundary. J. *Geophys. Res.* **86,** 6627-2230.

Paegle J., C. M. Kingtse and Nogues-Paegle, 1996: Dependence of simulated on surface evaporation during the 1993 summer floods. *Mon. Wea. Rev.*, **124,** 345-361.

Paul R. Remann: Flood analysis: 1993 Mississippi flood.

Randall, D. A., D. A. Dazilch, C Zhang, and A. S. Denning, 1996: A revised land-surface parameterization (SiB2) for GCMs. Part III: The Greening of the Colorado State University General Circulation Model. *Jour. Climate*. **9,** 738-763.

Rayner, P. J., I. G. Enting, and C. M. Trudinger, 1996: Optimizing the CO2 observing network for constraining sources and sinks, *Tellus*, **48B**, 433-444.

Ritter, M. E. 1997: Earth Online: An Internet Guide for Earth Science, Wadsworth Publishing Belmont, CA 264p.

Saleska, S. R. S. D. Miller, D. M. Matross, M. L. Goulden, S. C. Wofsy, H. R. da Rocha, P. B. de Camargo, P. Crill, B. C. Daube, H. C. de Freitas, L. Hutyra, M. Keller, V. Kirchhoff, M. Menton, J. W. Munger, E. H. Pyle, A. H. Rice, H. Silva, 2003: Carbon in Amazon forests: unexpected fluxes and disturbance-induced losses. *Science*, **302,** 1554-1557.

Salati E., Dall' Olio, Matsui, E. and Gat, J. R, 1979: Recycling of water in Amazon Basin: and isotopic study. *Water Resour. Res,* **15,** 1250-1258.

Salati, E., and E. Matsui. 1981. "Isotopic hydrology in the Brazilian Amazon Basin." Inter-American Symposium on Isotope Hydrology Bogota, Colombia, August 1980, Instituto de Asuntos Nucleares, Bogota, pp. 111-120.

Sellers, P. J., 1981: Vegetation type and catchment water balance: A simulation Study. Ph. D. Thesis, Leeds University, 836pp.

____, 1985: Canopy reflectance, photosynthesis and transpiration. *Int. J. Rem Sens,* **6(8),** 1335-1372.

____, and J. G. Lockwood, 1981: A computer simulation of the effects of differing crop types on the water balance of small catchments over long time period. *Quart. J Roy. Meteor. Soc.,* **107,** 395-414.

Sellers, P. J., 1985: Canopy reflectance, photosynthesis, and transpiration. *Intern.Jour. Remote Sens*., **6**, 1335-1371.

Sellers, P. J., 1987: Canopy reflectance, photosynthesis, and transpiration II. The role of biophysics in the linearity of their interdependence. *Remote Sens. Eniron.* **21**, 143-183.

Sellers, P. J. Y. Mintz, Y. C. Sud, and A. Dalcher, 1986: A simple Biosphere Model (SiB) for use within general circulation models. *J. Atmos. Sci*., **43**, 505-531.

Sellers, P. J., J. A. Berry, G. J. Collatz, C.B. Field, and F. G. Hall, 1992: Canopy reflectance, photosynthesis, and transpiration. III. A reanalysis using enzyme kinetics-electron transfer models of leaf physiology. *Remote Sens. Eniron*., **42,** 1-20.

Sellers, P. J., F. G. Hall, G. Asrar, D. E. Strebel, and R. E. Murphy, 1992: An overview of the First International Satellite Land Surface Climatology Project(ISLSCP) Field Experiment(FIFE). *Jour. Geophys. Res.,* **97,** 18345-18371.

Sellers, P. J., M. D. Heiser, and F. G. Hall, 1992: Relations between surface conductance and spectral vegetation indices at intermediate (100m^{2}to 15km^2) length scales. *Jour. Geophys. Res.* **97**, 19033-19059.

Sellers, P. J., D. R. Randall, J. A. Collatz, J. A. Berry, C. B. Field, D. A. Dazlich, and G. D. Collelo, 1996: A revised land-surface parameterization (SiB2) for GCMs. Part I: Medel formulation. *Jour. Climate*. **9,** 676-705

Seller, P. J., S. O. Los, C. J. Tucker, C. O. Justice, D. A. Dazlich, G. J. Collatz and D. A. Randall, 1996 : A revised land-surface parameterization (SiB2) for GCMs. Part II: The generation of global fields of terrestrial biophysical parameters from satellite data. *Jour. Climate*. **9,** 706-737

Sellers, P.J., R.E. Dickinson, D.A. Randall, A.K. Betts, F.G. Hall, J.A. Berry, C.J. Collatz, A.S. Denning, H.A. Mooney, C.A. Nobre and N. Sato, 1997: Modeling the exchanges of energy, water, and carbon between the continents and the atmosphere. *Science*, **275**, 502-509

Shukla, J., and Y. Mintz, 1982: Influence of land-surface evaporation on the earth's climate. *Science*, **215,** 1498-1501.

Skole, D., and C. Tucker. 1993: Tropical deforestation and habitat fragmentation in the Amazon: Satellite data from 1978 to 1988. *Science*, **260**: 1905-09.

Spittlehourse, D. L., And T. A. Black, 1981: a growing-season water balance model applied to two Douglas fir stands. *Water Resour. Res.*, **17,** 1651-1656.

Trenberth, K. E. and C. J. Guillemot, 1996: Physical processes involved in the 1998 drought and 1993 floods in North America, *Jour Climate*, **9,** 1288-1298.

Wilson, M. E. and Henderson-Sellers, 1985: A global archive of land cover and soils data for use in general circulation models. *Jour. Climate*, **5**, 119-143.